DOT/FAA/CT-88/27

FAA Technical Center
Atlantic City International Airport
N.J. 08405

AD-A209 330

Electro-Impulse De-Icing Research

(Fatigue and Electromagnetic Interference Tests)

G. W. Zumwalt
R. A. Friedberg
J. A. Schwartz

Institute for Aviation Research
Wichita State University

March 1989

Final Report

U.S. Department of Transportation
Federal Aviation Administration

NOTICE

This document is disseminated under the sponsorship of the U. S. Department of Transportation in the interest of information exchange. The United States Government assumes no liability for the contents or use thereof.

The United States Government does not endorse products or manufacturers. Trade or manufacturers' names appear herein solely because they are considered essential to the objective of this report.

Technical Report Documentation Page

1. Report No.	2. Government Accession No.	3. Recipient's Catalog No.
DOT/FAA/CT-88/27		

4. Title and Subtitle

ELECTRO-IMPULSE DE-ICING RESEARCH
(FATIGUE AND ELECTROMAGNETIC INTERFERENCE TESTS)

5. Report Date

March 1989

6. Performing Organization Code

8. Performing Organization Report No.

7. Author(s)

G. W. Zumwalt, R. A. Friedberg, and J.A. Schwartz

9. Performing Organization Name and Address

Institute for Aviation Research
Wichita State University
Wichita, KS 67208

10. Work Unit No. (TRAIS)

DOTFA03-86-C-00041

11. Contract or Grant No.

12. Sponsoring Agency Name and Address

U.S. Department of Transportation
Federal Aviation Administration
Technical Center
Atlantic City International Airport, NJ 08405

13. Type of Report and Period Covered

Final Report

14. Sponsoring Agency Code

ACD-200

15. Supplementary Notes

Program Manager: Charles Masters
Aviation Safety Division FAA Technical Center

16. Abstract

Electro-Impulse De-Icing (EIDI) has been recently developed and tested with very encouraging results. Questions remain, however, regarding the fatigue life and electromagnetic compatibility of the system.

Fatigue tests were conducted on two production aluminum wing leading edges and one composite material leading edge. These were done at realistic temperatures and impulse energies for an estimated aircraft lifetime of ice protection. Coil mounting brackets were the main casualties. Wing components did not fail.

Tests were also conducted for metal and composite wings of electromagnetic radiation of EIDI over a wide frequency range. The aluminum wing was found to be an excellent shield. All wires external to the aluminum wing were shown to require careful shielding. The composite wing required all wiring and the metal doublers to be shielded and grounded. keywords: Deicing systems;

17. Key Words

Aircraft Ice Protection,
Fatigue Tests,
Electromagnetic Interference.
Aircraft Icing

18. Distribution Statement

Document is available to the public through the National Technical Information Service, Springfield, Virginia 22161

19. Security Classif. (of this report)	20. Security Classif. (of this page)	21. No. of Pages	22. Price
Unclassified	Unclassified	60	

PREFACE

The work reported herein was performed under contract with the Institute for Aviation Research at Wichita State University. Professor Glen W. Zumwalt was the Wichita State University Project Director. Personal from the Federal Aviation Administration Technical Center, Aviation Safety Division, administered the contract. The Contracting Officers' Technical Representatives were Messrs. Caesar Caiafa and John Reed. Technical guidance, including personal participation in the electromagnetic interference testing, was provided by Mr. Charles Masters.

TABLE OF CONTENTS

LIST OF FIGURES

LIST OF ABBREVIATIONS

ADF	Airborne Direction Finder
AIAA	American Institute of Aeronautics
EIDI	Electro-Impulse De-Icing
EMI	Electromagnetic-Interference
dB	decibels
FAA	Federal Aviation Administration
FAR	Federal Aviation Regulations
GHz	Giga-Hertz, billions of cycles per second
Hz	Hertz, cycles per second
I.D.	Inside Diameter
KHz	Kilo-Hertz, Thousands of cycles per second
LORAN-C	C Model of Long Range Navigation system
NASA	National Aeronautics and Space Administration
NAV/COM	Combined NAVigation and COMmunication system
MHz	Mega-Hertz, millions of cycles per seconds
ms	milli-seconds
O.D.	Outside Diameter
RCVR	Receiver (Fig. 3-1)
RNAV	Radio NAVigational system
VAC	Volts Alternating Current
WSU	Wichita State University

EXECUTIVE SUMMARY

Electro-Impluse De-Icing (EIDI) Systems produce a very high intensity, electromagnetic induced mechanical shock in an aircraft's surface to dislodge ice buildups, thus fostering questions about electromagnetic interference and fatigue life which have not been adequately answered in previous EIDI development work. These questions both relate directly to aircraft safety and thus are of great concern to the Federal Aviation Administration. In view of the increasing use of composite materials in aircraft, it was necessary that both aluminum and composite materials be included in the testing.

Tests were performed on two aluminum wing leading edge models and one composite leading edge model. The aluminum models were identical except for skin thickness. Both were 6 feet long with ribs at 1.5-foot intervals. They were made at the Cessna plant in Wichita to make this a test of a typical production quality wing section. (The composite model had been made earlier by the Learfan Aircraft Company. It was a Kevlar® composite leading edge of 38-inch span.) The models were all fitted with EIDI coils, and soft aluminum doublers were bonded to the inner wing surfaces opposite the coils. The models were placed in a cold box for the fatigue tests. Coils were impulsed at four spanwise positions for each metal model and two positions for the composite model. There were 15,000 impulses delivered to each metal wing coil position and 20,000 impulses to each composite wing coil position. The impulse energy levels were those previously determined to be needed for effective de-icing.

Damage was limited to coil beam mounting brackets and end closure ribs which were peculiar to these test models. No changes could be detected for the composite model.

Electromagnetic interference tests used the same models as the fatigue tests. Tests in a shielded room revealed that EIDI is well shielded by an aluminum wing, but in a composite wing every component of the system must be individually shielded to meet emissions standards. More work is suggested to determine good shielding for EIDI in composite structures.

1. INTRODUCTION

A project to develop the Electro-Impulse De-Icing (EIDI) system for aircraft was conducted from 1982 to 1986 at Wichita State University (WSU) under NASA Lewis Research Center funding. This was a joint effort of NASA, WSU and ten aerospace industries. The results of this project are given in references 1 through 9. At the termination of NASA funding the basic parameters in designing an EIDI system had been defined and the satisfactory operation of this de-icing method demonstrated on a wide range of aircraft elements in ten icing tunnel tests and in three sets of flight tests.

However, some important questions were left unanswered. One question which comes to mind upon hearing EIDI described is, what are the cumulative effects of impacting the surface? Is fatigue of the skin material a problem? Upon further thought, the question expands to cover the fatigue of all the leading edge structure, the coil mounts, lead wires and insulation. No systematic set of tests had been performed to define the extent of the fatigue problem. These tests had been postponed at WSU out of concern that the weak link in the system might be the power and sequencing box, upon which many other tests depended. After the pressure to perform icing tunnel tests subsided, and a back-up power supply was available, it was clearly time to do fatigue testing. Incidentally, the fears for the vulnerability of the power-and-sequencing box proved to be unfounded. Over 100,000 additional impulses have been added without failure.

A second naturally arising question concerns the possible electromagnetic interference (EMI) with aircraft control, communication or navigation systems. High voltage pulses with extremely high transients are discharged in leading edges of wings, tails and engine inlets. This may be in close proximity to many sensors, transmitters or control elements. Flight tests had indicated that EMI was not a problem, and a cursory test at one of the participating industries had given confirmation for one case. But the extent of the EMI danger was still uncertain.

The third question was a more difficult one. System design by semi-empirical methods was being done, but the physical processes involved in de-bonding, shattering and expelling ice were not clearly understood. There was a need to observe the actual movement of a surface under EIDI impulsive forces both with and without ice on the surface. There was the hope that such observations could lead to a single criterion for de-icing a given type of ice. Possible criteria were maximum normal velocity or acceleration, or surface curvature or rate of change of curvature. Perhaps these would be functions of ice thickness or temperature. Computer codes have been developed which predict surface movement for a given structure with a specified EIDI electrical and coil design. The de-icing criterion could be added to these codes to provide a complete design methodology, if the criteria were sufficiently general and trustworthy. These tests and results will be contained in a separate report.

The tests reported here help to answer these questions. They were performed during 1986 to 1988 under funding and guidance from the Federal Aviation Administration Research Grant No. DTFA03-86-C-00041 to the Institute for Aviation Research at The Wichita State University.

2. FATIGUE TESTS

2.1 METAL LEADING EDGES

For fatigue testing of metal leading edges, it was decided that the most meaningful tests would be those of typical assembly line products. Therefore, arrangements were made with Cessna Aircraft Company to make sections of leading edges in their production shop. The workmanship in the fitting, riveting and bonding would then be representative of actual aircraft. The Cessna model 206 had been flight tested with an EIDI system installed, so the EIDI coil mounts had already been designed by Cessna and their fabrication method was established.

2.1.1 Test Models

Two Cessna 206 aluminum leading edge models were tested. These were identical except for skin thickness. One was 0.025 and the other 0.040 inches thick 2024 T-3 aluminum. Each was a six-foot span section from the inboard portion of the Cessna 206 wing. In this section, the wing is neither tapered, twisted nor sweptback. The span was divided into four 18 inch bays by ribs which were bonded and riveted to the leading edge. The main spar was 10.5 inches from the leading edge, which is a large distance for a spar-mounted coil. In addition, control cables occupy the aft part of the "D-section" in the actual airplane. For these reasons, the coils were supported by composite beams whose ends were attached to ribs by aluminum brackets. These can be seen in Figure 2-1. The coil beams had U-shaped cross sections. The bottom of the U was concentric with the nose arc, so that a coil could be contoured and mounted directly on the outside of the U, with a proper gap between it and the skin. The metal-to-metal gap is nominally 0.10 inches. The beams were made of fiberglass on the compression (outer) side of the beam and Kevlar on the tension (inner) side of the U beam.

One EIDI coil was mounted in each bay. The coil was centered spanwise in the bay, and chordwise the coil was slightly below the highlight to center over the average stagnation line. The coils were made from copper ribbon wire having a cross section of 0.025 x 0.190 inches. Each coil consisted of 40 turns with 0.25 inch I.D. and 2.25 inch O.D. The coils were series connected to alternating bays. That is, coils in bays 1 and 3 were connected and those in bays 2 and 4 were connected so that alternate bays were impulsed together.

Opposite each coil, a doubler plate was bonded to the inside of the skin. These doublers were 0.050 inch thick unalloyed aluminum with a diameter only slightly greater than the coil. These were needed to increase the electrical conductivity of these thin skins for EIDI eddy currents to develop in the skin. The coil gap was, of course, measured from the doubler surface.

The two leading edge models were inspected upon delivery from Cessna. It was found that the outboard rib on the thin-skin model was a special, hand-installed closure rib. The rivet holes appeared to be hand drilled and hole alignment was imperfect. This rib was not bonded as were the other ribs. Where poor hole alignment occurred, the rivets created a slight pucker in the skin, putting extra stress on the rivet. The thick-skin model also had a non-standard, non-bonded outboard closure rib.

The coils had been made by Cessna with techniques developed at WSU. In the initial inspection, it was found that in one of the bays of each model, one of the coils had a connecting pin that was poorly covered by insulation, as shown in Figure 2-2. This was corrected by grinding the pin and covering it with fiberglass and epoxy. This would likely have caused a short across the 0.1 inch gap between the coil and doubler. The short could be dangerous to personnel as well as seriously reducing the de-icing capability of the unit.

2.1.2 Test Procedure

To simulate the freezing conditions encountered during flight, the models were placed in a freezer chest and allowed to cold soak for 30 minutes at about 0 degrees F. This was done principally to provide a worst case condition for the bonded junctions. The coils were then pulsed and a current trace (plot of current vs. time) was made for comparison with a trace to be taken at the end of the test. The current plot is very sensitive to changes in the coil-to-skin gap.

The impulsing then began from the power supply in the room to the model in the cold box. A counter and timer was set for ten-second intervals between pulses. The capacitor voltage was 1,000 and the capacitance was 400 microfarads, resulting in 200 joules per impulse. These values had been determined as adequate for de-icing in icing tunnel and flight tests for the C-206 wing. The ten second interval was decided by monitoring the coil temperature and maintaining 5 degrees F.

During the fatigue test, about once each hour inspection was made of the current trace, rivets, bonds and skin. This was to detect any equipment malfunction, change in peak current or rise time, fretting or loosening of rivets, debonding of ribs or deformation of skin.

Bays 1 and 3 were impulsed for about two hours (about 700 impulses), then the power box channel was changed to bays 2 and 4 for the next two hours. This cycling was continued throughout the test. At 7,500 impulses, the model was removed from the cold box, the spar removed, and the components thoroughly inspected visually. The model was then returned to the cold box for a second 7,500 impulses, thus completing the 15,000 impulses estimated as the lifetime expected of de-icing required for this aircraft.

A final current trace was plotted for comparison with that at the start of the test. The model was disassembled and inspected for damage.

2.1.3 Results for the Thin-Skin-Model

At 3,400 impulses, inspection revealed fretting had begun around two rivets on the outboard rib, and at 7,500, these rivets showed signs of peeling, as shown in Figure 2-3. The inspection at 7,500 impulses showed no signs of debonding, cracking, delamination of the coil support beam or deformation of the skin.

At 11,200 impulses, a change in sound was detected, and the inspection covers were removed to reveal a broken coil-beam mounting bracket in bay number 2, as shown in Figure 2-4. Since the bracket was still lodged in place, no change in current trace was indicated.

After 15,000 impulses, dissembly and inspection showed a hairline crack in the outboard end closure ribs, shown in Figure 2-5. No other damage could be detected. The stability of the electrical parameters can be seen in the data of Table 1, and in the current trace in Figures 2-6 and 2-7.

2.1.4 Results for the Thick-Skin Model

At the 7,500 impulse dissemble and inspection, no changes could be detected. At 11,700 hits, a change in peak current was noted for the bays 1 and 3 circuit. Inspection revealed that a coil beam mounting bracket had broken as shown in Figure 2-8. The coil mount had shifted about 0.10 inches, which had caused the change in peak current. At the end of the test of 15,000 impulses, dissembly and inspection revealed that bays 2 and 4 also had cracks in one of their mounting brackets; these are shown in Figures 2-9 and 2-10. There was also a hairline crack in the nose of the outboard closure rib (Figure 2-11). Current traces are shown in Figure 2-12 and 2-13.

2.1.5 Conclusions

The results both relieve fears about fatigue damage and give warnings about fatigue. For the structure made by standard manufacturing methods, no debonding, cracking or deformation took place. But for a poorly designed mounting bracket, a warning is sounded. This stretch-formed aluminum bracket was not well suited to a system with fatigue possibilities. A stronger bracket is obviously required. A machined bracket with large radius fillet would avoid the stress concentration.

Similarly, the end closure rib which was rather casually inserted, showed the danger of ignoring fatigue considerations. The rivet holes misalignment and failure to bond the rib led to hairline cracking. The main conclusion is that fatigue is a solvable problem, but the EIDI system can cause fatigue breakage when stress concentration points are permitted in the design.

2.2 COMPOSITE LEADING EDGE

2.2.1 Test Model

A leading edge for fatigue tests of a composite model was obtained from the Learfan aircraft. It also represented an aircraft company production quality item. This was made of Kevlar, a composite which has very good energy absorption characteristics for bird strike survivability. This wing was designed for a higher speed than the metal models, with a small nose radius and nearly straight upper and lower surfaces just behind the nose. This called for a coil pair at each span station, one on the upper and one on the lower surfaces. The span length was 38 inches with ribs at the ends only. Two spanwise coil stations were used, giving 19 inches to be cleaned by each coil station. The two stations were impulsed separately and supplied with 800 volts and 550 microfarads stored energy, giving 111 joules per foot per impulse. Doublers were bonded to the skin opposite the coils; these were made from unalloyed aluminum 0.050 inches thick. The coils were 30 turns of copper wire 0.025 x 0.125 inches cross section, giving a 2.00 inch O.D. and 0.50 inch I.D.

An ultrasonic scan was made of the model before the test to insure that there were no voids or delaminations.

The leading edge was supported by its spar, as shown in Figure 2-14. Figure 2-15 shows the coils mounted on the spar and Figure 2-16 shows the leading edge with doublers bonded in place. The closure ribs were screwed to the model at each end as seen in Figure 2-16.

2.2.2 Test Procedure

The test procedure was similar to that for the metal models. The composite model was placed into the cold box and cold soaked for 30 minutes. Impulses were ten seconds apart, with coil stations impulsed alternatively. The model was removed for inspection every 5,000 cycles until 20,000 total impulses had been delivered. Current traces were taken at the beginning and end of the test for comparison.

2.2.3 Test Result

No changes in the leading edge structure, coils nor mounts could be detected visually. An ultrasonic scan was then made and found to be essentially identical with the one made before the test.

2.2.4 Conclusions

The composite leading edge of Kevlar suffered no damage from 20,000 impulses at a level which icing tunnel test had shown to be needed for deicing. This energy level is generally a little greater than that required by metal leading edges, but did not cause fatigue damage.

2.3 SKIN-MOUNTED COIL

A coil mounting method which appears superior to others is the skin-supported design termed the "band aid." A semi-rigid rectangular fiberglass plate has a coil at its center and is bonded to the skin at its ends, resembling an oversized adhesive bandage. See Figure 2-17. Its advantages are light weight (about 4 ounces) and more effective de-icing. The greater effectiveness is because all of the energy is put into the skin rather than having part of it lost in flexing the mounting supports (about 70% as much energy is needed). This superiority had been shown in several icing tunnel tests. The only drawback was that the impulsive force puts the adhesive bond in tensile "peel," perhaps the worst stress condition. Early versions tended to de-bond after a few impulses. Riveting the mount to the leading edge is an obvious alternative, but many structural designers dislike punching holes in their leading edges.

Similar peeling problems have occurred for doublers bonded to the skin. The impulsive loads had the same effect as blows with a ball peen hammer; the edges tended to curl and initiate de-bonding. A bonding agent was needed which would not become brittle, but would retain a rubbery consistency with adequate strength. Number 3840 urethane by Hexell had been found to be good for the doublers and was used in these fatigue tests for the coil mount.

2.3.1. The Test Model

Figure 18 shows the band-aid coil mount laying in the 0.040" thick metal leading edge used in the tests described in section 2.1. This coil was bonded over the doubler. The coil had 33 turns of 0.025 x 0.125 inch copper ribbon wire, giving 0.50" I.D. and 2.25" O.D. The gap between coil and doubler was 0.70 inches. Only this one skin mounted coil was used in the test.

2.3.2 Test Procedure

As before, the model was cold soaked in the deep freeze box, and an initial current trace was made. Impulses at ten second intervals were imposed from capacitor voltage of 800 and capacitance of 400 microfarads, giving 128 joules per impulse. The model was removed from the box and inspected every 5,000 cycles until a total of 20,000 cycles were delivered.

Several days later, to add a more extreme test, another 1,000 impulses were delivered at 1200 volts and 550 microfarads, equaling 396 joules per impulse.

2.3.3 Results

Neither visual inspection nor current traces revealed changes. The bonding agent had passed the test.

2.3.4 Conclusions

The fatigue test was successful, indicating that the skin-mounted coil can be used and its benefits realized. The only doubt may be the effect of long term changes on the bond. It is not known whether or not the rubbery consistency changes over a period of several years.

2.4 RELATED TESTS AT BOEING

Boeing Commercial Airplane Company was one of the participating industries in the EIDI Consortium. The WSU research group acted as consultant for a set of laboratory and flight tests to evaluate EIDI for the next generation Boeing transport. The test aircraft was a model 757 which had coils placed in two leading edge slats on the left wing; no. 2 (second inboard from the tip) and no. 5 (inboard slat). Fatigue tests were run in the laboratory before the flight tests. A lifetime maximum impulse total of 60,000 hits was predicted and, to allow for the possible effects of combined stresses, a multiple of this number was deemed to be required.

The EIDI system chosen by Boeing differed considerably from that previously tested. In an effort to minimize weight, a 3,000 volts system was designed. Previous testing had not exceeded 1500 volts. Since energy varies as the square of the voltage, this quadrupled the energy. The current was about 3500 amps. Thus, the impulse was several times as great as any system with which the WSU team had experience. The skin was 7075-T6 aluminum 0.062 inches thick. There was only one coil per span station in the slat.

At 69,000 cycles cracking of the skin over the coil was seen. A new model was prepared with a doubler bonded opposite the coil. The doubler had tapered edges to avoid stress concentration. The fatigue test was started again and this time, no damage was seen even after 230,000 impulses. Note that the doubler was added strictly for skin strengthening, not for the electrical benefits.

TABLE 2-1

FATIGUE TESTS FOR METAL SKINS

THIN SKIN (0.025) (1000 volts/400 microfarads)			THICK SKIN (0.040) (1000 volts/400 microfarads)		
COILS 2 & 4			COILS 2 & 4		
CYCLES	M/S*	AMPS	CYCLES	M/S*	AMPS
0	174	2454	0	174	2484
1095	175	2446	2194	174	2498
1114	174	2454	2380	174	2460
1450	174	2510	3411	175	2486
3300	174	2510	6046	175	2538
5260	175	2532	6735	170	2382
6045	175	2404	6760	174	2468
6700	178	2416	7500	174	2414
8226	175	2478	9000	174	2448
10400	177	2518	11000	176	2634
11590	178	2584	13300	176	2530
12900	178	2582	14000	176	2604
14900	178	2584	14400	176	2554
15000	176	2546	14900	176	2560
			15000	176	2548
COILS 1 & 3			COILS 1 & 3		
0	175	2446	0	174	2400
1504	172	2510	1340	174	2400
2347	170	2404	3650	174	2414
3425	172	2394	3770	174	2462
6315	170	2500	7275	175	2402
7310	170	2498	7500	176	2420
9033	172	2509	7900	176	2422
11200 **	172	2508	9000	176	2446
11686	176	2598	10150	176	2462
13840	176	2610	10900	176	2474
14100	176	2602	11100	176	2530
14350	174	2614	11700 ***	169	2359
15000	174	2598	12300	169	2344
			13700	169	2516
			14220	169	2508
			14700	168	2474
			15000	170	2364

* M/S = milliseconds to peak current.

** Broken coil mounting bracket on bay no. 2 detected by sound at 11,200 hits.

*** Broken coil mounting bracket on bay no. 3 detected by current change at 11,700 hits.

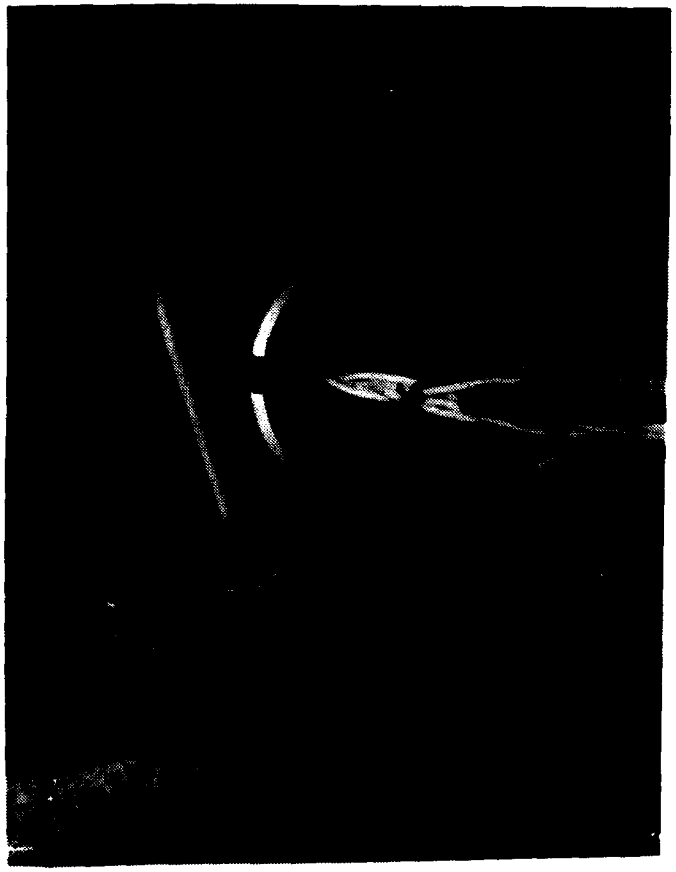

Figure 2-1
Rib and Coil
Mount Bracket

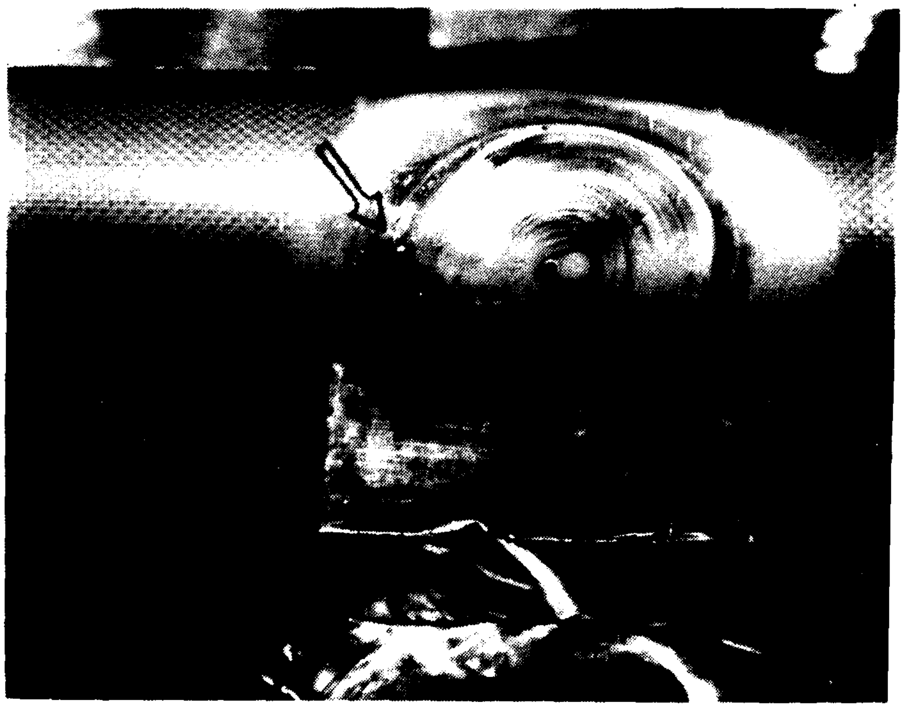

Figure 2-2
Coil Mounted on Semi-Cylindrical Beam. Poorly
Insulated Pin is on Left Side of Coil.

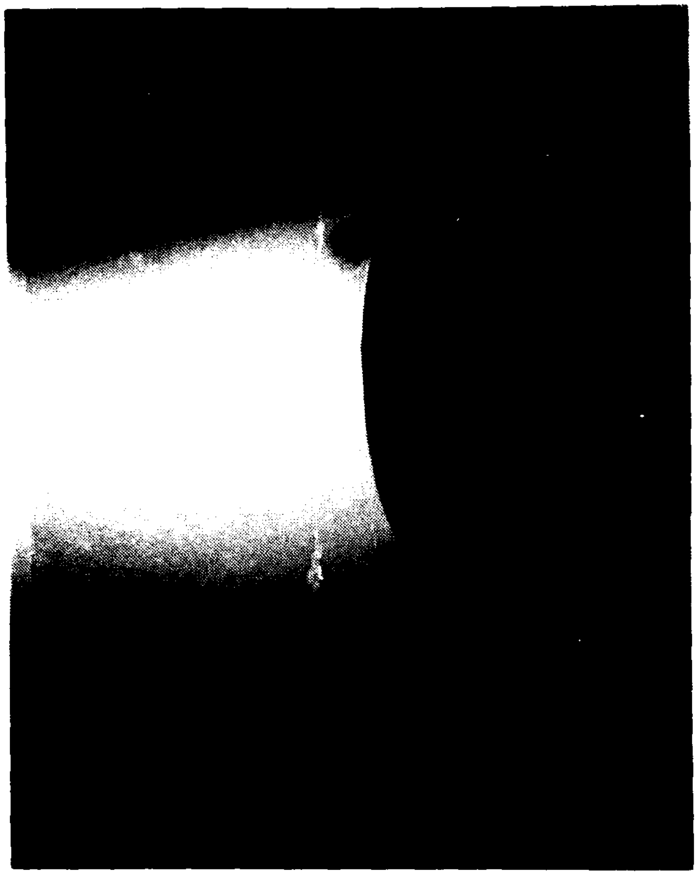

Figure 2-3
Rivet Hole Failure
After 7,500 Impulses
(0.025 Inch Skin)

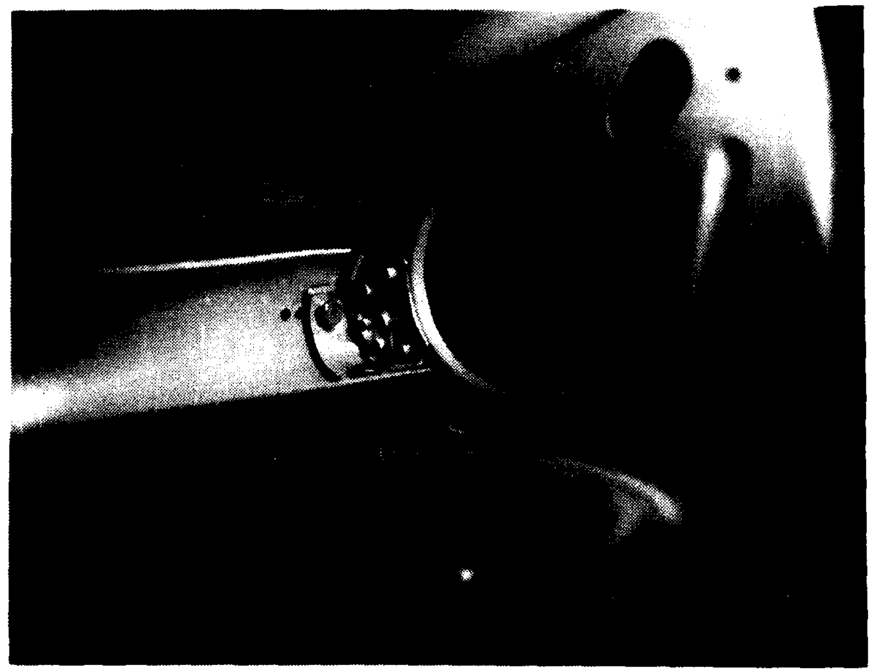

Figure 2-4
Broken Bracket
After 11,200 Impulses
(0.025 Inch Skin)

Figure 2-5
Hairline Crack on End Rib (Crack is at Upper Right Corner of Rib) (0.025-Inch Skin)

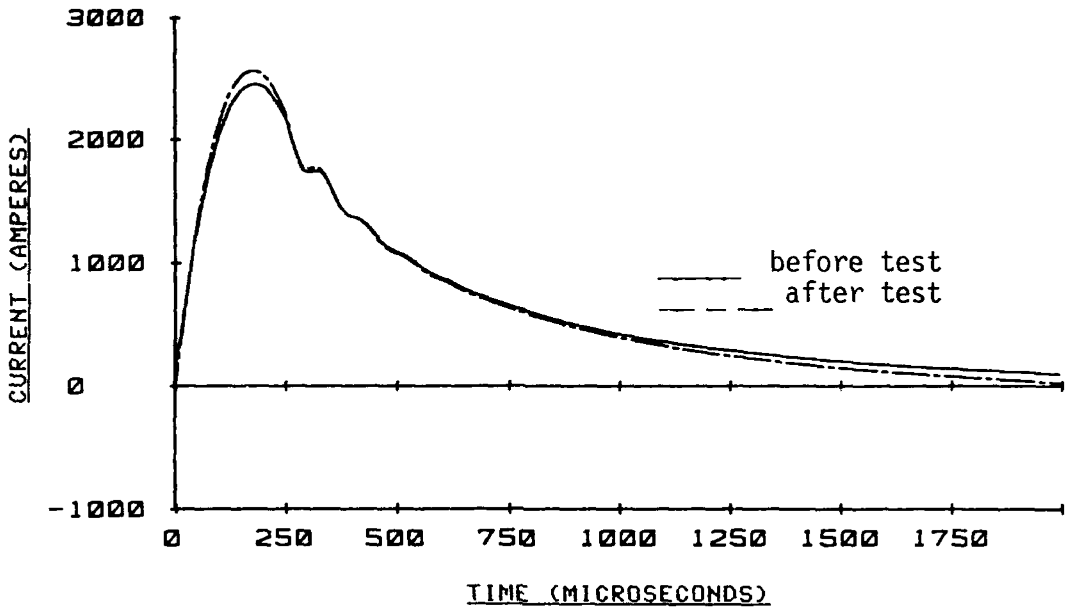

SKIN .025 BEFORE AND AFTER BAY 1 AND 3

Figure 2-6
Current Traces

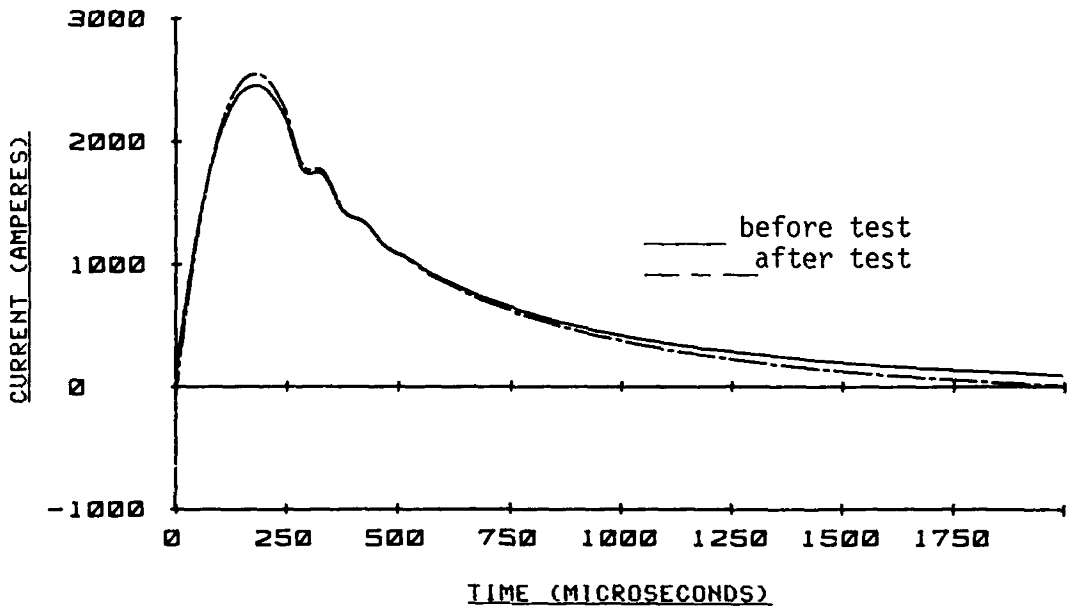

SKIN .025 BEFORE AND AFTER BAY 2 AND 4

Figure 2-7
Current Traces

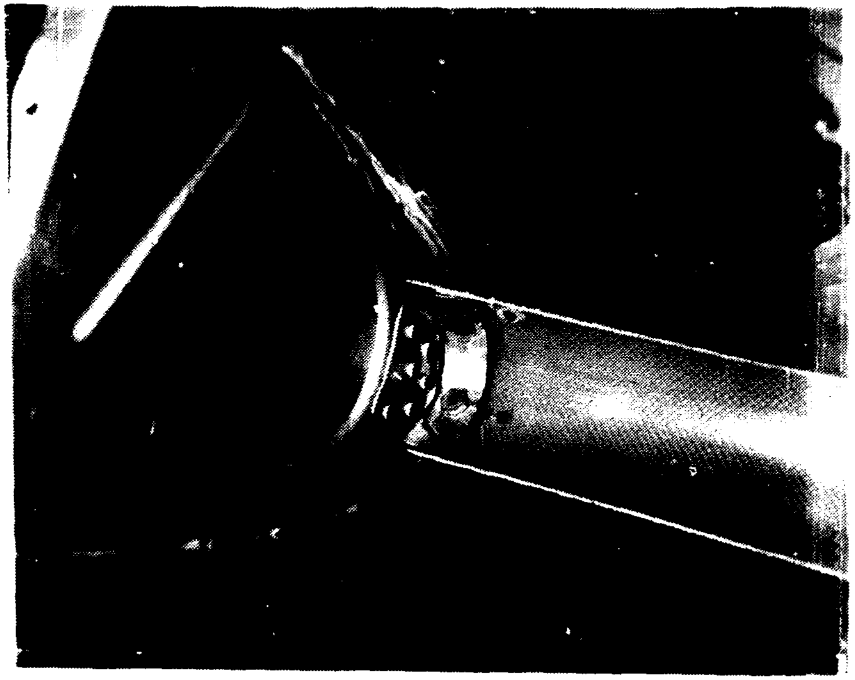

Figure 2-8
Broken Bracket on 0.040-Inch Skin
Model (Bay 3) After 11,700 Impulses

Figure 2-9
Broken Bracket on 0.040
Inch Model (Bay 2).

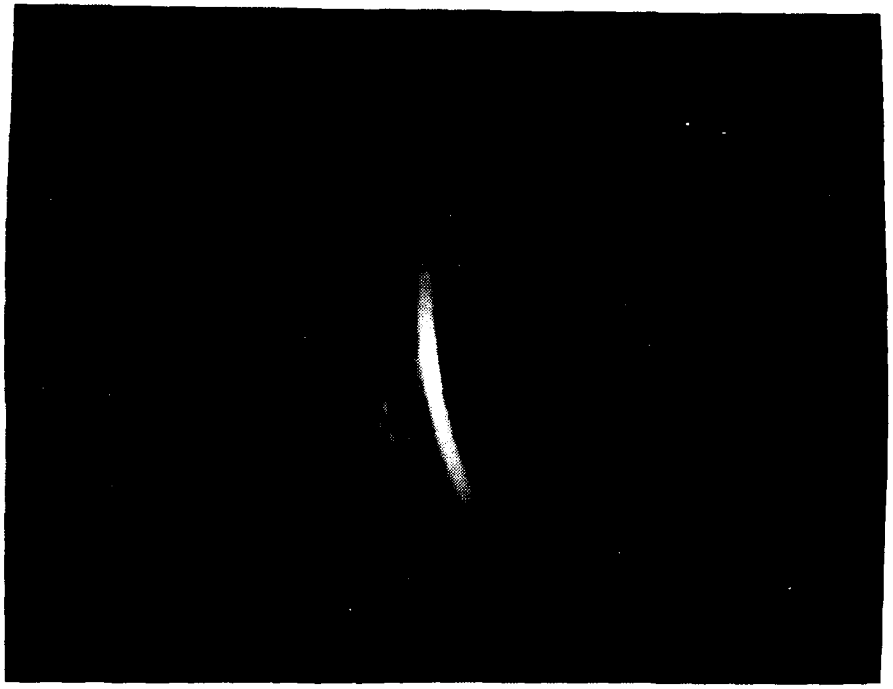

Figure 2-10
Broken Bracket on 0.040
Inch Skin Model (Bay 4)

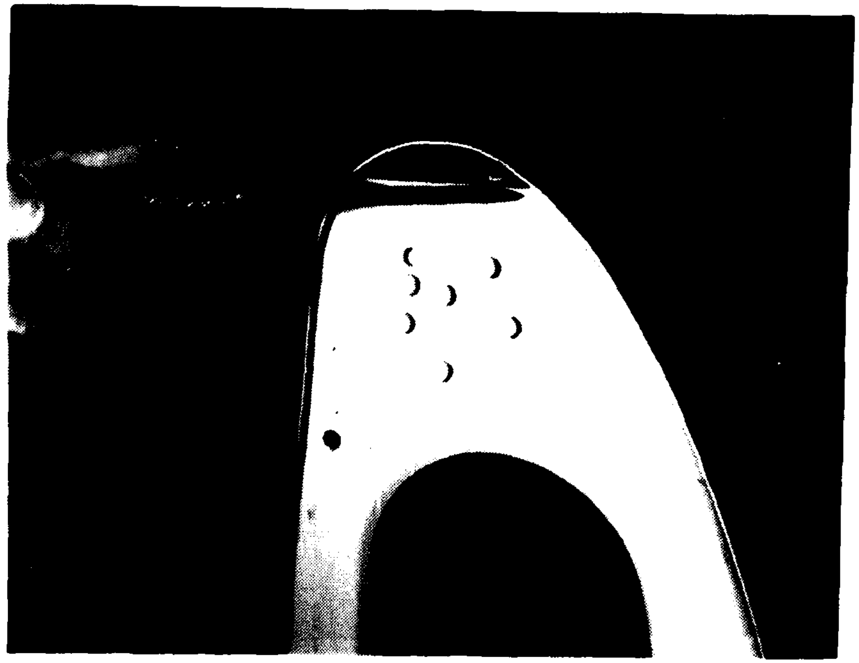

Figure 2-11
Hairline Crack on End Rib
of 0.040 Inch Skin Model

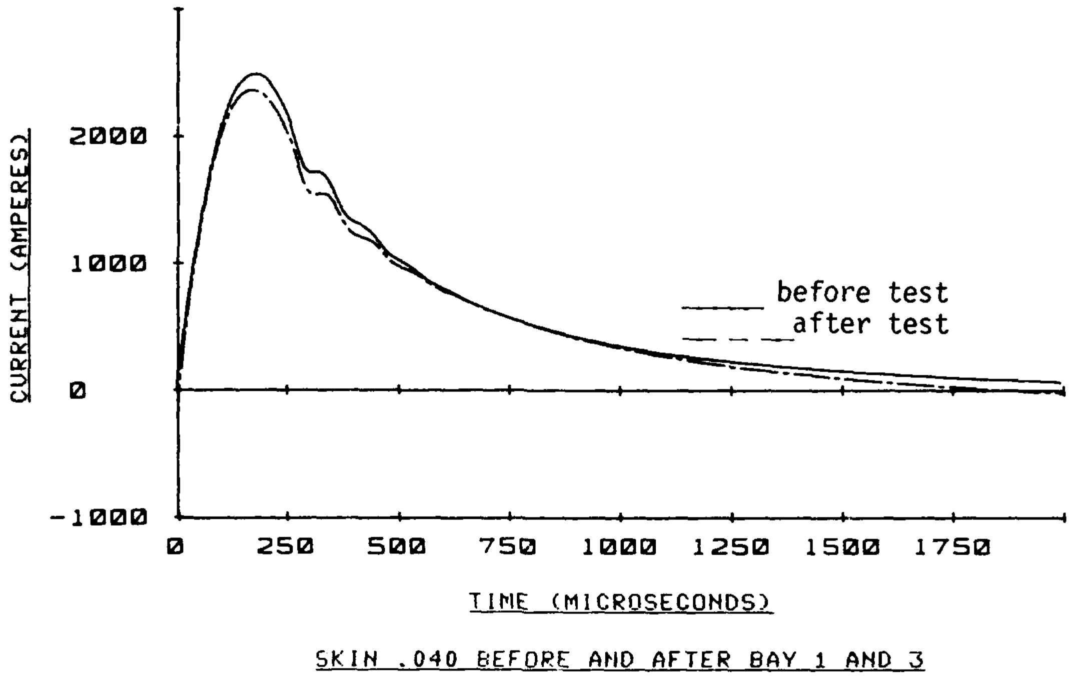

Figure 2-12
Current Traces

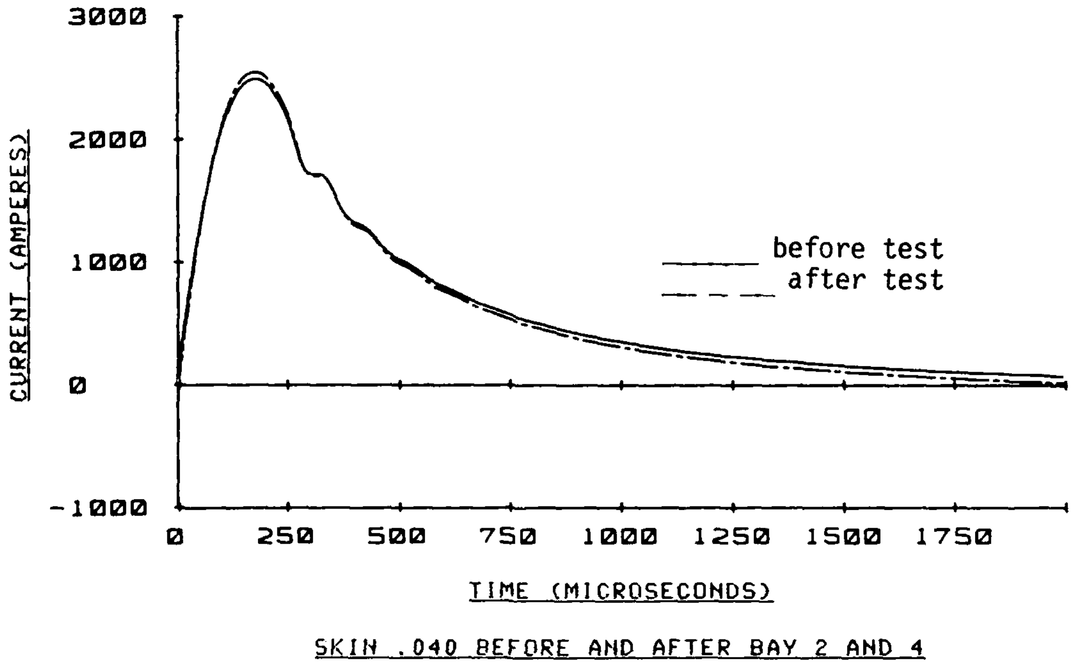

Figure 2-13
Current Traces

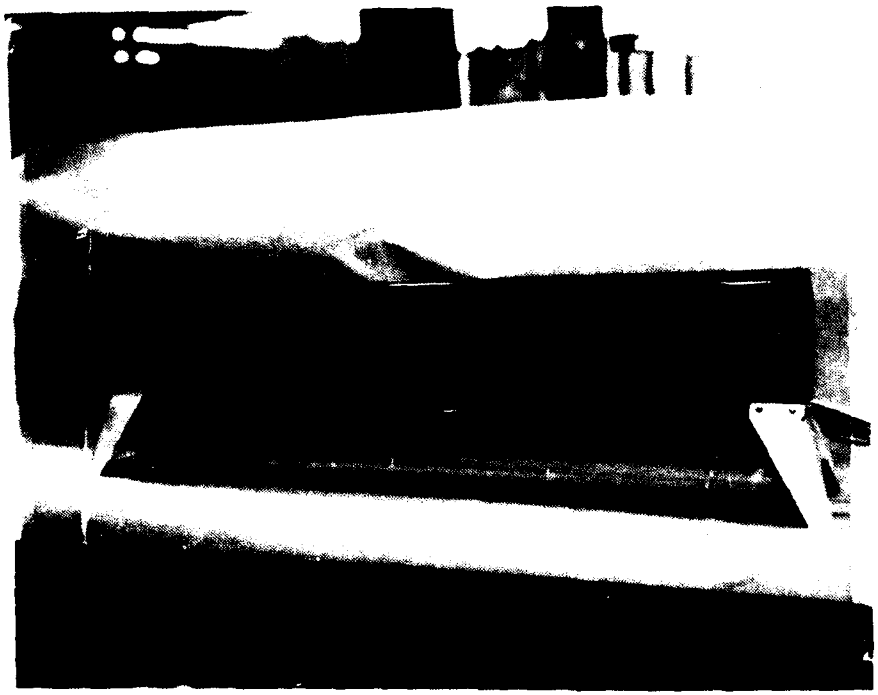

Figure 2-14
Composite Leading Edge Model

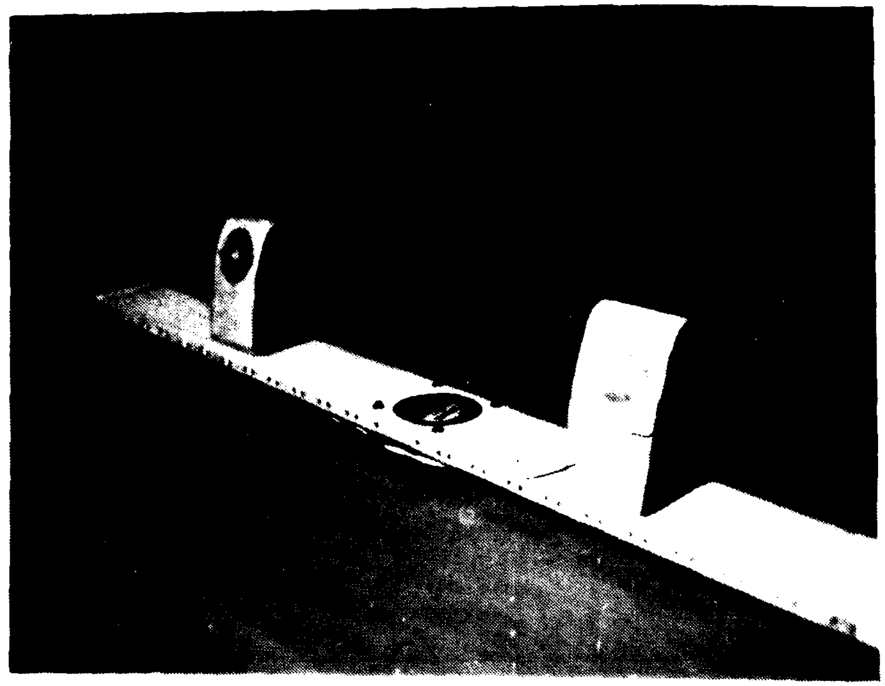

Figure 2-15
Spar and Coil Mounts for
Composite Model

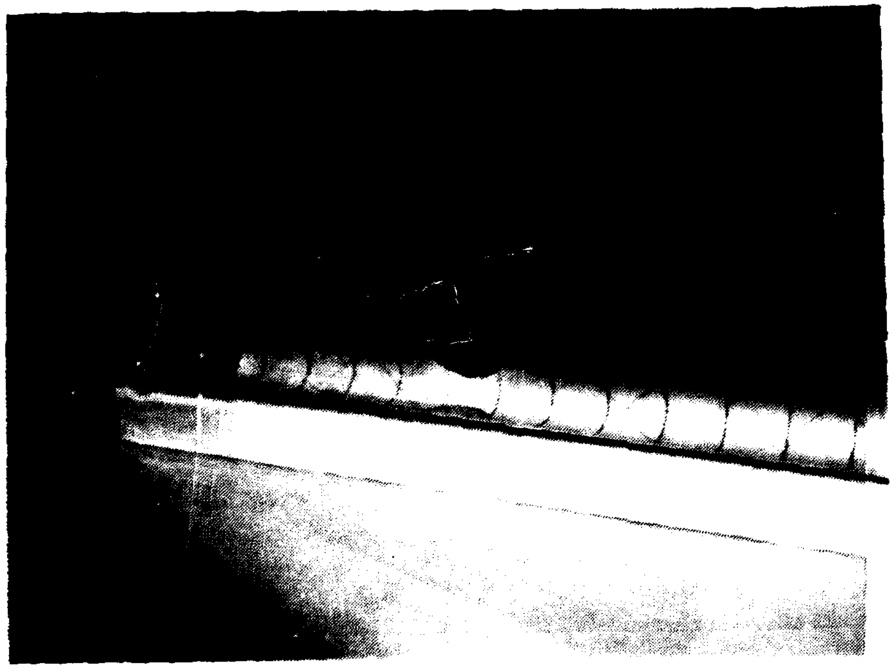

Figure 2-16
Inside View of Composite Model

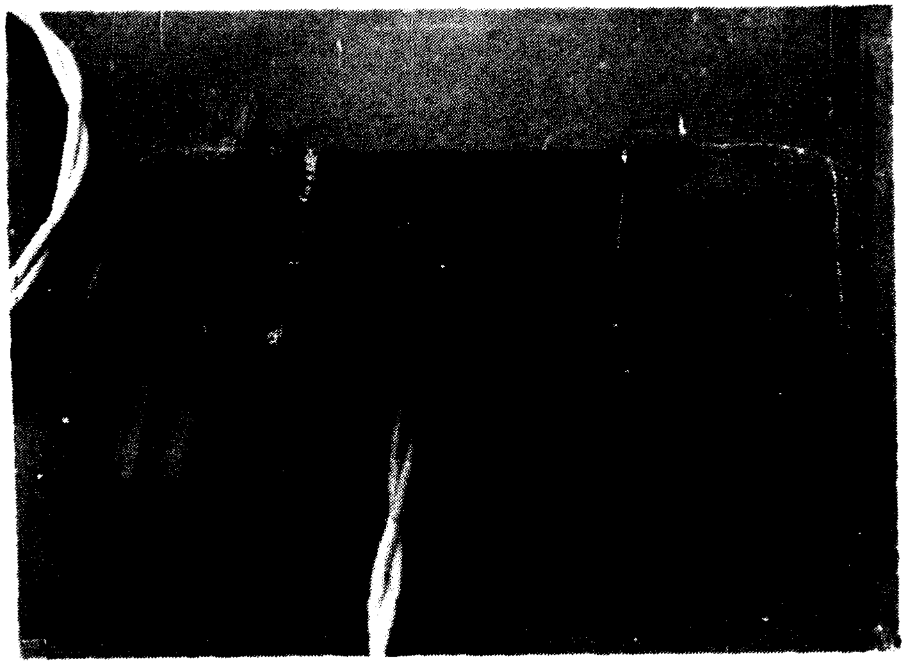

Figure 2-17
Band Aid Coil Mount

Figure 2-18
Band Aid Coil Before Bonding
Over the Doubler

3. ELECTROMAGNETIC INTERFERENCE TESTS

The purpose of the tests was to measure the radiated emissions from the EIDI system installed in a metal wing as compared to those from a similar system installed in a wing of composite (non-metallic) construction. A secondary purpose was to provide a method, for both installations, which allowed radiated emissions to meet the requirements of the applicable specifications.

3.1 PRIOR EXPERIENCE

In 1983, near the start of the EIDI research at WSU, an EMI test of an EIDI system was made by one of the industrial partners, Simmonds-Precision, Engine Systems Division, Norwich, New York. Two coils provided by WSU were mounted against the front wall of a "simulated wing," which was actually a trapezoidal-shaped box. The box was made of 0.032 inch thick aluminum and sat directly on a ground plane. The two coils connected in series were supplied with impulses from capacitors charged at 1500 volts and 395 microfarads (a higher energy than generally used for a thin-skinned aircraft). The maximum energy direction was found to be directly ahead of the wing. The radiated emissions were well within the limits of MIL-STD-461A, notice 3. When one end was removed from the wing, low frequency emissions were near the permissible limits.

Flight tests with the EIDI system gave opportunity to observe any electromagnetic interference. The NASA icing research aircraft, a DeHavilland DHC-6 Twin Otter, was fitted with a 50 inch long wing cuff (or "glove") over the leading edge at about two-thirds semi-span from the fuselage. Four nose coils were placed in the cuff. These were impulsed from 1000 volt, 400 microfarad capacitors, with two coils connected in series. Twenty-one flights were made in which natural ice was removed by EIDI. No EMI problems could be found, even though all flight and data acquisition instruments were turned on and monitored.

Shortly after the NASA flights a Cessna 206 aircraft was tested with EIDI in the right wing and wing strut. This involved eight coil positions, with a single nose coil at each spanwise station. The power-and-sequencing box was in the passenger compartment and the cables were fed into the leading edge directly from the cabin. Fifteen flights were made with either natural icing or ice formed in the wake of a water-spray tanker airplane. There was no evidence of any electromagnetic interference on any of the flights. Equipment installed on all flight included two digital NAV/COMs, ADF, RNAV, autopilot and a weather radar mounted on the right wing. In addition, a LORAN-C was installed for a few flights specifically to test for EMI.

Subsequently, the Cessna 206 was fitted with a complete EIDI system; both wings, struts, and horizontal and vertical tails had coils. A number of flights have been made both with natural and tanker ice, but no EMI effects have been observed by the pilots.

In 1987, another EIDI Consortium member, Boeing Commercial Airplane, Co., Seattle, tested EIDI on a 757 transport aircraft. Two left wing slats, no. 2 (second from wingtip) and no. 5 (inboard) were EIDI-equipped. An unusual electrical design used 3,000 volts with 400 microfarads fired through series connected coils at two stations. Each span station had a single coil. The inboard slat shared an inside-the-wing space with wires for a digital engine control system. For this, some EMI was detected for single-phase power but disappeared when two-phase power was used. Otherwise, no EMI was detected.

3.2 TEST PLAN

The test methodology was that of MIL-STD-462, Notice 2, RE02 (Reference 10) over the frequency range 14 kHz through 150 kHz, above which frequency the test methods of RTCA/DO-160B (Reference 11) Chapter 21, Radiated Emissions for class Z equipment, were used (150 kHz through 1215 MHz). Test specifications were MIL-STD-461C RE02 (Reference 12) for 14 kHz through 150 kHz and RTCA/DO-160B (Reference 11) for the 150 kHz through 1215 MHz portion for test.

The only departure from RTCA/DO-160B Chapter 21 test instructions was the use of a peak detector for all measurements, both narrow and broadband. This was based on MIL-STD-462 which dictates peak detector function for all measurements, and also on the nature of the signal which simply was not detectable at all by a carrier or continuous wave detector.

The power supply was not an aircraft configuration, but was a general purpose laboratory device. Its emissions were not measured, since it was outside the shielded room. To the extent that the voltage levels of the capacitor charges and the energy discharged into the coils are representative of a final configuration de-icing system, the emission levels disclosed herein are valid representations of an actual aircraft installation.

3.3 TEST SITE AND MODELS

3.3.1 Test Site

The testing was performed at the Electromagnetic Interference (EMI) test facility of the Boeing Company in Wichita, Kansas. The general test set up is shown in Figure 3-1. The power supply was installed in a small 10 x 10 foot shield room (Figure 3-2) adjoining the main shield room in which the wing sections were installed and measurements made.

The shield rooms are double wall, zinc clad, steel enclosures. Attenuation is at least 135 dB for electric fields and plane waves, and at least 70dB for magnetic fields. Attenuation to these fields is at least 100 dB from 1 GHz to 10 GHz. The screen rooms are double wall, copper screen, providing sufficient isolation from the laboratory area for the supporting test equipment. All rooms contain benches which serve as ground planes, covered with 0.022 inch copper bonded to the wall approximately every 18 inches. All power entering the shield and screen rooms is fully filtered. For this test, the power supplied to the EIDI power box was 115 VAC, 60 Hz, single phase.

Figure 3-3 shows the EMI receiver/plotter in the screen room. Also in this room was the remote band switching unit shown in Figure 3-4. The two large power supplies sent DC power to the rod antenna. The small power supply (right rear), through the switch box (foreground), controls the octave band impedance matching networks in the antenna base.

Antennas used were a rod antenna (Figure 3-5) for lower frequencies, 14 kHz to 25 MHz, and three higher frequency antennas shown in Figure 3-6; clockwise from top left are biconical (25-200 MHz), logconical (200-1000 MHz) and double ridge guide horn (1-18 GHz).

3.3.2 Test Models

The Electro-Impulse De-Icing (EIDI) system was installed in two wing sections. These were two of the three wing leading edges previously described for the fatigue test (Section 2 of this report). The thicker-skin aluminum model (0.040 inches) and the composite model were used here.

The metal wing leading edge model was from a Cessna 206 aircraft. It was six feet in span and divided by ribs into four 18 inch bays. One EIDI coil was in each bay, supported on a composite beam suspended between two ribs. See Figures 2-1 and 2-2. For the EMI test, two alternate bays had their coils electrically connected in series and were impulsed simultaneously. In accordance with standard EIDI design, the coils were centered in their bays with a small gap between coil and skin. The antenna was centered in front of the model so as to be about equidistant from each coil. The back of the model was enclosed by an aluminum spar which was solid except for a hole through which the power wires entered the model. The ends had ribs which had large lightening holes in them. These were electrically sealed by copper tape for the later tests. In Figure 3-7 the outline of the end hole can be seen under the tape.

The composite model was also the leading edge from a wing. It was made of Kevlar-epoxy with a span of 38 inches. Two coil stations were located at the 1/4 and 3/4 span positions, so that each coil station had 19 inches to de-ice. There were two coils at each span station, located just behind the nose on the upper and lower sides of the leading edge. There were no ribs except for closure ribs added at the ends. Figures 2-14 and 2-15 show the model and the coil support methods. Aluminum doublers were bonded to the skin opposite the coils, as shown in Figure 2-16. For this test, only one coil station was used.

3.4 TEST PROCEDURE

3.4.1 Development of Adjusted Specifications

The method selected for presenting the emissions data was to present the raw uncorrected data from the test and to compare it to the appropriate specification, with the specification adjusted for the appropriate factors. Therefore, in the data plots, raw data appears with an adjusted specification from Ref. 11 or 13 superimposed on the plot. The adjustments were made for antenna factor and cable losses. These were programmed into the EMI Test Receiver for plotting.

3.4.2 General Data Taking Methods

The discharge of a capacitor into a coil is by its very nature an impulsive phenomenon, similar to a delta function. The Fourier spectrum of a delta function is the ultimate broadband signal, with equivalent energy density spread from zero to infinite frequencies. The test procedure had to be tailored to the expected signal, and this differed from the usual EMI measurements in several ways.

(a) Narrowband specifications do not apply to the impulsive signals; only the broadband specifications have significance. Nevertheless, in an attempt to conform with specifications in References 10 and 11, narrowband data were taken for the first test setup, but will not be reported in this report.

(b) Because the EIDI power supply was timed to discharge at 10 second intervals (to avoid overheating the coils), there was no way to get a continuous plot of signal strength vs. frequency in a reasonable amount of time. A dwell time (gate) at each data point was selected that was longer than the discharge period, but nowhere near long enough to guarantee a "hit" at each frequency. The time selected was long enough to get five to ten data points per scan. The peaks of the plotted spikes can be considered to be the envelope of the full plot.

(c) Closely related to the above consideration was the fact that it was not necessary to pick measurement bandwidths to overlap the step size. Normally the measurement bandwidth should be larger than the step size to guarantee that all frequency components are measured. But since only a few frequency components were to be measured, the requirement to overlap steps with bandwidths is superfluous. Therefore, there was no relationship between the bandwidths selected and the frequency step size, other than a general attempt to keep the step size no larger than the bandwidth. The bandwidths selected were within the range suggested by Reference 11, Chapter 21 on radiated emissions, where applicable, and in accord with Reference 10 below 150 kHz.

(d) A passive rod antenna, rather than an active rod, was used to make measurements below 25 MHz. Active rods have lower dynamic range and are easily overloaded by signals with wide bandwidth. Preliminary tests made with an active rod antenna at reduced voltage EIDI discharges indicated that a full voltage impulse would likely saturate or burn out the active antenna electronics.

(e) Peak detection was used for all measurements in accordance with MIL-STD-462 (Ref. 10), but not in accord with RTCA/DO-160B, Chapter 21 (Ref. 11), which specifies carrier or continuous wave detection. Because of the nature of the impulsive signal, the continuous wave detector cannot capture the fast rise/fast decay signature.

3.4.3 Procedure for First Setup

The first test set up was for the purpose of measuring radiated emissions from the metal and composite wing models with no power wire shielding. This is shown in Figure 3-8 for the metal wing and in Figure 3-9 for the composite wing. At upper left the power wires can be seen feeding through the metal bulkhead.

The metal wing was not closed, but had large holes in the end ribs. The wing was raised off the table and thus not grounded to the power supply reference, as it would be for an aircraft installation. The power wires external to the wing were not shielded and were only partially shadowed by the wing model.

Each pair of coil stations were impulsed by the 400 microfarad capacitor charged to 1000 volts. Similarly, the composite wing had unshielded wires, both internal to the model and external to it. The pair of coils at the one span-station was impulsed by a 550 microfarad capacitor charged to 800 volts, with discharges at ten second intervals.

Data were taken over the frequency range from 14 kHz to 1215 MHz in accordance with MIL-STD-461 (Reference 10), and the specification lines adjusted as described above in Section 3.4.1

The emission levels measured from both models were in excess of the specified limits from 14 kHz to 100 MHz, so shielding was called for in the rest of the tests.

3.4.4 Procedure for the Second Setup

The metal wing test setup was altered to seal the ends of the wing, shield the external wiring and ground the wing to the shield room groundplane. Figure 3-10 shows the end sealed with copper tape. Before adding the tape, the non-conductive surface finish was sanded down. Also visible in Figure 3-10 is the L-shaped piece of copper sandwiched between the skin and the spar flange. These surfaces had been prepared by grinding off their non-conductive finish. The other leg of the L bracket can be seen soldered to the groundplane. This was done at both ends of the wing. The L-shaped brackets were about one foot in length.

Shielding of the external wiring was obtained by pulling an overbraid over the twisted wire pair emanating from the bulkhead and feeding into the wing. The shield was terminated to the wing and bulkhead as shown in Figure 3-11. Good electrical contact was insured by sanding away paint. In addition to shielding the wires, they were shaded as much as possible from the measurement antenna by placing the wire on the far side of the groundplane and underneath the raceways at the back of the tables. The overall test setup is shown in Figure 3-12. The metal wing is in the foreground and the composite wing in the left background.

For the composite wing model, the wires inside the model, as well as those external to it, had to be shielded. This was required since the composite material is almost perfectly transparent to the emissions. The wiring shield had to be brought as close as possible to the coil, and the end of the shield must provide a closed end. This was done by adding a small metal plate to the back of the coil mount and terminating the shield against the plate. This still left about three inches of unshielded wire inside the coil mount.

An additional shielding was found to reduce emissions substantially. A wire was run from the metal plate on the coil mount to each doubler. The wire was soldered to the doubler, thus grounding it and shielding the coil itself.

Data were again taken over the emission frequency range from 14 kHz to 1215 MHz in accordance with Reference 3-1 and plotted against adjusted specification lines.

The metal wing model coils were again impulsed at ten second intervals from the 400 microfarad capacitors charged to 1,000 volts. The composite wing model coils were supplied from 550 microfarad capacitors charged to 800 volts.

3.4.5 Procedure For the Third Setup

To demonstrate the effect of unshielded lead wires, the metal wing model had the overbraid removed from its external wires. These wires were then placed in front of the wing so that they were not shadowed in any way. However, the wing remained grounded and sealed. This is illustrated in Figure 3-13 and 3-14.

The composite wing model was altered simply by disconnecting the wire to the doubler. Thus the lead wires remained shielded, but the doubler was no longer grounded.

Each of the models was then impulsed at the same power levels used for the first and second setups.

3.5 RESULTS

The results are presented in plots of emissions in decibels versus frequency in MHz (Figures 3-15 to 3-20 in the Appendix). The spikes represent the impulses and an envelope of spikes gives the emissions curve.

For setup no. 1, the emitted radiations exceeded the permissible limits for both the aluminum and composite models. This can be seen in Figures 3-15c through 3-15h for the aluminum model, covering 25 to 150 MHz. Figure 3-15i is a repeat of 3-15h and illustrates the difference due to selective frequency test points. Figures 3-15j and k show the drop in emissions with increasing frequency up to 1,000 MHz's. For the composite model, Figures 16c through 16h show exceedance for the same frequency range as for the metal model. (Figure i again repeats h.) As with the metal wing, emissions are below acceptable levels from 200 to 1,000 MHz. Composite model emissions were only slightly greater for limited frequencies (e.g., 30 to 200 MHz). The similarities between the two models were an indication that the major part of the radiation was coming from the unshielded lead wires running from the room bulkhead to the model. The second setup made changes to test this hypothesis.

Sealing the ends of the aluminum model, grounding the wing and shielding the exposed wires led to the results seen in Figures 3-17a though 3-17f. The emissions are scarcely discernible from the background noise. Plots for frequencies above 25 MHz are omitted since they resembled 3-17f.

The no. 2 setup for the composite model had shielded wires and grounded doublers. Figures 3-18a through e show the results. While greatly reduced from the first setup, the emissions from the composite model are greater than from the aluminum model, and some spikes equal or exceed the limits. Considering that only discrete frequencies were tested, one must assume that the emissions probably exceed the limits at some frequencies which were skipped over. Results for frequencies above 200 MHz had negligible emissions spikes and plots are omitted.

In the third setup, only the wing was sealed, but the exterior lead wires were exposed. Comparing Figures 3-19a through 3-19d with the first metal wing setup plots for the same frequencies (Figures 3-15d through 3-15g) shows very small differences. This indicates that the exterior wires were the main radiation sources in setup number one.

For the composite model in the third setup, the emissions exceeded the limits in the low frequency range shown in Figure 3-20. For higher frequencies the results of the second setup are essentially repeated. In the 2 to 5 MHz frequency range, grounding the doublers significantly reduced the emissions.

3.6 CONCLUSIONS

The test results indicate that an EIDI system in an aluminum wing would cause negligible electromagnetic interference outside the wing if the exposed wires were inside the skin or shielded. The wing would automatically be grounded. If space inside the wing is shared with other electronic system wires, shielding of one of them is probably required. This is in accord with previous aircraft experience.

If the wing is made from non-metallic composite materials, the EMI is a greater problem. The shielding of wires must be complete. Also, the emissions exceed specifications unless the doublers are grounded. Even then, compliance with the regulations is marginal at best. A complete geometric survey of emissions was not made, so there may be some directions in which EMI is clearly unacceptable for composite wings. A more complete shielding, perhaps with a light metal foil, around the coil area may insure emissions containment.

At the end of the EMI tests, with the aluminum model having unshielded leads, a radio interference test was tried. The EMI receiver was tuned to a local radio station at 1410 kHz. The EMI antenna was placed in the shield room with the door closed enough to permit only a minimal radio signal.

EIDI operation at the same time did not result in any audible or measured response for continuous wave detector setting. The explanation is that the power density of this broadband signal is low enough that it does not disturb small bandwidth reception. The frequency and type of broadcast was chosen because it is close to the characteristics of high frequency reception in aircraft.

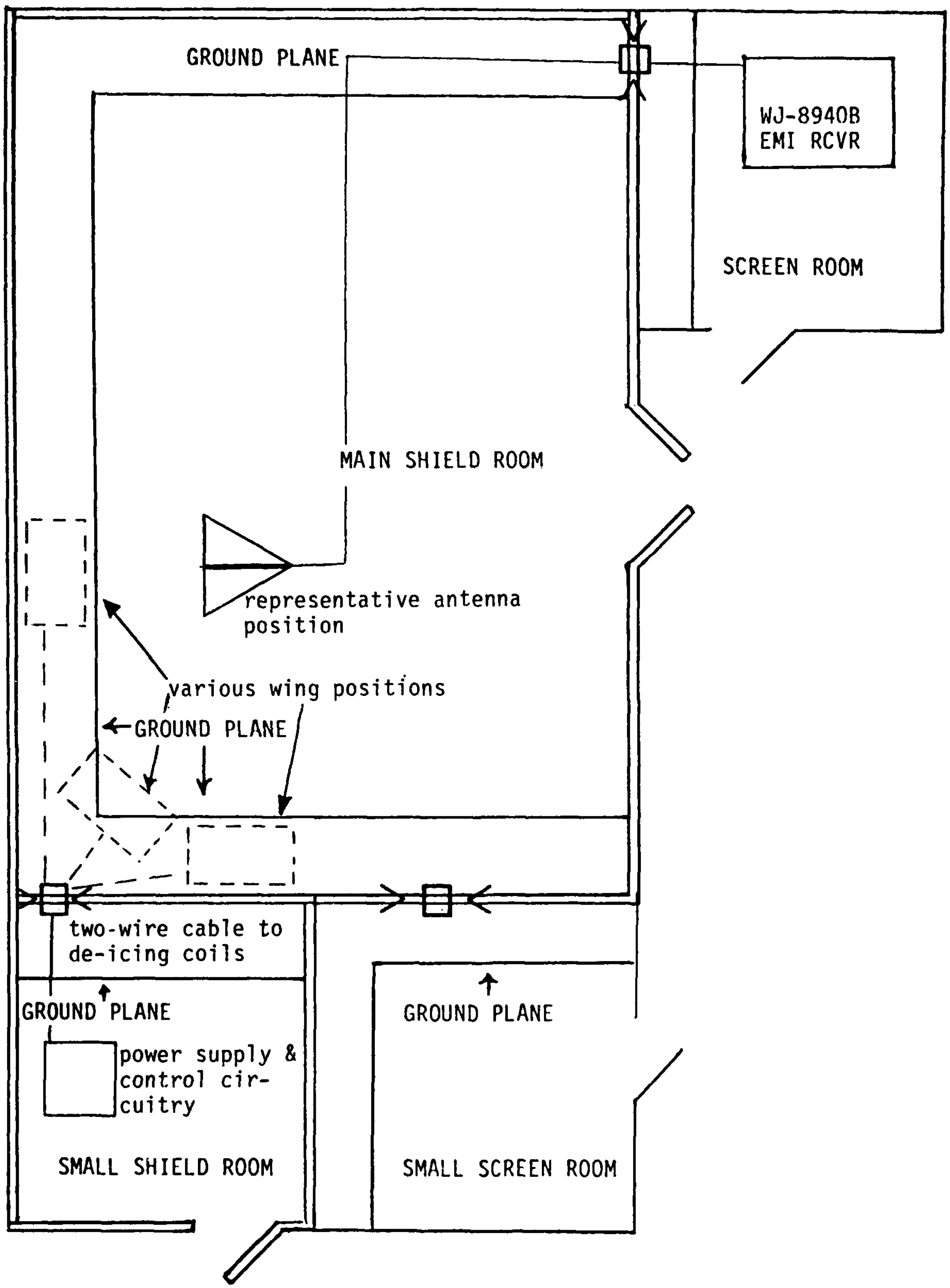

Figure 3-1
EMI Test Layout

Figure 3-2
Small Shield Room. From Left to Right are Power Supply (in large wooden box), Control Unit, Timer and Power Wires Leading into Main Shield Room.

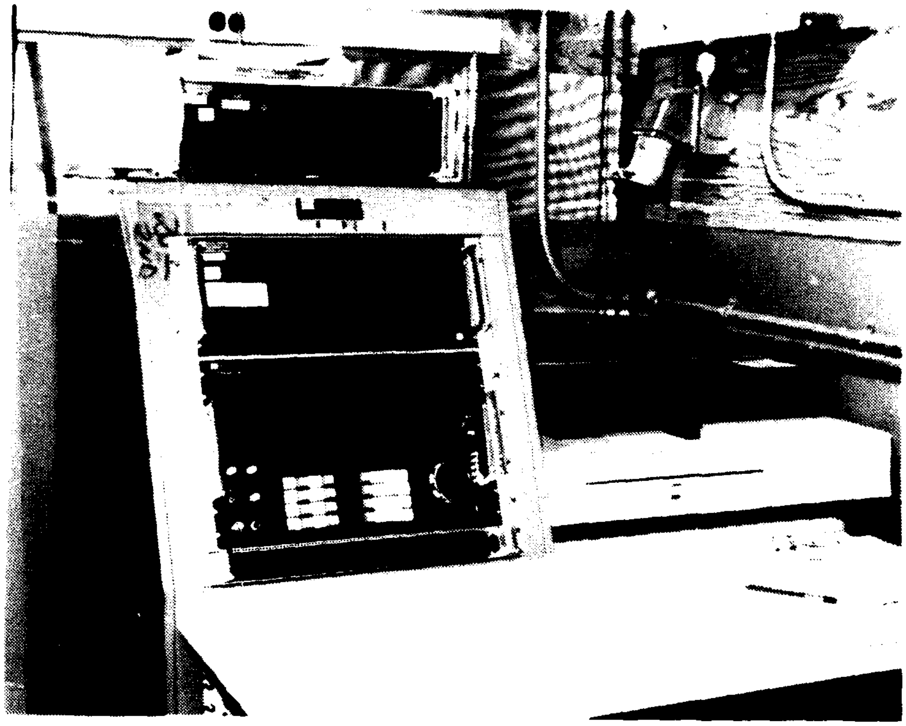

Figure 3-3
EMI Receiver in the Screen Room

Figure 3-4
Power Supply and Band Switching
Unit for the Rod Antenna

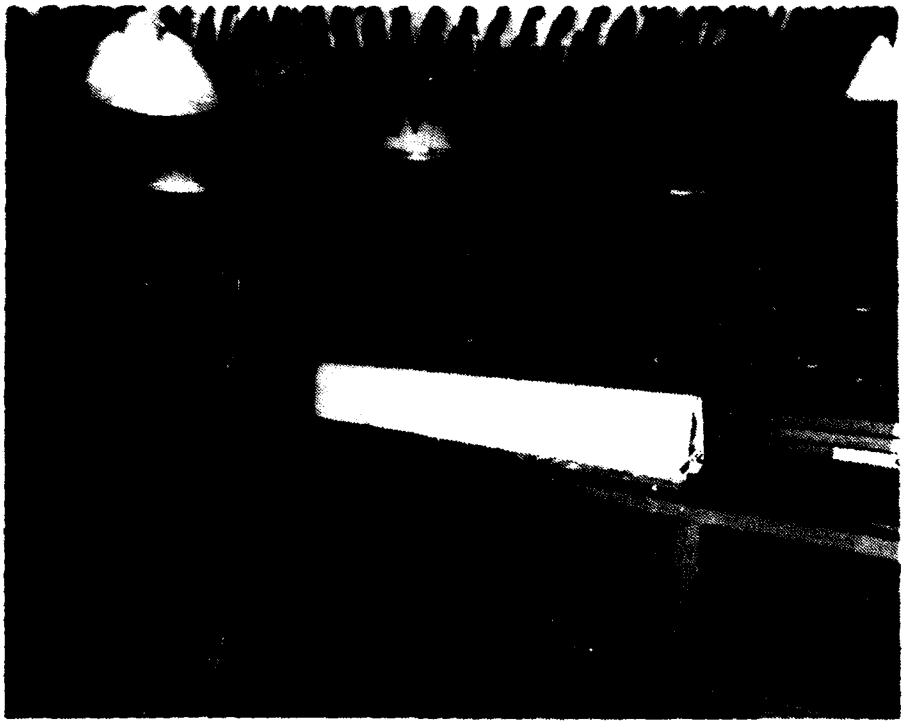

Figure 3-5
Rod Antenna

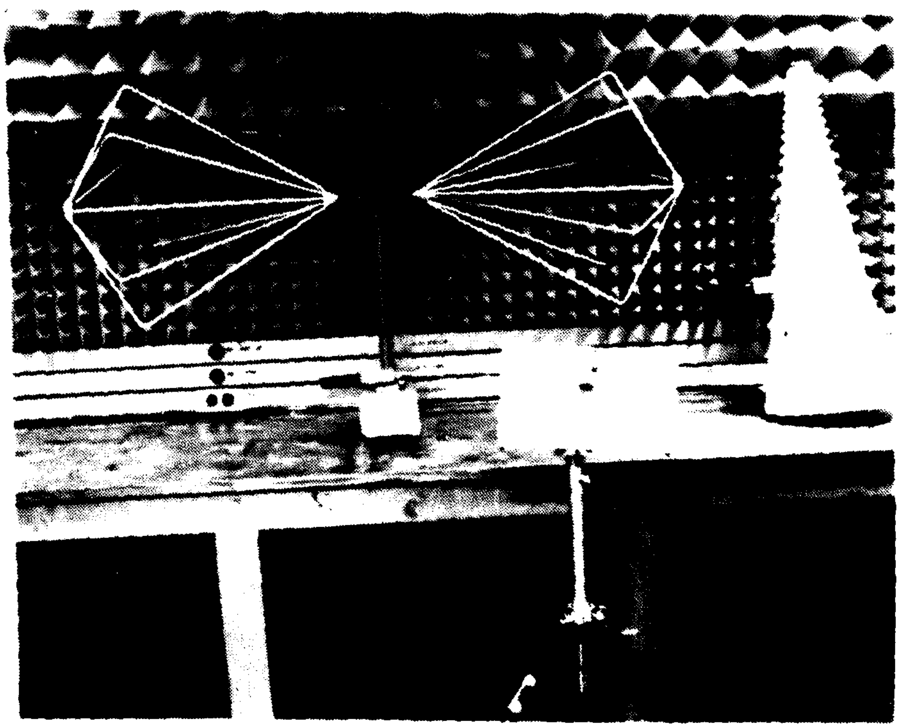

Figure 3-6
High Frequency Antennas

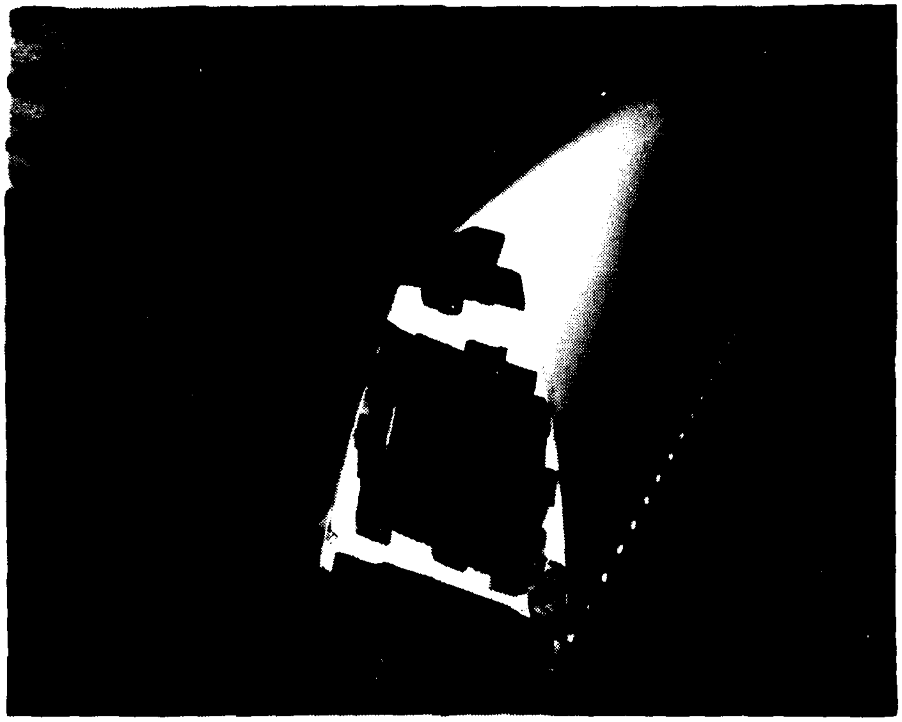

Figure 3-7
Rib at End of the Metal Model
Sealed by Copper Tape

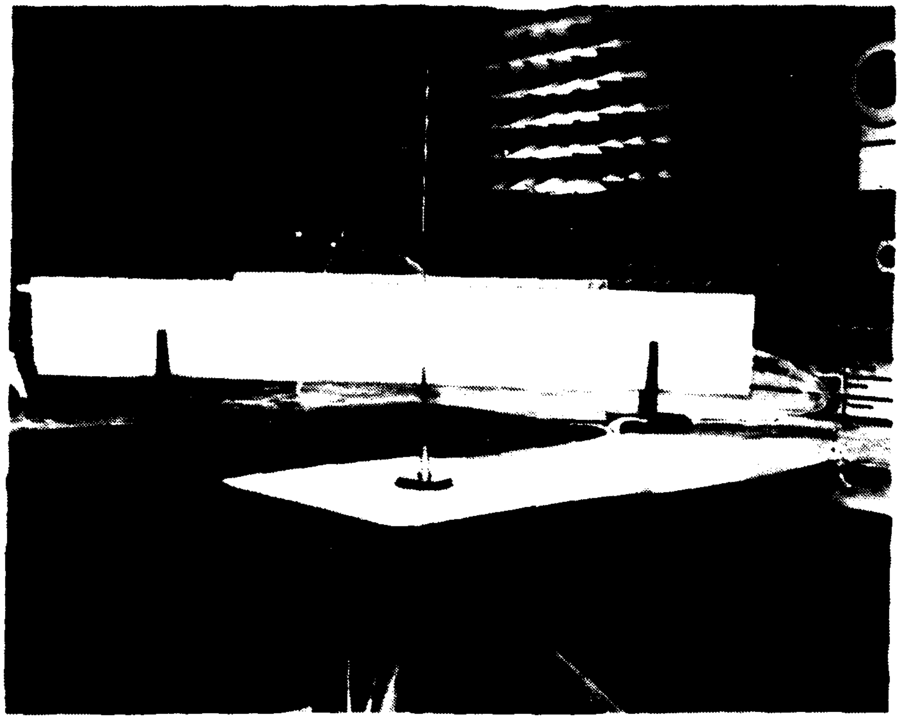

Figure 3-8
First Test Setup for Metal Wing

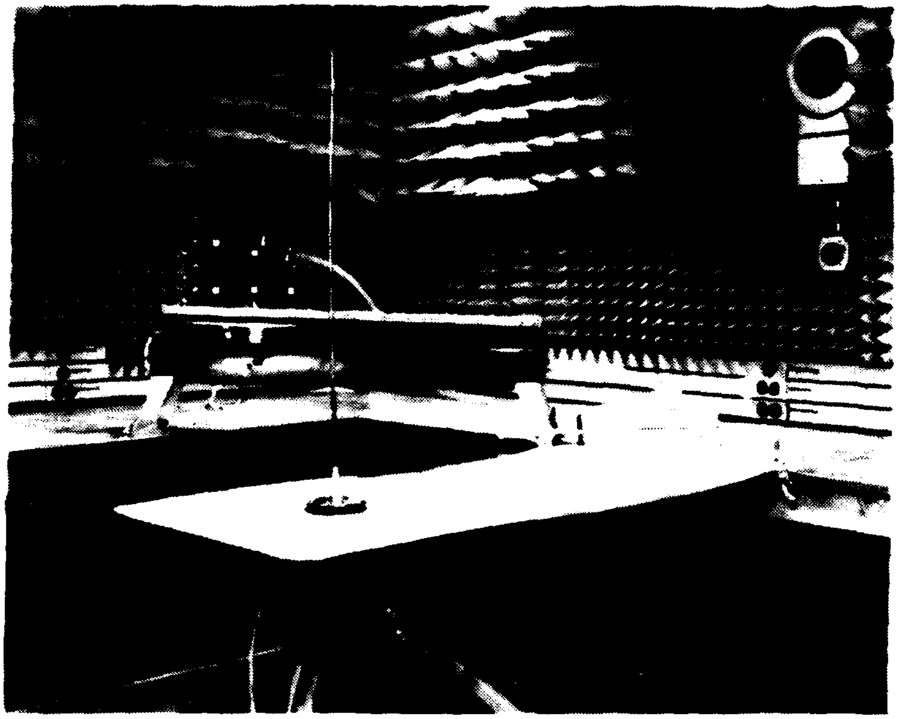

Figure 3-9
First Test Setup for Composite Wing

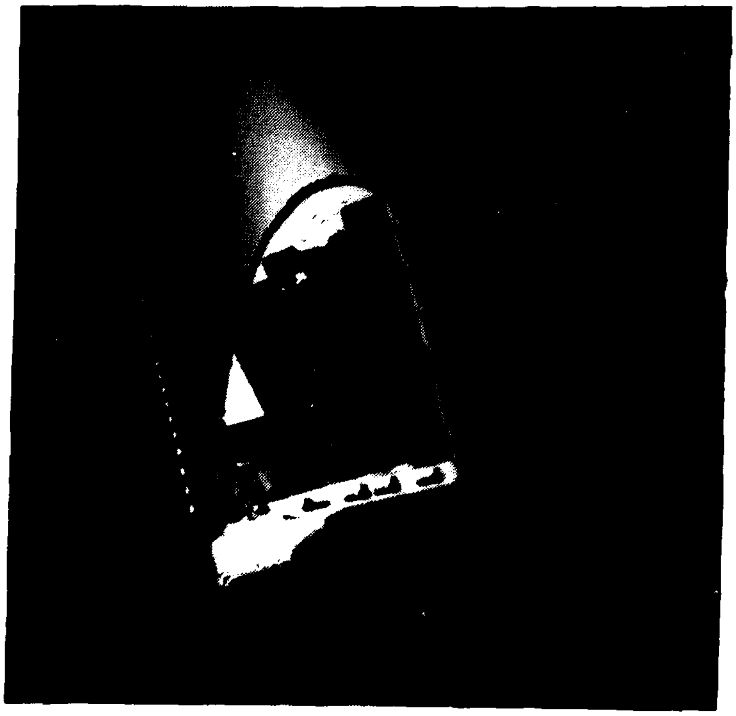

Figure 3-10
Second Test Setup for Metal Wing

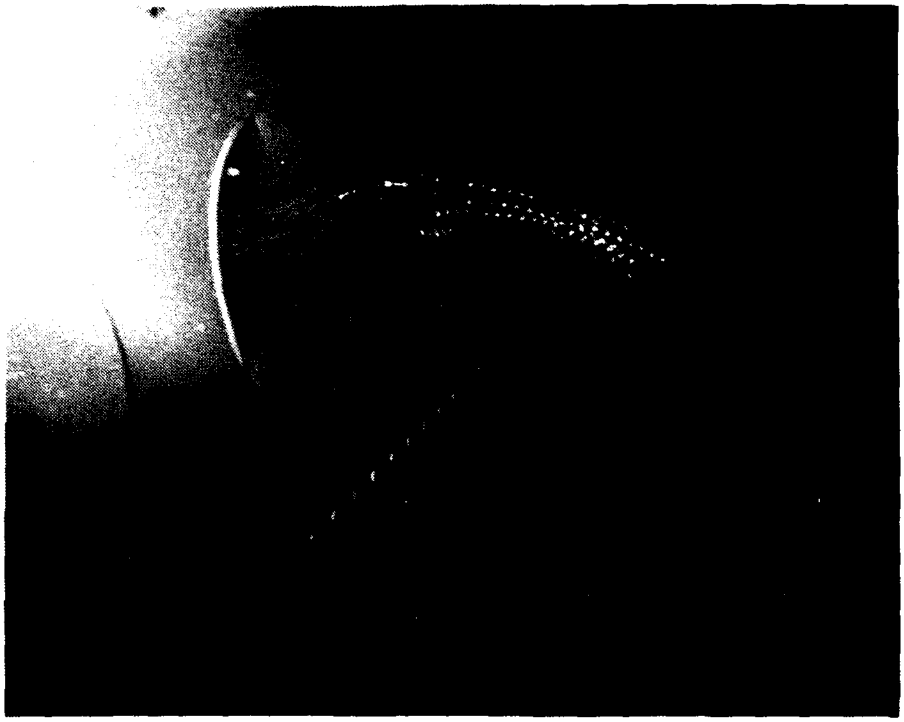

Figure 3-11
Shielded Wires Coming Out of the
Model for Second Test Set

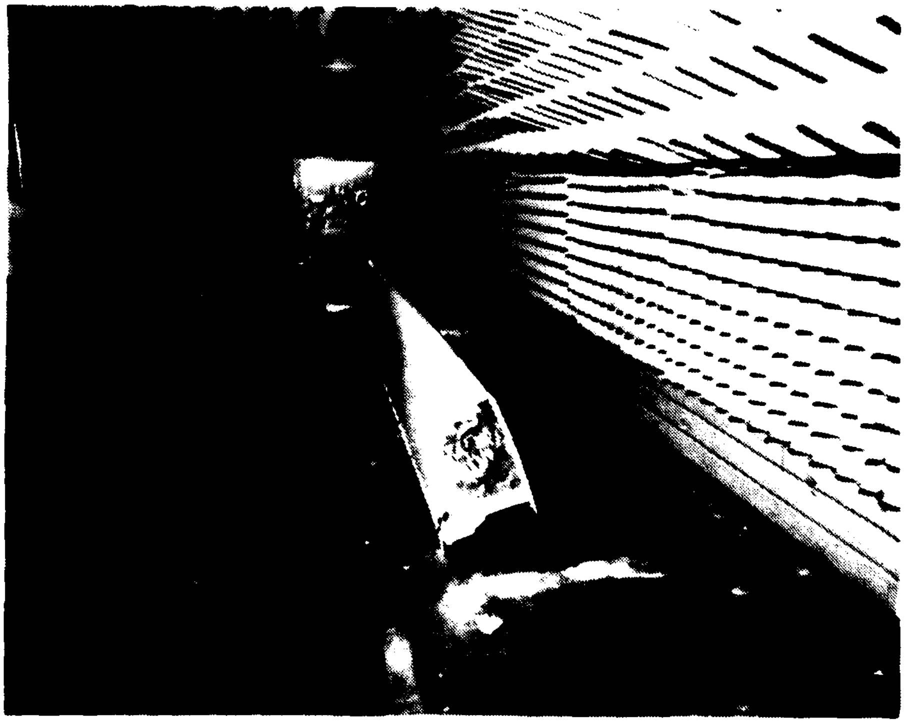

Figure 3-12
Setup for Second Test Set

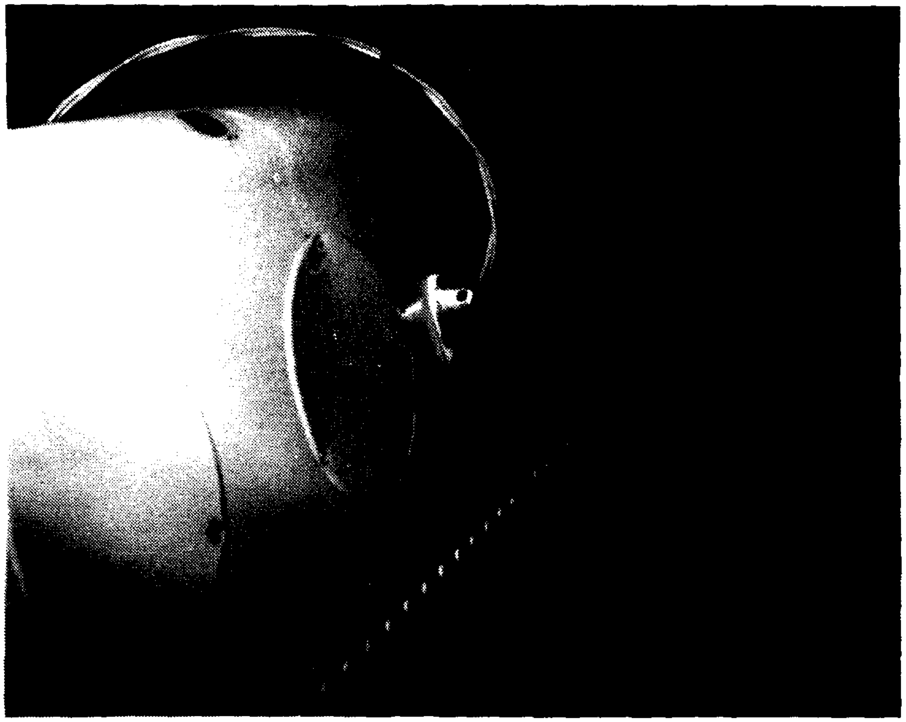

Figure 3-13
Third Test Setup Power Wire Unshielded

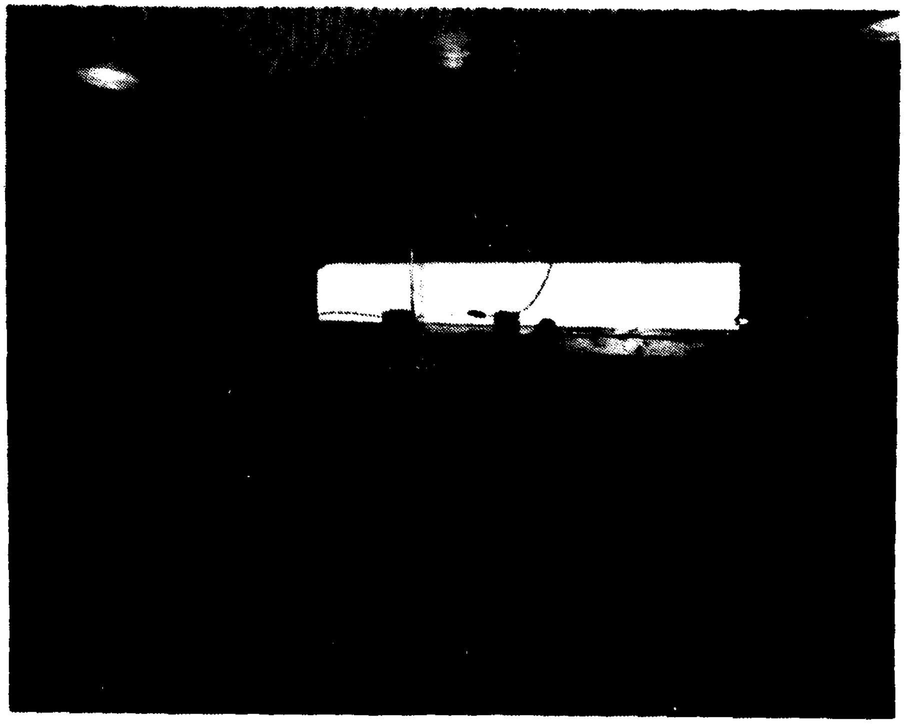

Figure 3-14
Third Test Setup

4. REFERENCES

1. Schrag, R.L. and Zumwalt, G.W., "Electro-Impulse De-Icing: Concept and Electrodynamic Studies," AIAA 22nd Aerospace Sciences Meeting, Reno, NV, Jan. 9-12, 1984, Paper No. 84-0021.

2. Bernhart, W.D. and Zumwalt, G.W., "Electro-Impulse De-Icing: Structural Dynamic Studies, Icing Tunnel Tests and Applications," AIAA 22nd Aerospace Sciences Meeting, Reno, NV, Jan. 9-12, 1984, AIAA Paper No. 84-0022.

3. Zumwalt, G.W., "Icing Tunnel Tests of Electro-Impulse De-Icing of an Engine Inlet and High-Speed Wings," AIAA 23rd Aerospace Sciences Meeting, Reno, Nevada, January 14-17, 1985, AIAA Paper No. 85-0466.

4. Zumwalt, G.W. and Mueller, A.A., "Flights and Wind Tunnel Tests of an Electro-Impulse De-Icing System," AIAA/NASA General Aviation Technology Conference, Hampton, VA, July 10-12, 1984, AIAA Paper No. 84-2234.

5. Zumwalt, G.W., "Electromagnetic Impulse De-Icing Applied to a Nacelle Nose Lip," AIAA/SAE/ASME/ASEE 21st Joint Propulsion Conference," Monterey, CA, July 8-10, 1985, AIAA Paper No. 85-1118.

6. Zumwalt, G.W. and Friedberg, R.A., "Designing an Electro-Impulse De-Icing System," AIAA 24th Aerospace Sciences Meeting, Reno, NV, Jan. 6-9, 1986, AIAA Paper No. 86-0545.

7. Bernhart, W.D. and Schrag, R.L., "Electro-Impulse De-Icing: Electrodynamic Solution by Discrete Elements," AIAA 26th Aerospace Sciences Meeting, Reno, NV, Jan. 11-14, 1988, AIAA Paper No. 88-0018.

8. Zumwalt, G.W., Schrag, R.L., Bernhart, W.D. and Friedberg, R.A., "Analysis and Tests for Design of an Electro-Impulse De-Icing System," NASA CR-174919, May 1987.

9. Zumwalt, G.W., "Electro-Impulse De-Icing - A Status Report," AIAA 26th Aerospace Sciences Meeting, Reno, NV, Jan. 11-14, 1988, AIAA Paper No. 88-0019.

10. "EMI Characteristics, Measurement of," MIL-STD-462, Notice 2, May 1970

11. "Environmental Conditions and Test Procedures for Airborne Equipment," RTCA/DO-160B, July 1984

12. "Electromagnetic Emissions and Susceptibility Requirements for the Control of EMI," MIL-STD-461C, August 1986

APPENDIX

PLOTS OF EMISSIONS VERSES FREQUENCY

Figures 3-15a through k. Metal Model; First Test Setup.

Figures 3-16a through k. Composite Models; First Test Setup.

Figures 3-17a through f. Metal Model; Second Test Setup.

Figures 3-18a through e. Composite Model; Second Test Setup.

Figures 3-19a through d. Metal Model; Third Test Setup.

Figure 3-20. Composite Model; Third Test Setup.

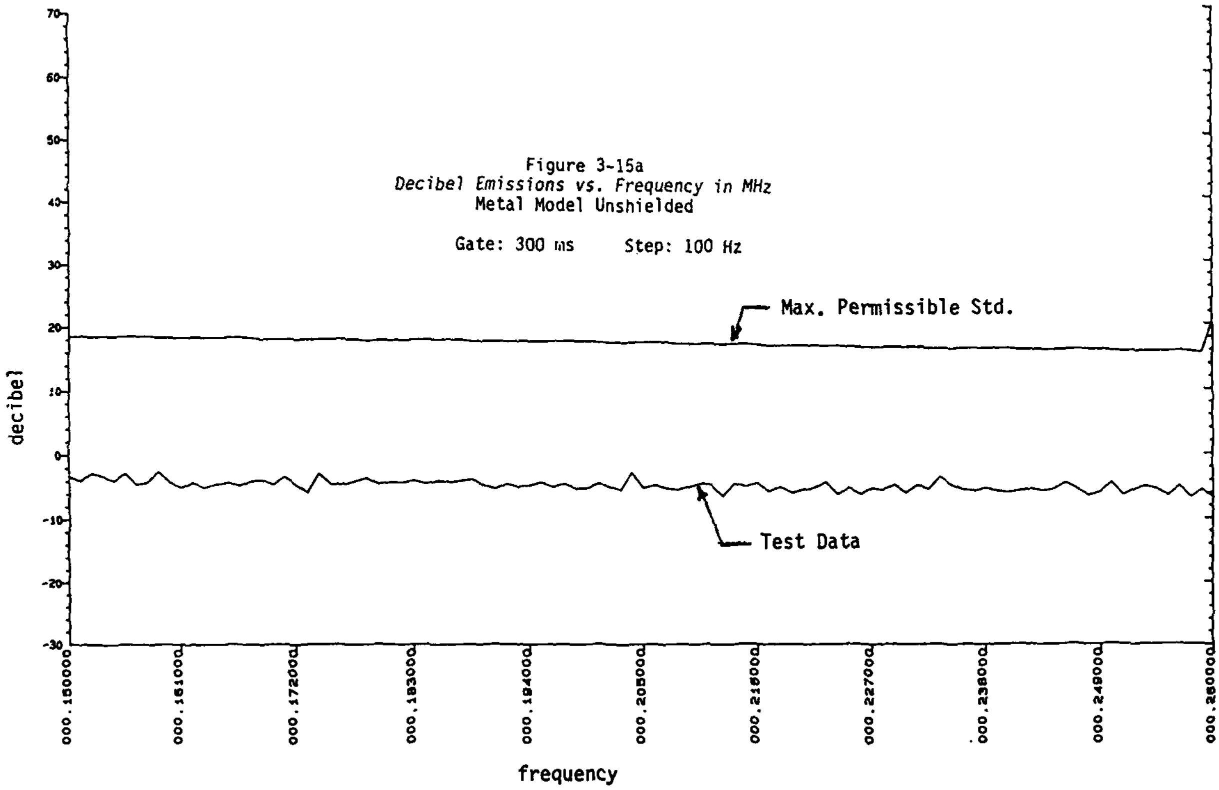
Figure 3-15a
Decibel Emissions vs. Frequency in MHz
Metal Model Unshielded
Gate: 300 ms Step: 100 Hz
Max. Permissible Std.
Test Data
decibel
frequency
70
60
50
40
30
20
10
0
-10
-20
-30
000.150000
000.161000
000.172000
000.183000
000.194000
000.205000
000.216000
000.227000
000.238000
000.249000
000.260000

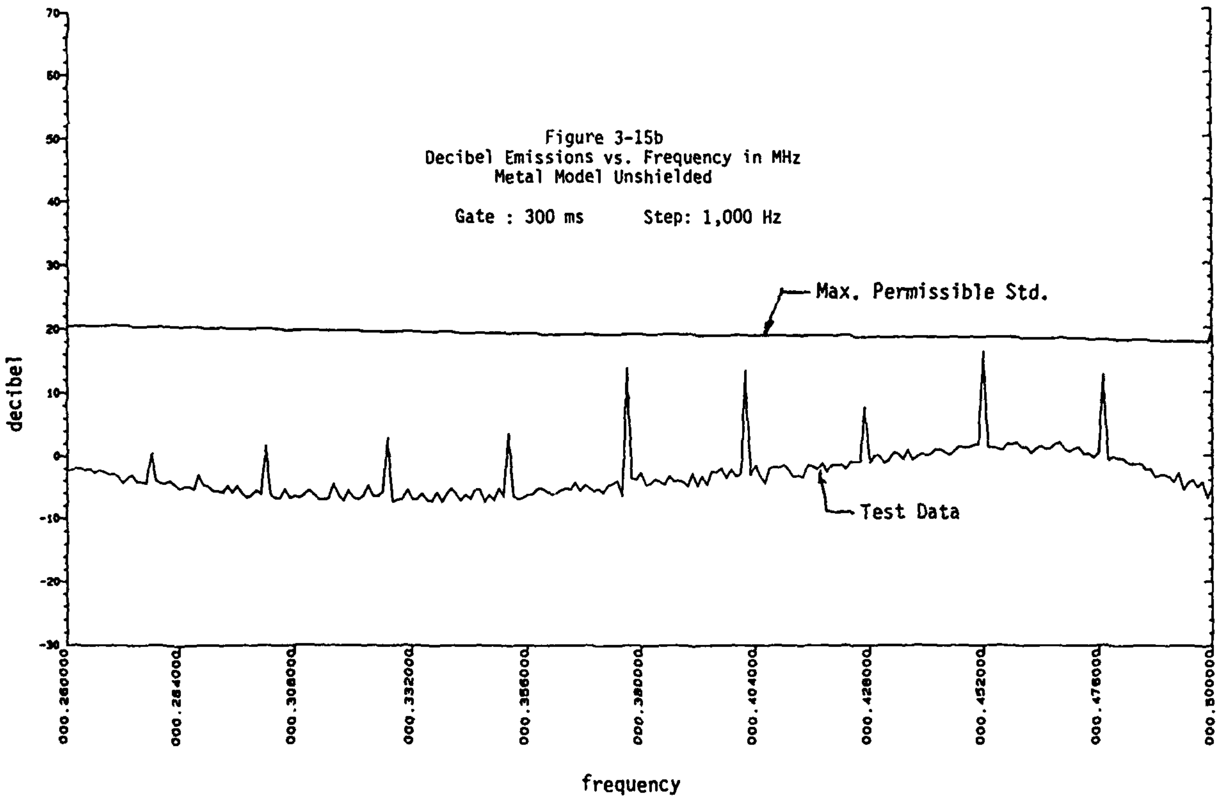
Figure 3-15b
Decibel Emissions vs. Frequency in MHz
Metal Model Unshielded
Gate : 300 ms Step: 1,000 Hz
Max. Permissible Std.
Test Data
decibel
frequency
70
60
50
40
30
20
10
0
-10
-20
-30
000.260000
000.284000
000.308000
000.332000
000.356000
000.380000
000.404000
000.428000
000.452000
000.476000
000.500000

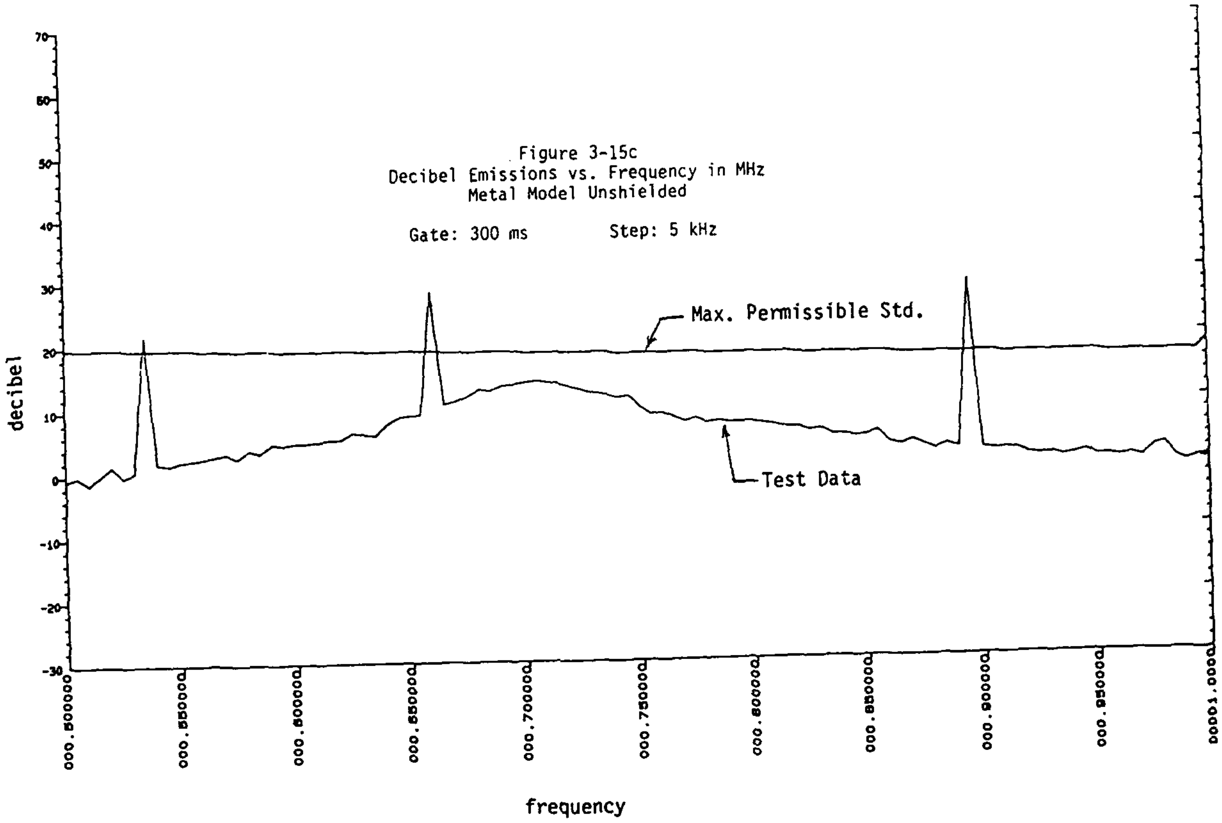

Figure 3-15c
Decibel Emissions vs. Frequency in MHz
Metal Model Unshielded
Gate: 300 ms
Step: 5 kHz
Max. Permissible Std.
Test Data
decibel
70
60
50
40
30
20
10
0
-10
-20
-30
000.500000
000.550000
000.600000
000.650000
000.700000
000.750000
000.800000
000.850000
000.900000
000.950000
00001.0000
frequency

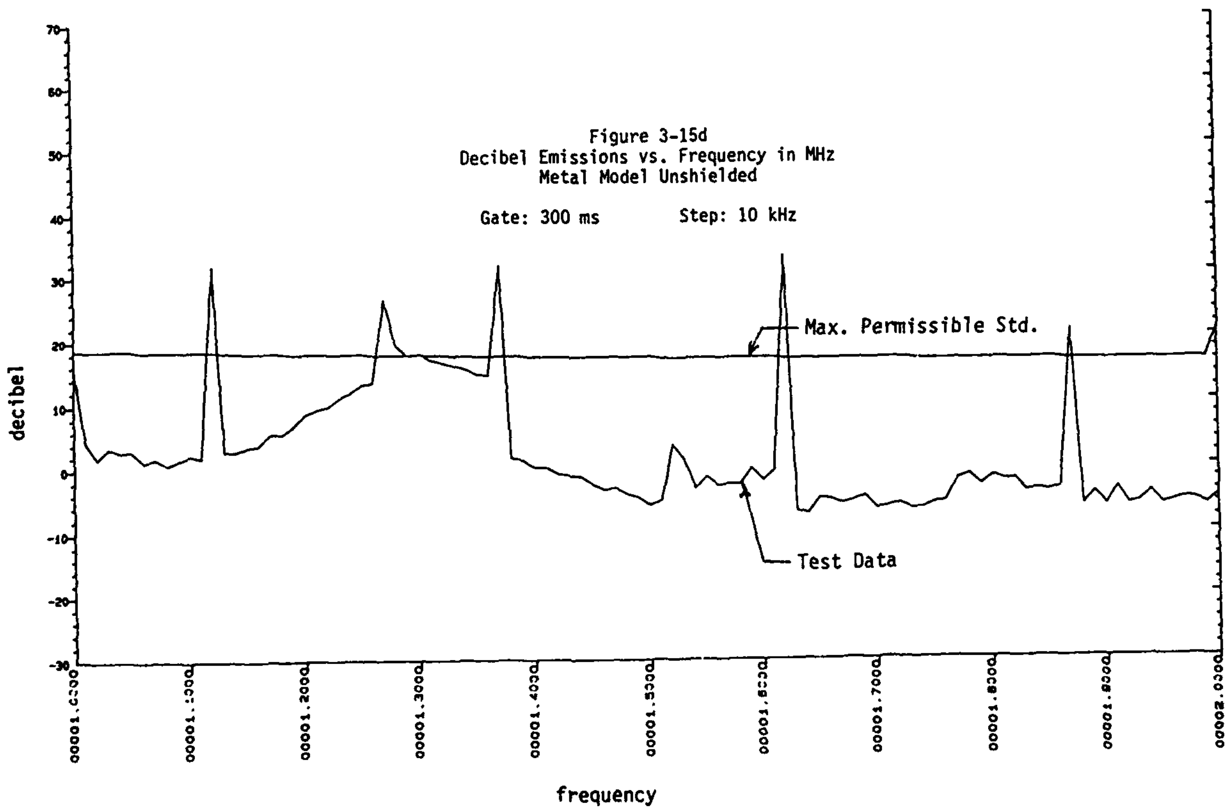

Figure 3-15d
Decibel Emissions vs. Frequency in MHz
Metal Model Unshielded
Gate: 300 ms
Step: 10 kHz
Max. Permissible Std.
Test Data
decibel
70
60
50
40
30
20
10
0
-10
-20
-30
00001.0000
00001.1000
00001.2000
00001.3000
00001.4000
00001.5000
00001.6000
00001.7000
00001.8000
00001.9000
00002.0000
frequency

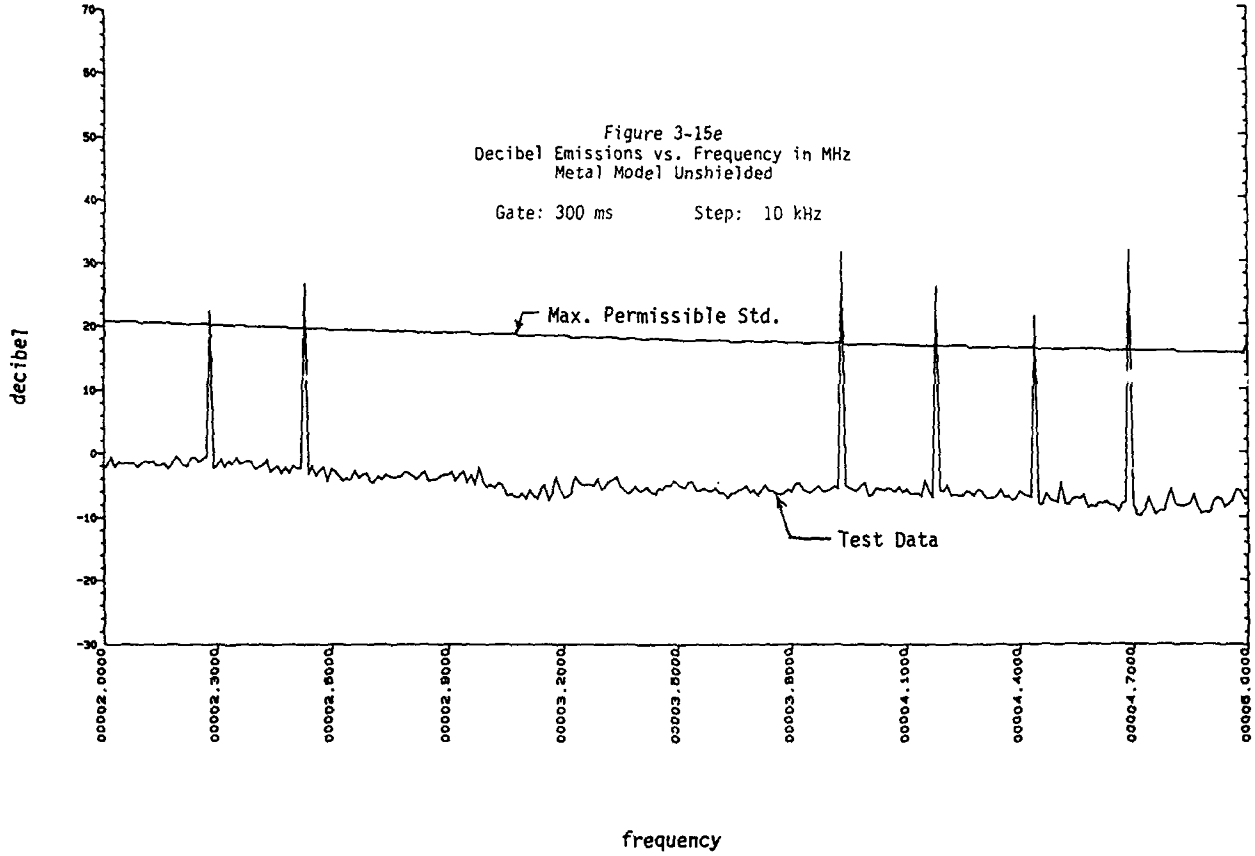

Figure 3-15e
Decibel Emissions vs. Frequency in MHz
Metal Model Unshielded
Gate: 300 ms
Step: 10 kHz
Max. Permissible Std.
Test Data
decibel
70
60
50
40
30
20
10
0
-10
-20
-30
00002.0000
00002.3000
00002.6000
00002.9000
00003.2000
00003.5000
00003.8000
00004.1000
00004.4000
00004.7000
00005.0000
frequency

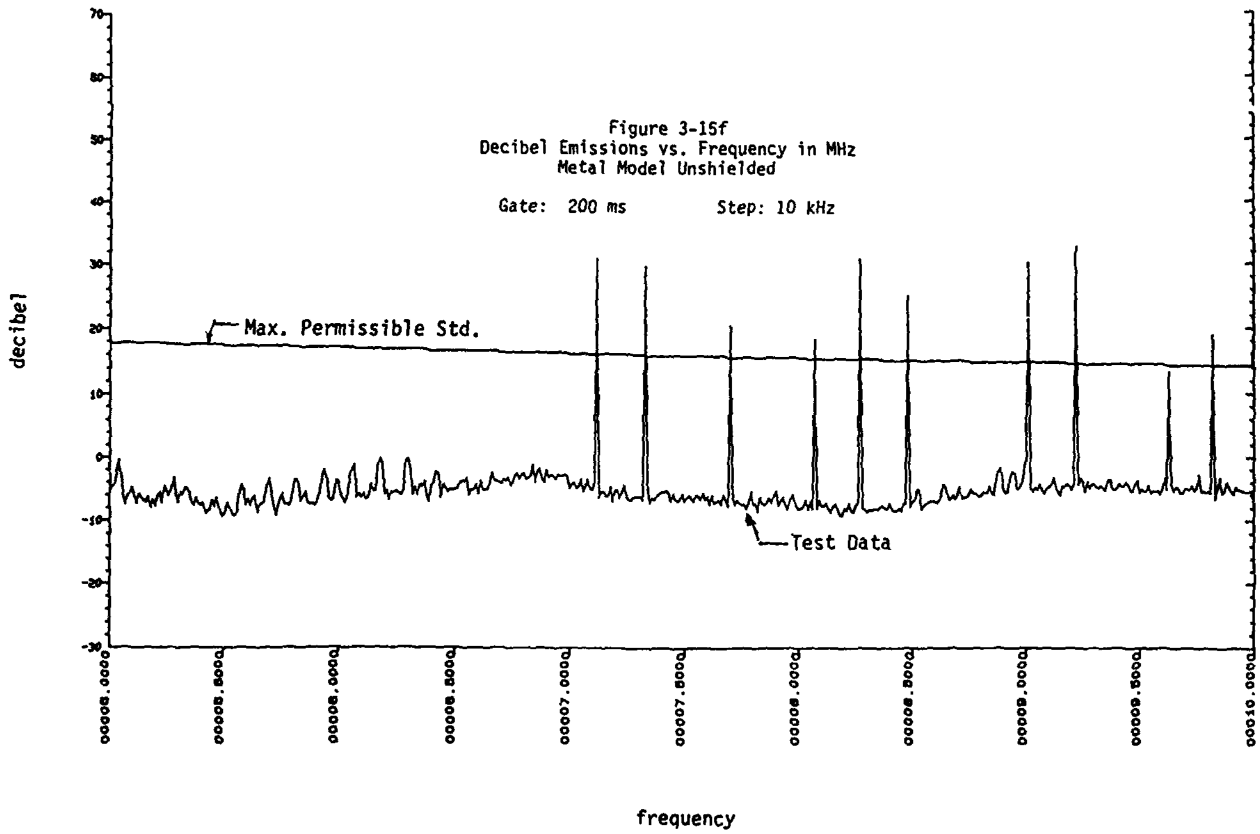

Figure 3-15f
Decibel Emissions vs. Frequency in MHz
Metal Model Unshielded
Gate: 200 ms
Step: 10 kHz
Max. Permissible Std.
Test Data
decibel
70
60
50
40
30
20
10
0
-10
-20
-30
00005.0000
00005.5000
00006.0000
00006.5000
00007.0000
00007.5000
00008.0000
00008.5000
00009.0000
00009.5000
00010.0000
frequency

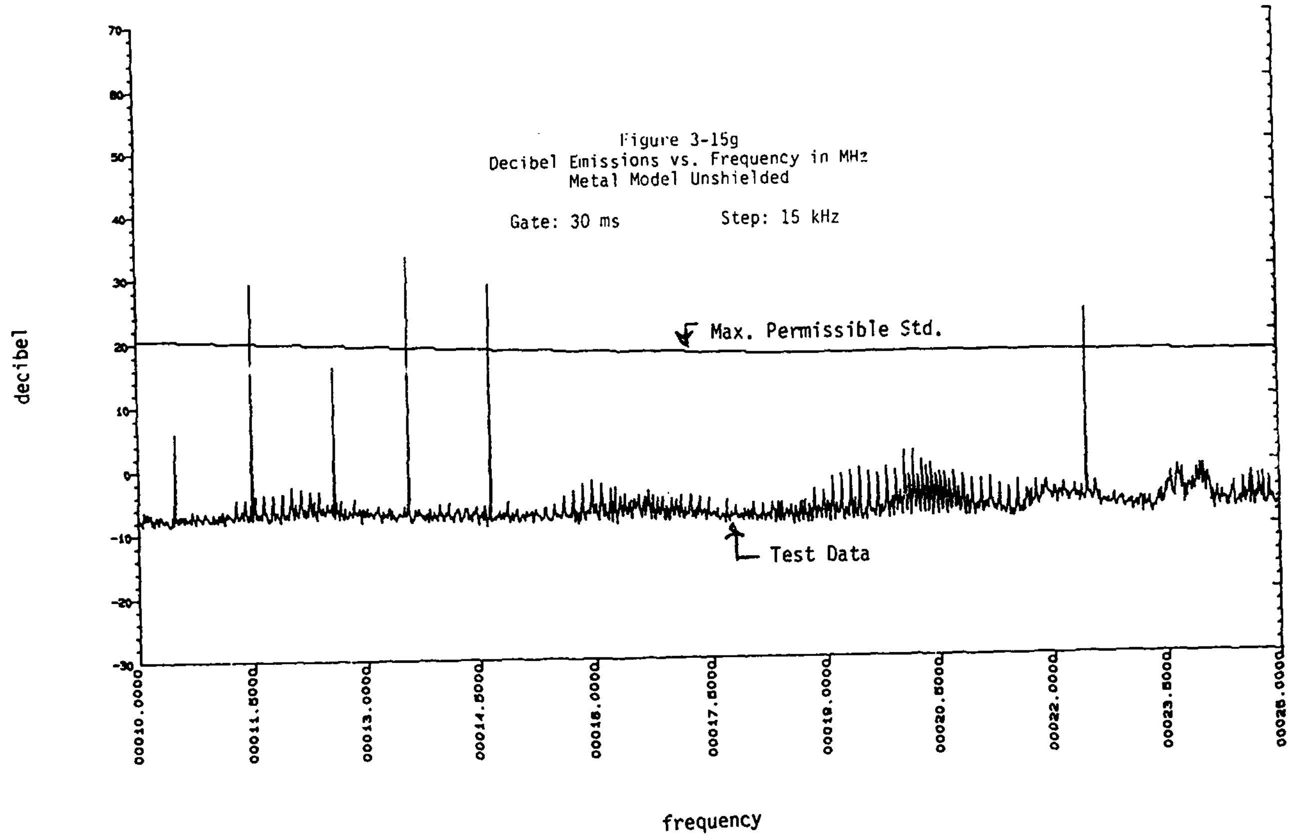

Figure 3-15g
Decibel Emissions vs. Frequency in MHz
Metal Model Unshielded
Gate: 30 ms
Step: 15 kHz
Max. Permissible Std.
Test Data
decibel
frequency

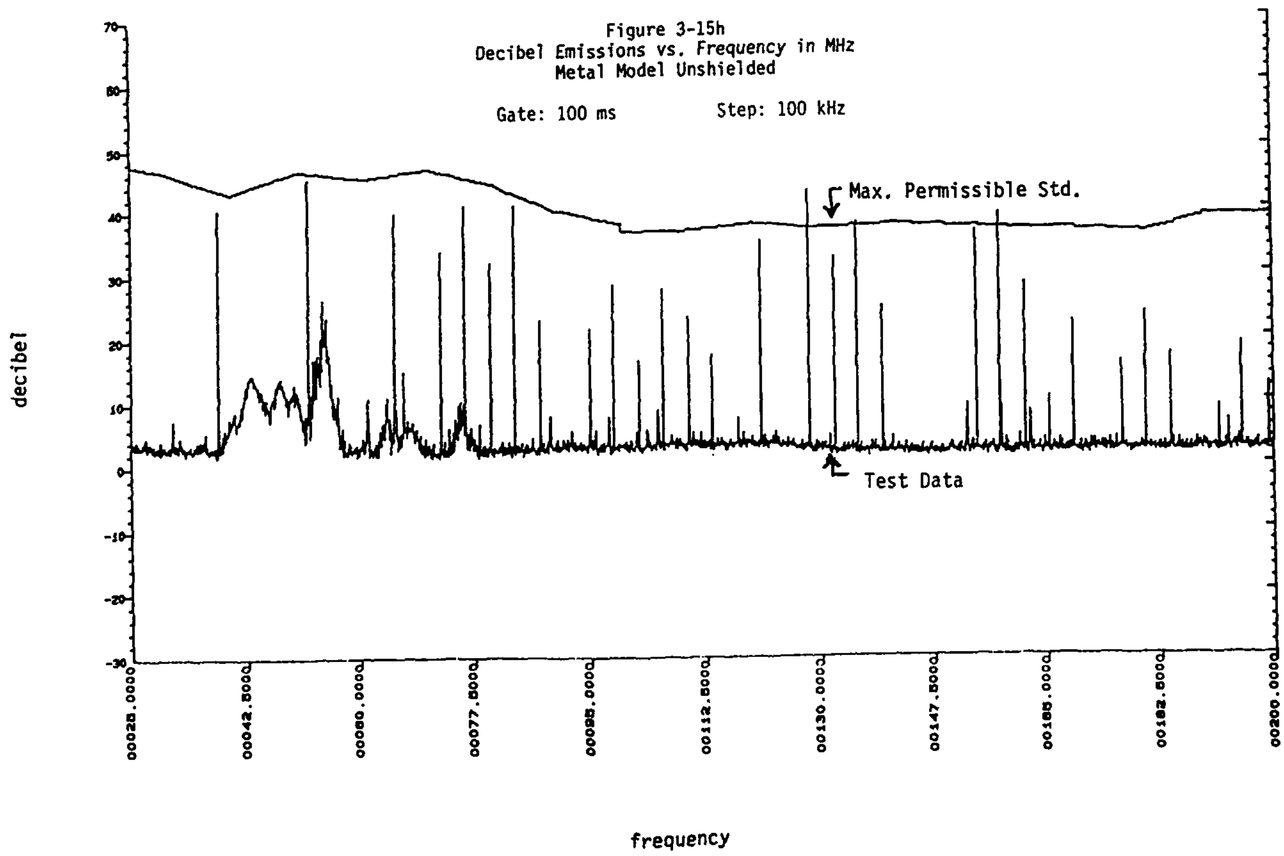

Figure 3-15h
Decibel Emissions vs. Frequency in MHz
Metal Model Unshielded
Gate: 100 ms
Step: 100 kHz
Max. Permissible Std.
Test Data
decibel
frequency

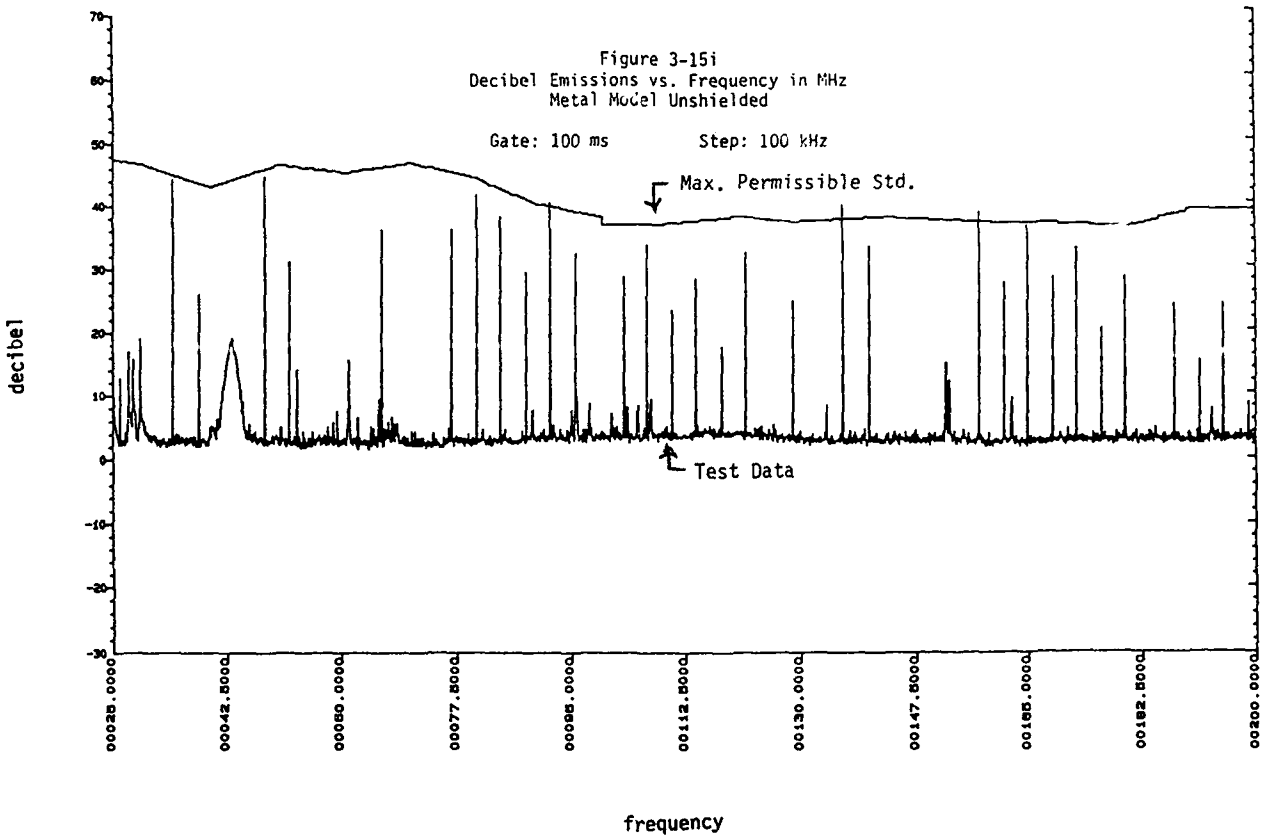
Figure 3-15i
Decibel Emissions vs. Frequency in MHz
Metal Model Unshielded
Gate: 100 ms
Step: 100 kHz
Max. Permissible Std.
Test Data
decibel
frequency
70
60
50
40
30
20
10
0
-10
-20
-30
00025.0000
00042.5000
00060.0000
00077.5000
00095.0000
00112.5000
00130.0000
00147.5000
00165.0000
00182.5000
00200.0000

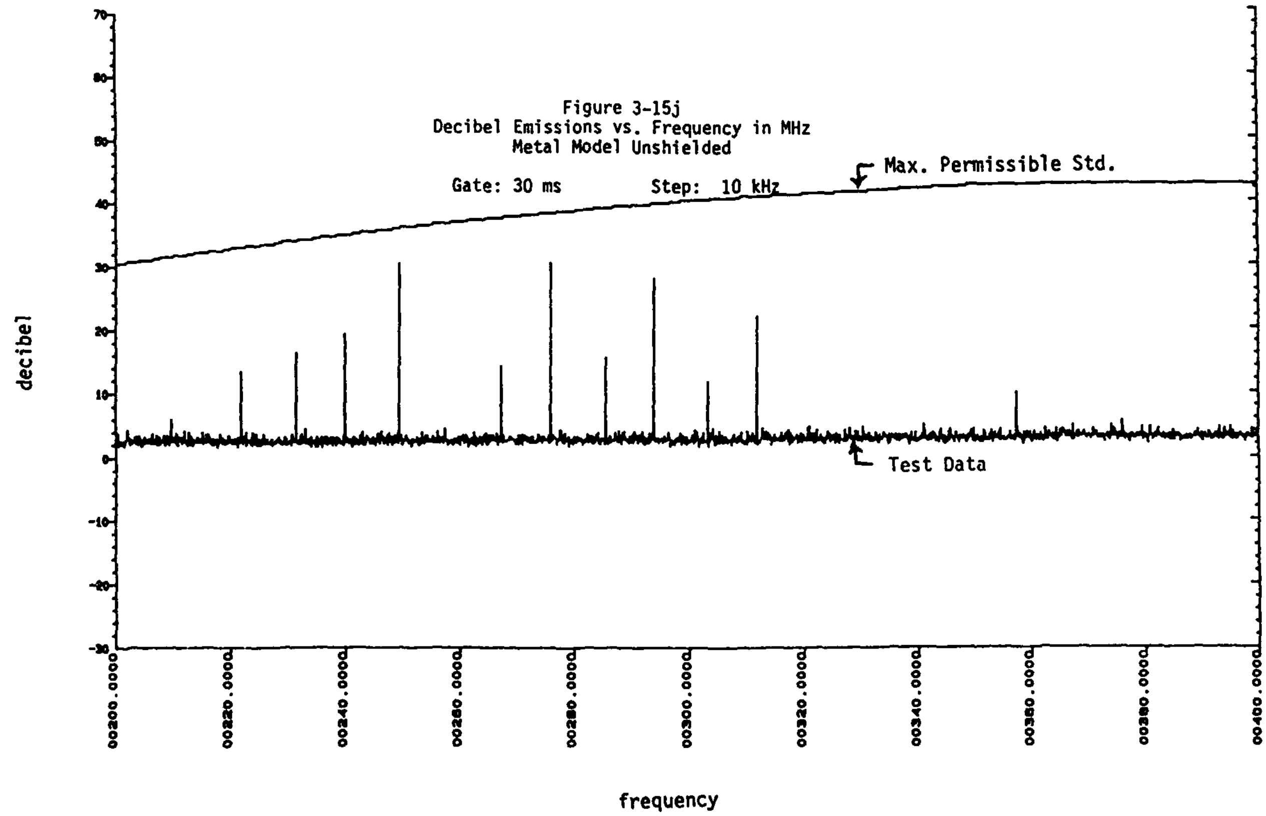
Figure 3-15j
Decibel Emissions vs. Frequency in MHz
Metal Model Unshielded
Gate: 30 ms
Step: 10 kHz
Max. Permissible Std.
Test Data
decibel
frequency
70
60
50
40
30
20
10
0
-10
-20
-30
00200.0000
00220.0000
00240.0000
00260.0000
00280.0000
00300.0000
00320.0000
00340.0000
00360.0000
00380.0000
00400.0000

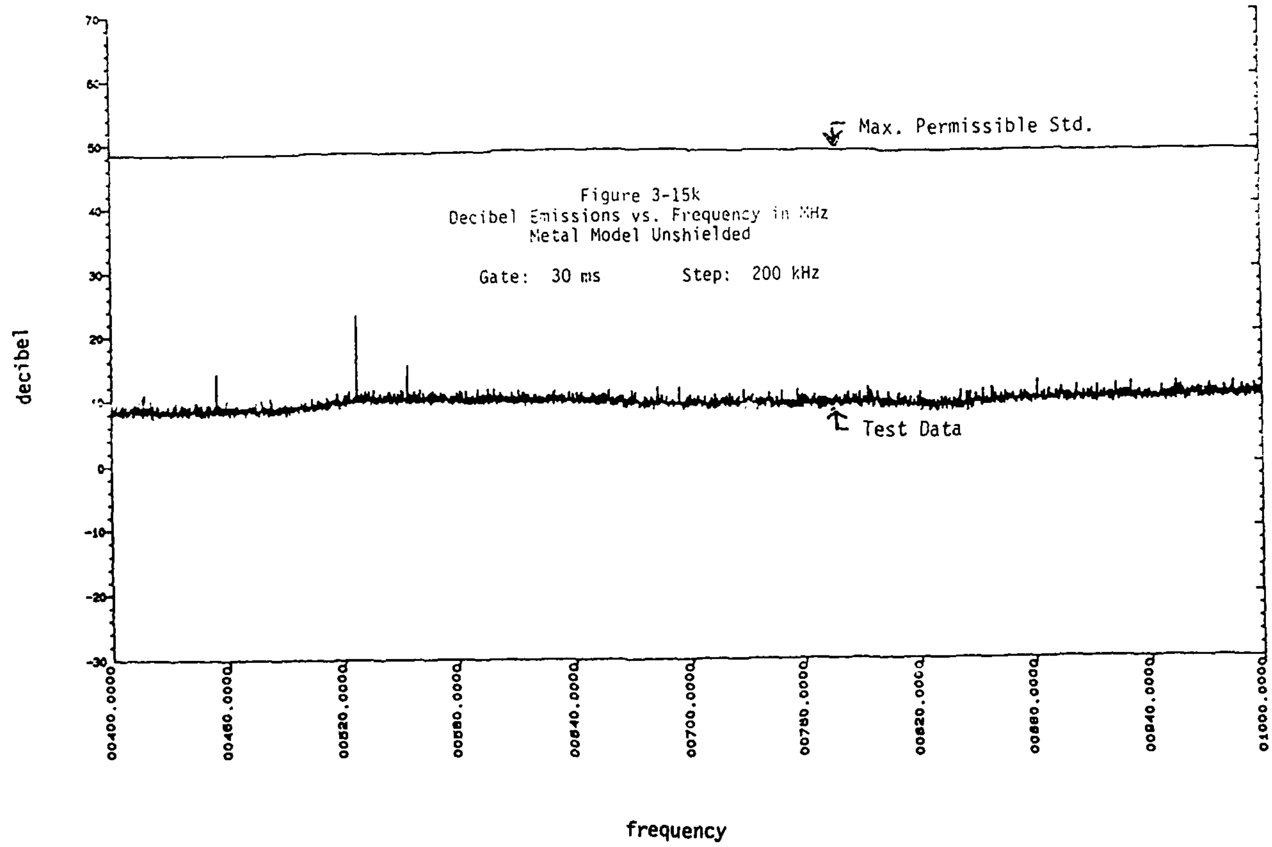

Max. Permissible Std.
Figure 3-15k
Decibel Emissions vs. Frequency in MHz
Metal Model Unshielded
Gate: 30 ms
Step: 200 kHz
Test Data
decibel
frequency

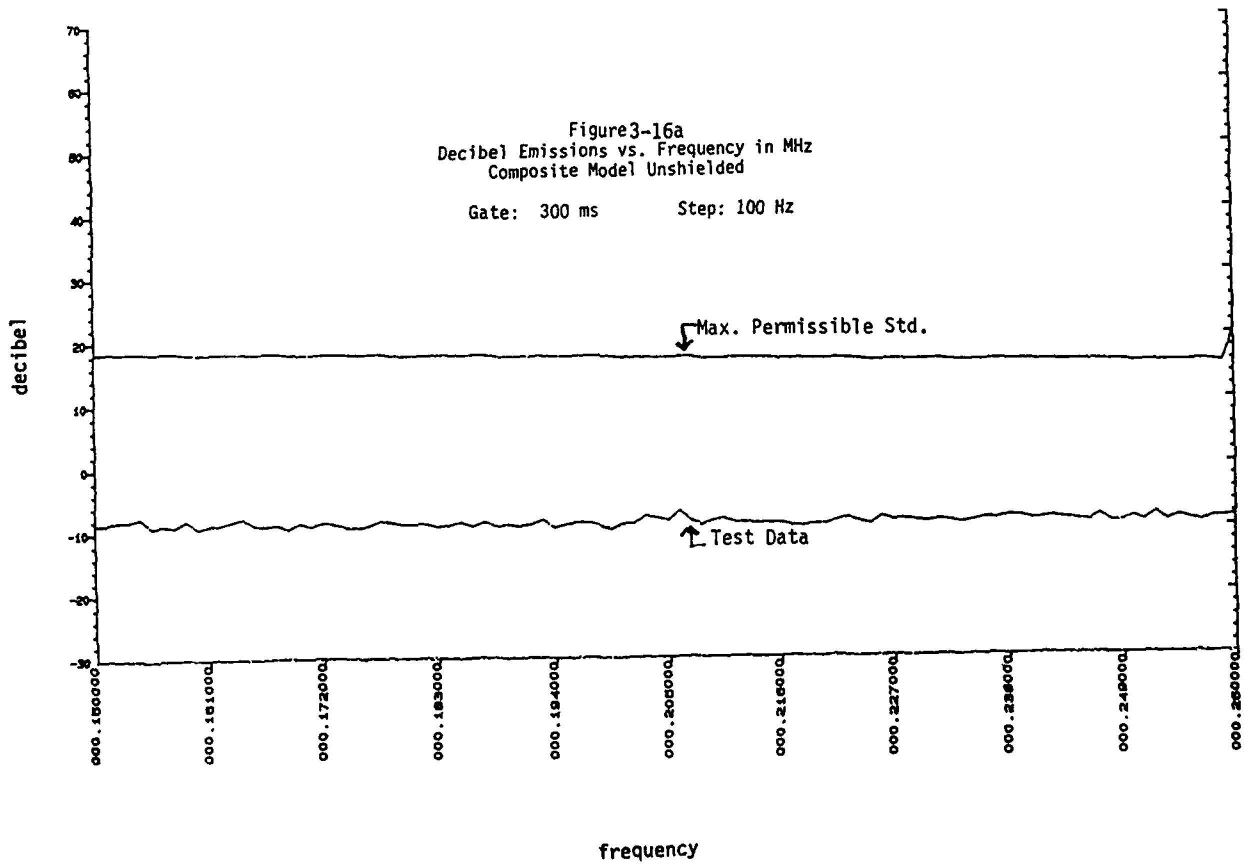

Figure3-16a
Decibel Emissions vs. Frequency in MHz
Composite Model Unshielded
Gate: 300 ms
Step: 100 Hz
Max. Permissible Std.
Test Data
decibel
frequency

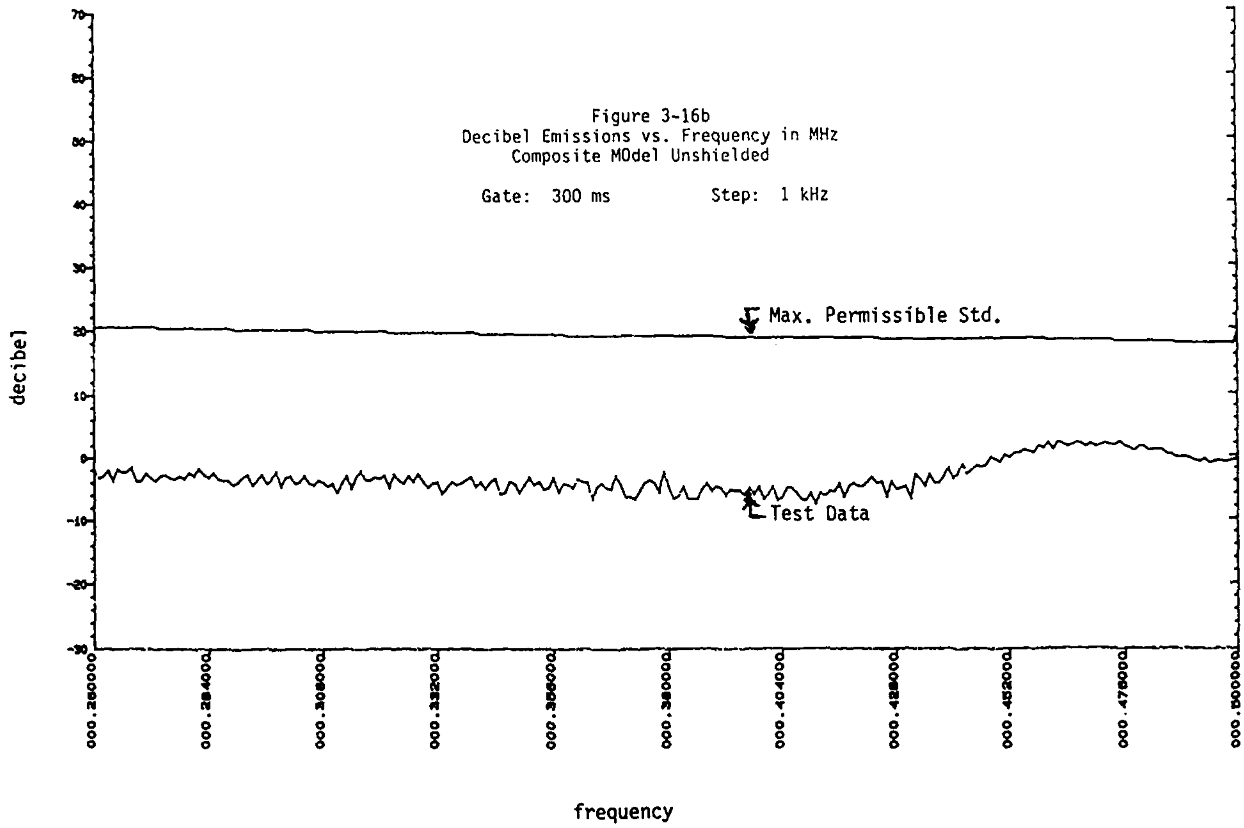
Figure 3-16b
Decibel Emissions vs. Frequency in MHz
Composite MOdel Unshielded
Gate: 300 ms
Step: 1 kHz
Max. Permissible Std.
Test Data
decibel
frequency

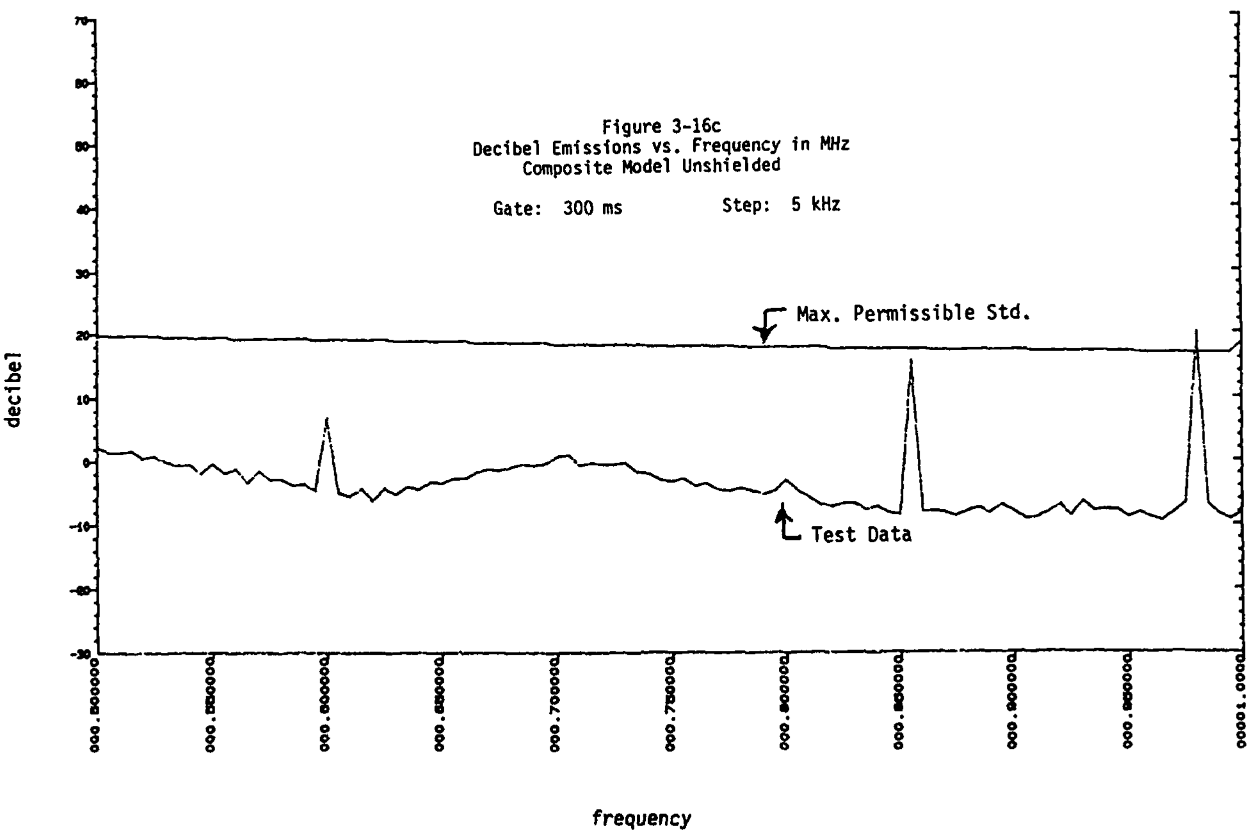
Figure 3-16c
Decibel Emissions vs. Frequency in MHz
Composite Model Unshielded
Gate: 300 ms
Step: 5 kHz
Max. Permissible Std.
Test Data
decibel
frequency

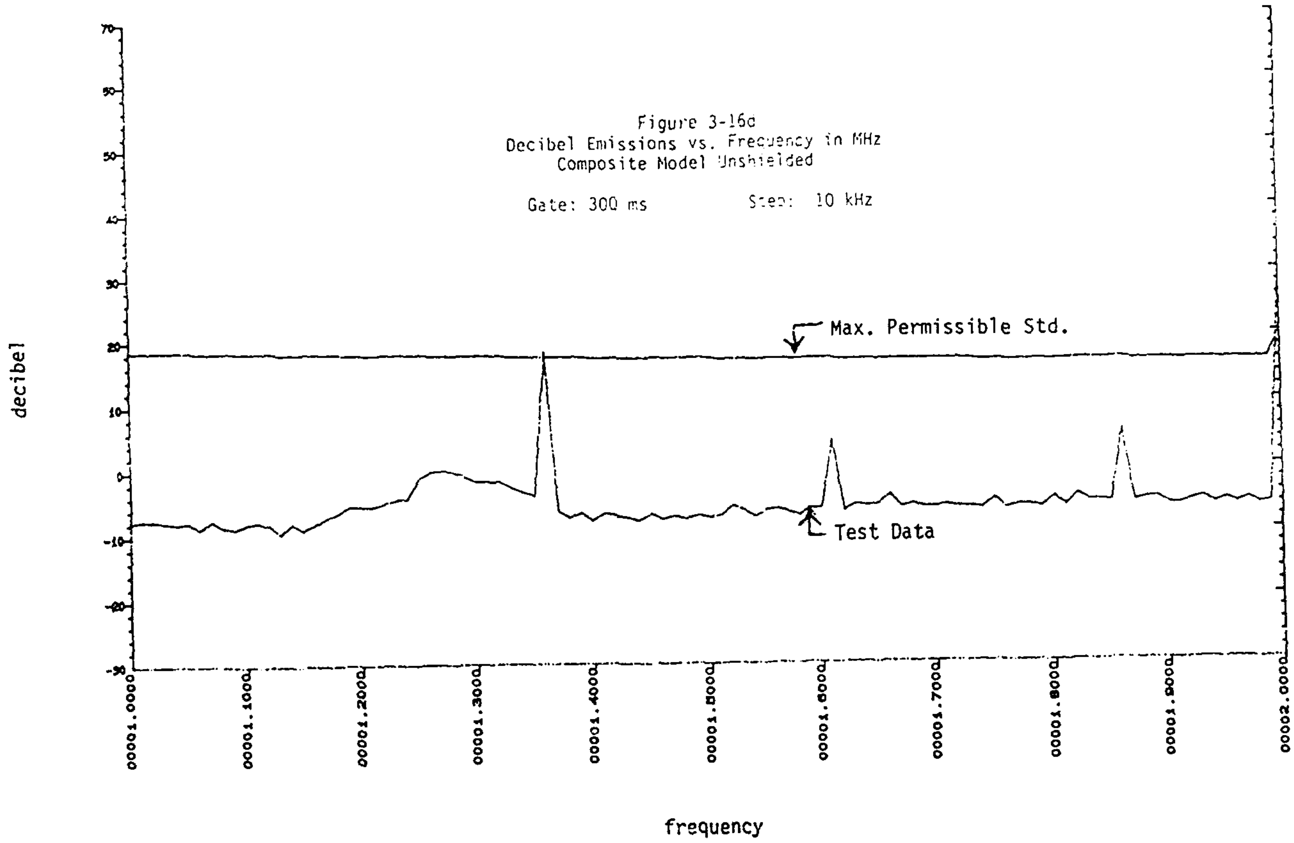

Figure 3-16d
Decibel Emissions vs. Frequency in MHz
Composite Model Unshielded
Gate: 300 ms
Step: 10 kHz
Max. Permissible Std.
Test Data
decibel
frequency
70
60
50
40
30
20
10
0
-10
-20
-30
00001.0000
00001.1000
00001.2000
00001.3000
00001.4000
00001.5000
00001.6000
00001.7000
00001.8000
00001.9000
00002.0000

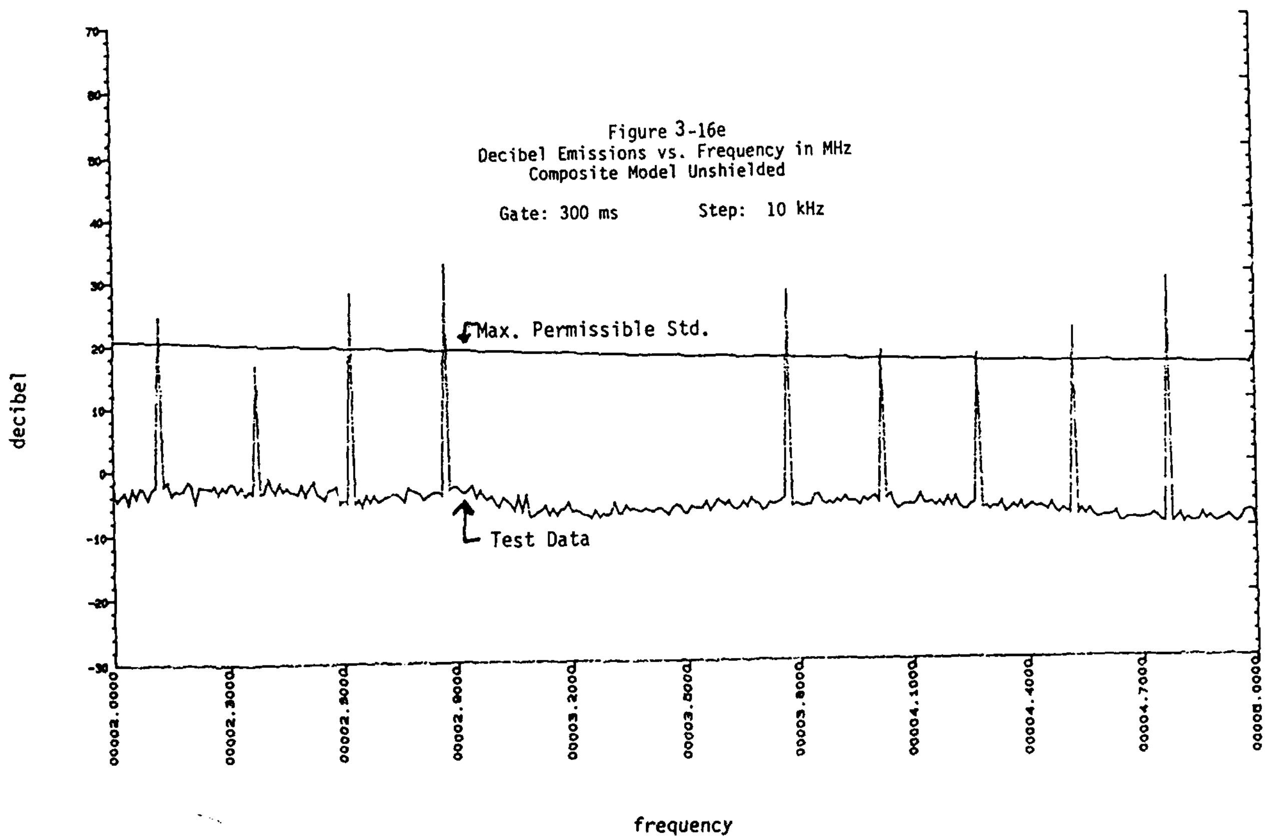

Figure 3-16e
Decibel Emissions vs. Frequency in MHz
Composite Model Unshielded
Gate: 300 ms
Step: 10 kHz
Max. Permissible Std.
Test Data
decibel
frequency
70
60
50
40
30
20
10
0
-10
-20
-30
00002.0000
00002.3000
00002.6000
00002.9000
00003.2000
00003.5000
00003.8000
00004.1000
00004.4000
00004.7000
00005.0000

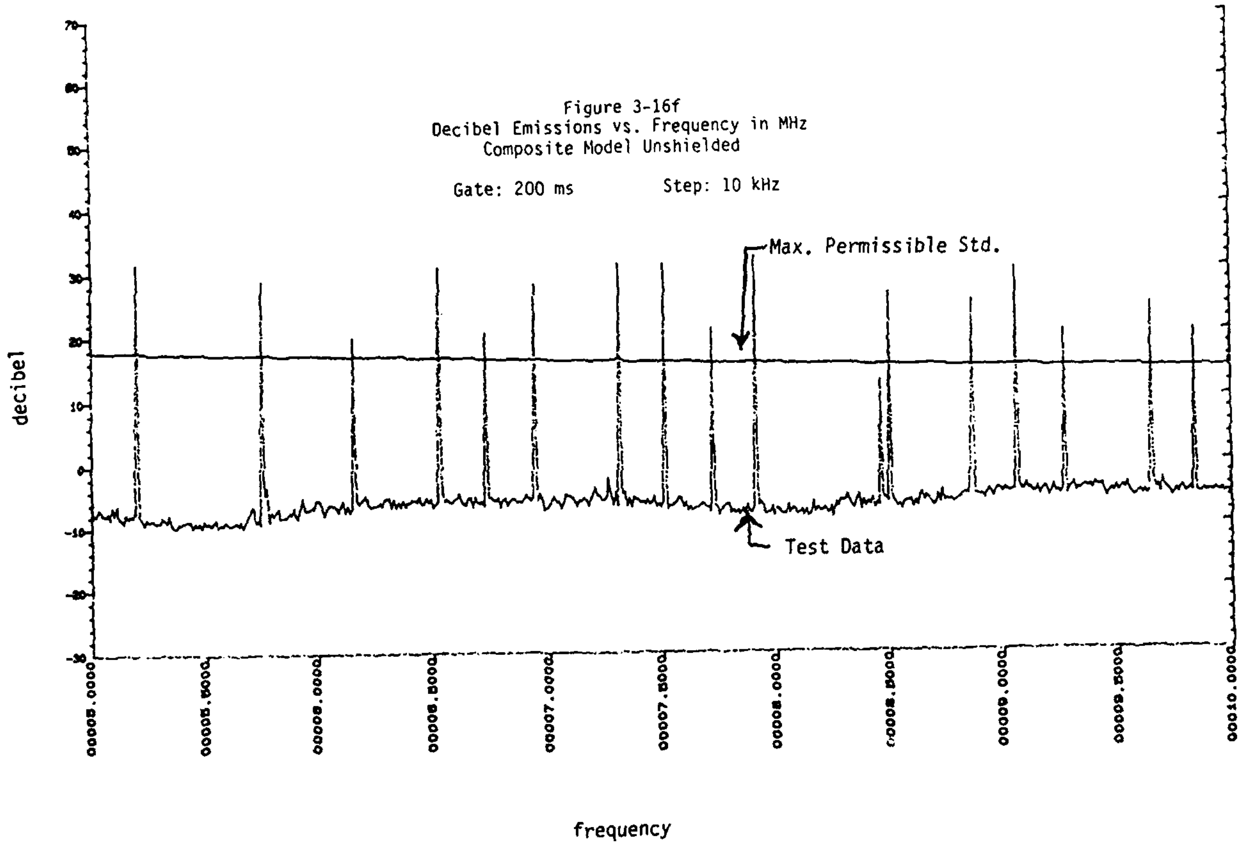
Figure 3-16f
Decibel Emissions vs. Frequency in MHz
Composite Model Unshielded
Gate: 200 ms
Step: 10 kHz
Max. Permissible Std.
Test Data
decibel
frequency

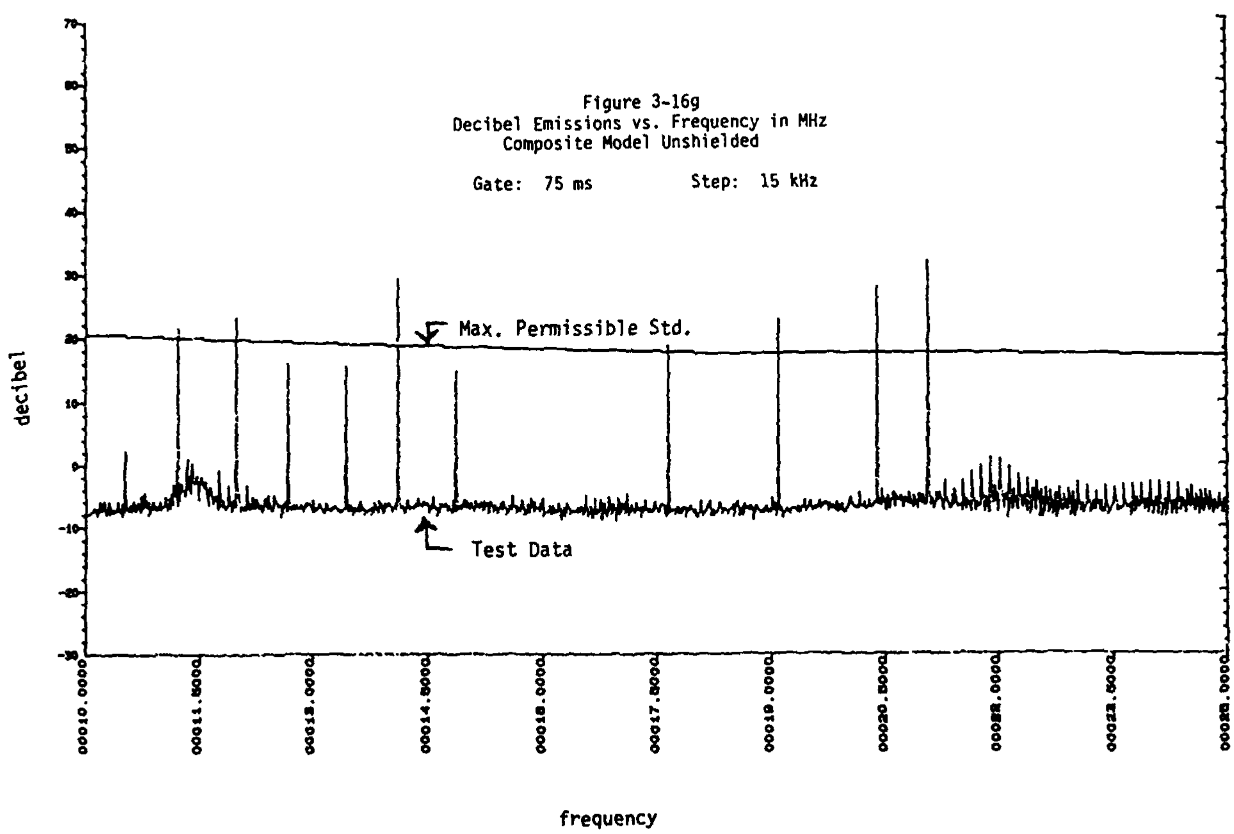
Figure 3-16g
Decibel Emissions vs. Frequency in MHz
Composite Model Unshielded
Gate: 75 ms
Step: 15 kHz
Max. Permissible Std.
Test Data
decibel
frequency

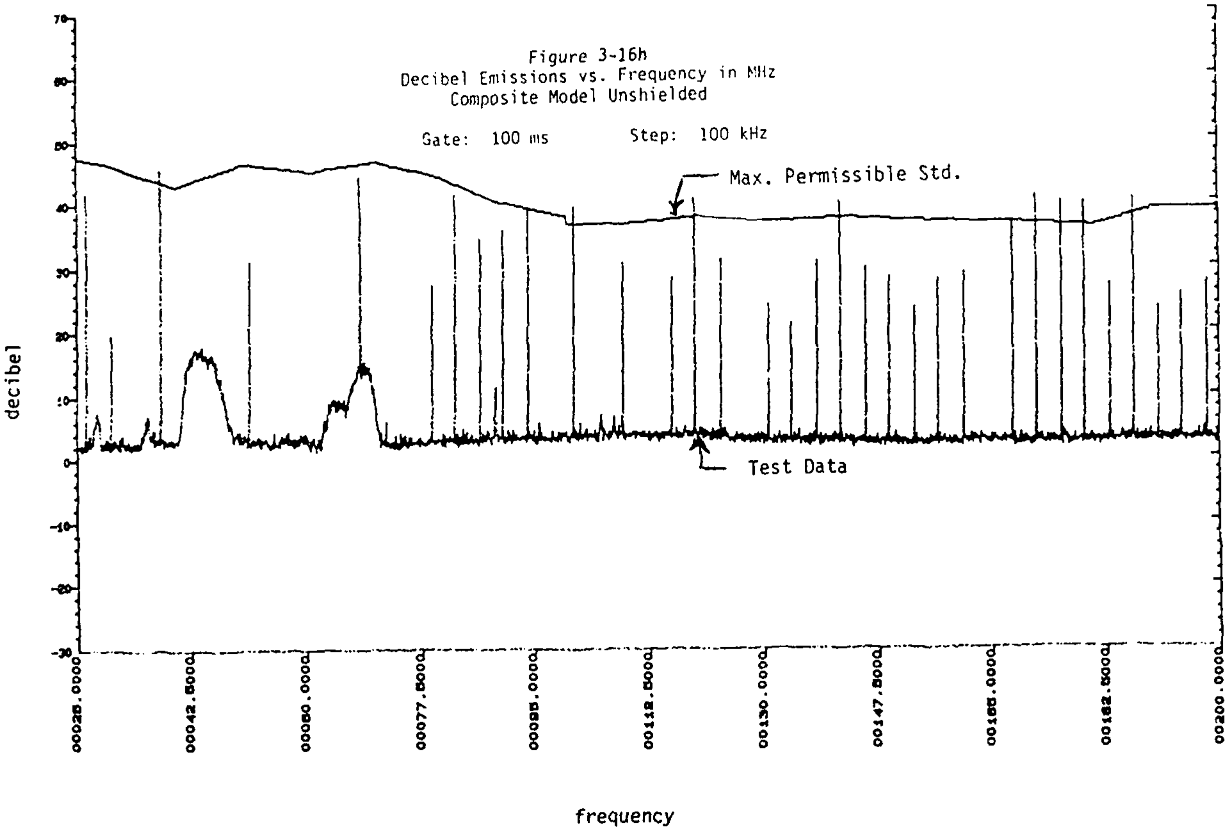

Figure 3-16h
Decibel Emissions vs. Frequency in MHz
Composite Model Unshielded

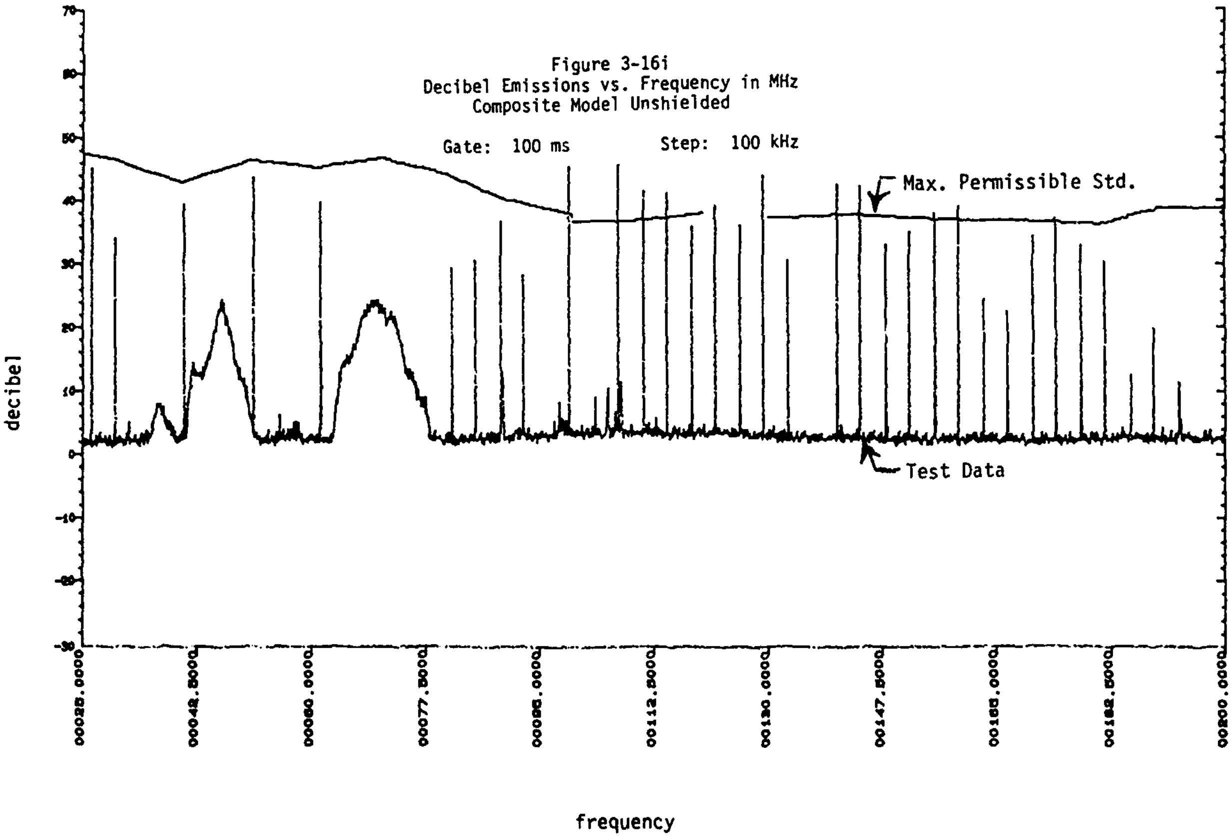

Figure 3-16i
Decibel Emissions vs. Frequency in MHz
Composite Model Unshielded

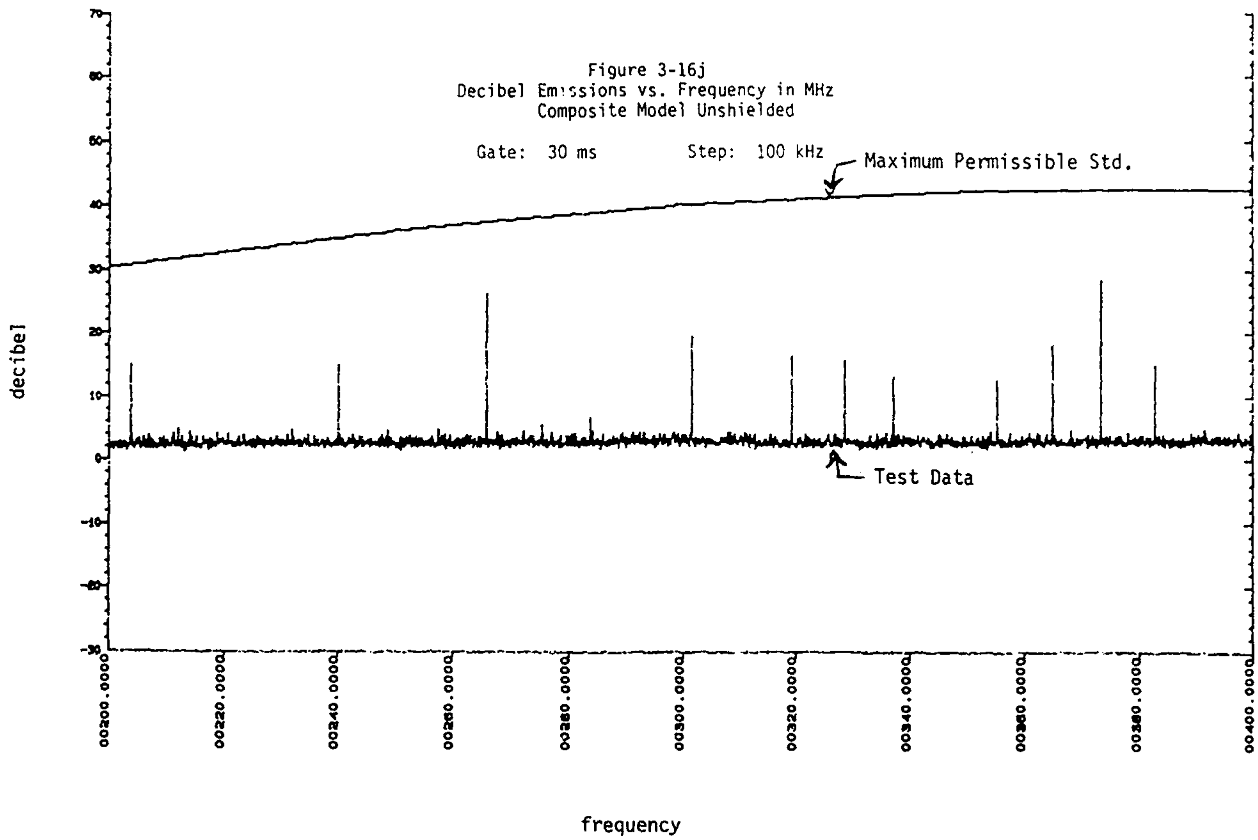
Figure 3-16j
Decibel Emissions vs. Frequency in MHz
Composite Model Unshielded
Gate: 30 ms Step: 100 kHz
Maximum Permissible Std.
Test Data
decibel
frequency
00200.0000
00220.0000
00240.0000
00260.0000
00280.0000
00300.0000
00320.0000
00340.0000
00360.0000
00380.0000
00400.0000

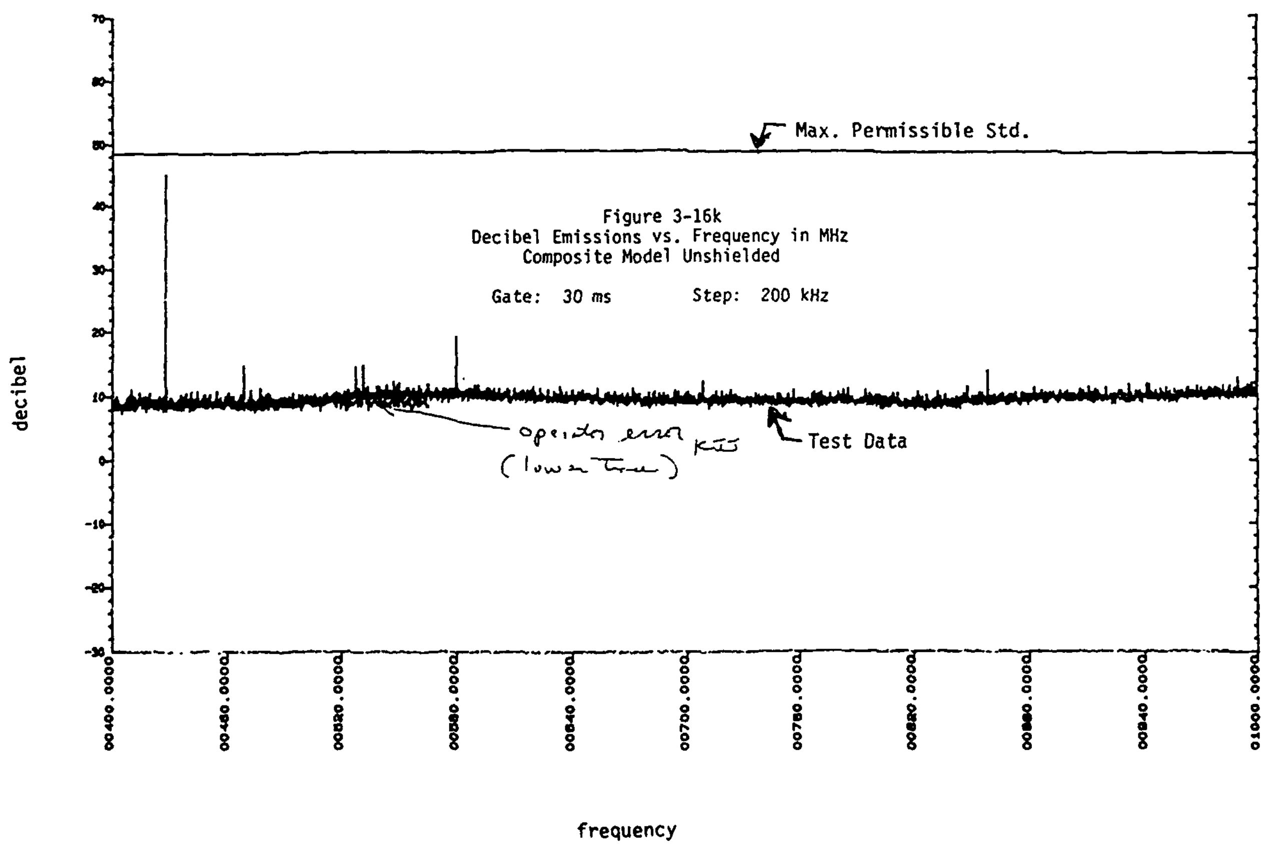
Max. Permissible Std.
Figure 3-16k
Decibel Emissions vs. Frequency in MHz
Composite Model Unshielded
Gate: 30 ms Step: 200 kHz
Test Data
operator error
(lower trace)
decibel
frequency
00400.0000
00460.0000
00520.0000
00580.0000
00640.0000
00700.0000
00760.0000
00820.0000
00880.0000
00940.0000
01000.0000

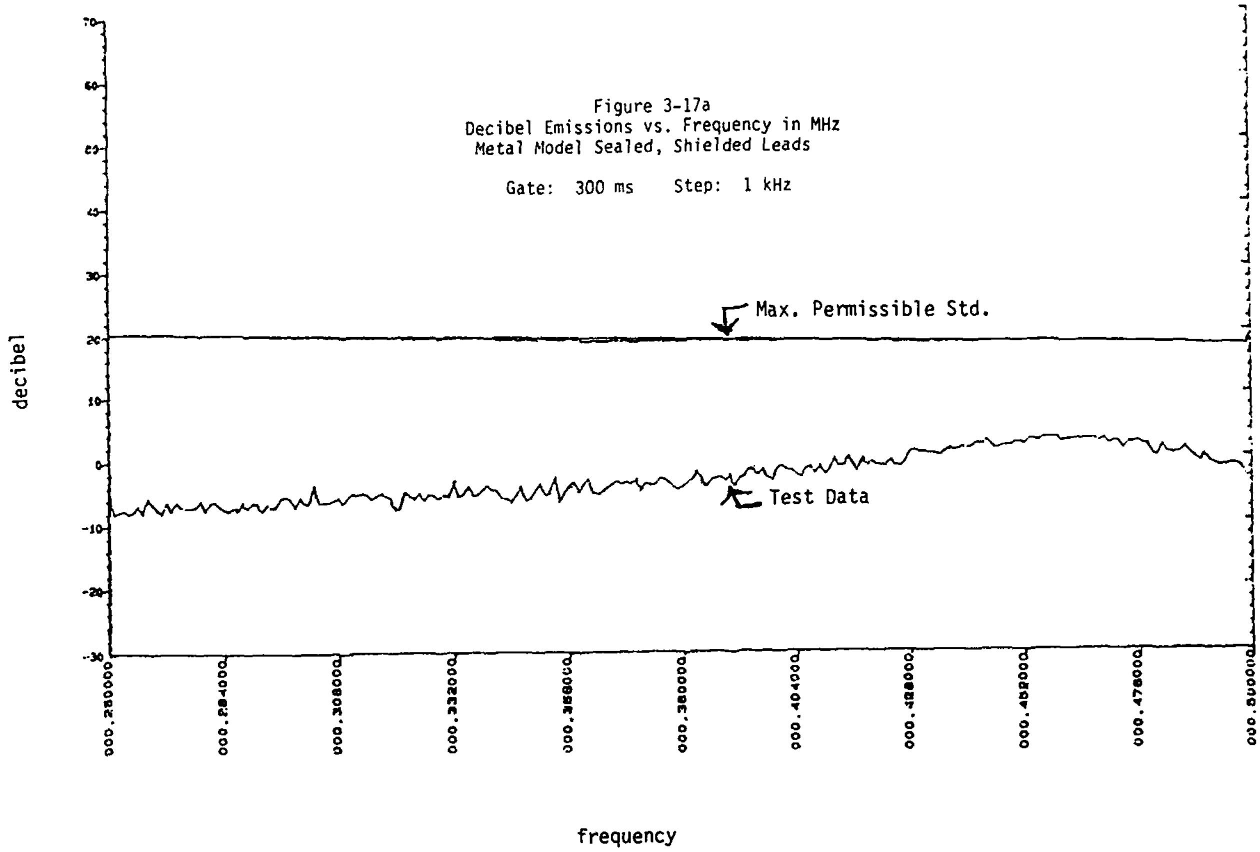
Figure 3-17a
Decibel Emissions vs. Frequency in MHz
Metal Model Sealed, Shielded Leads
Gate: 300 ms Step: 1 kHz
Max. Permissible Std.
Test Data
decibel
frequency

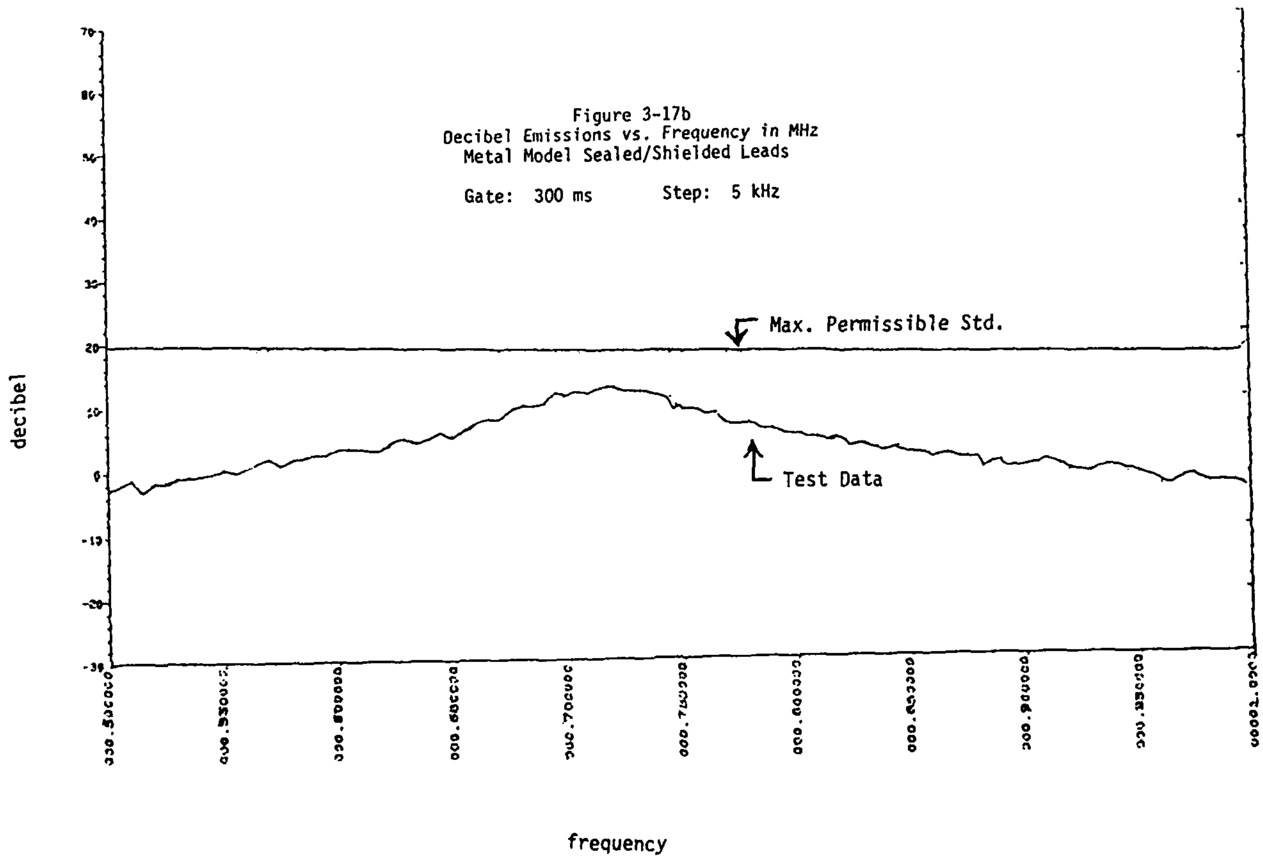
Figure 3-17b
Decibel Emissions vs. Frequency in MHz
Metal Model Sealed/Shielded Leads
Gate: 300 ms Step: 5 kHz
Max. Permissible Std.
Test Data
decibel
frequency

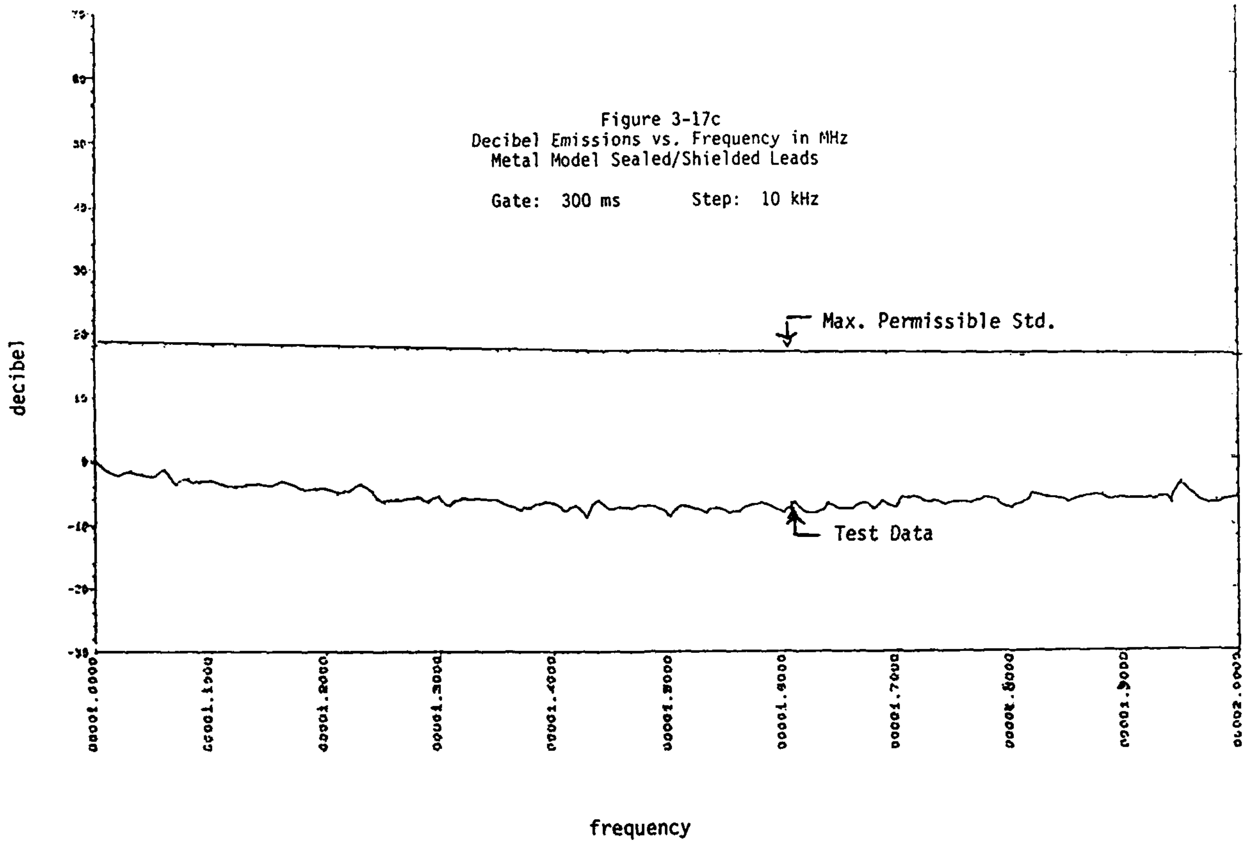

Figure 3-17c
Decibel Emissions vs. Frequency in MHz
Metal Model Sealed/Shielded Leads

Gate: 300 ms Step: 10 kHz

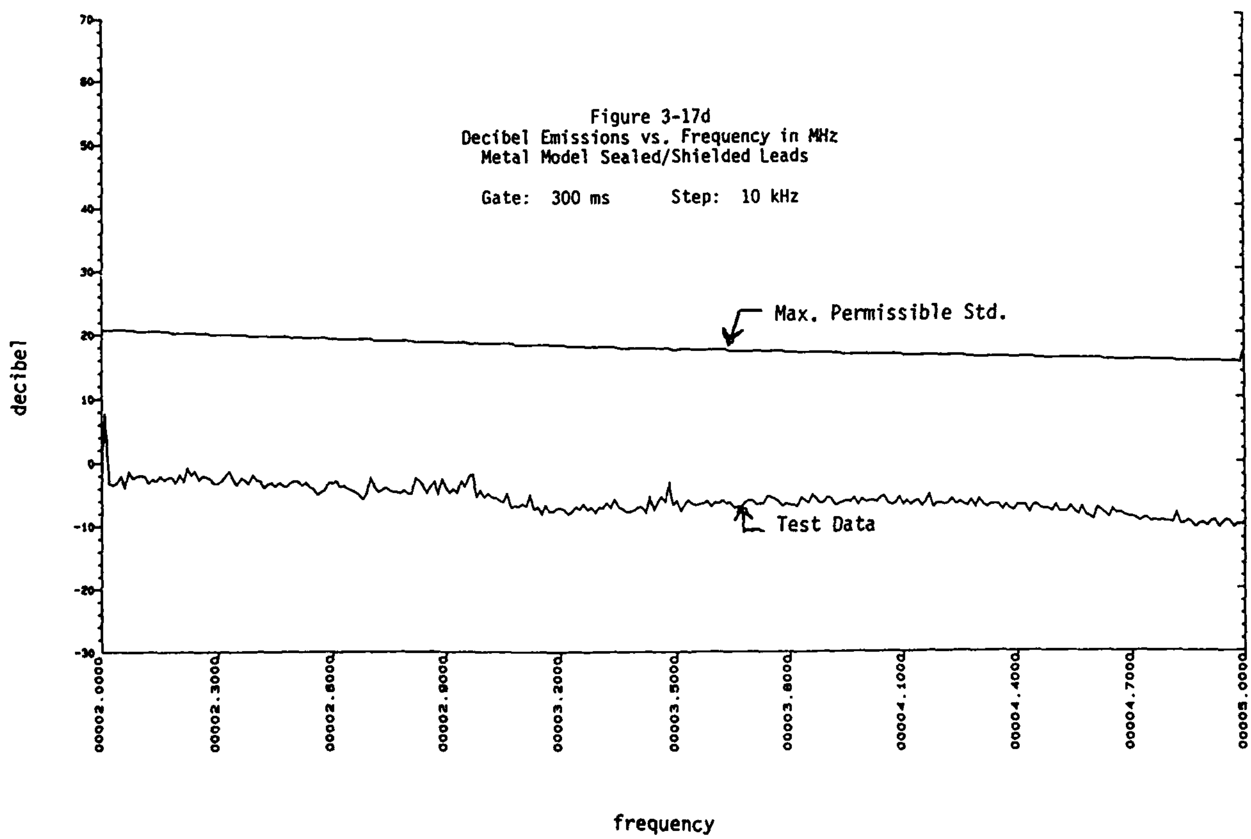

Figure 3-17d
Decibel Emissions vs. Frequency in MHz
Metal Model Sealed/Shielded Leads

Gate: 300 ms Step: 10 kHz

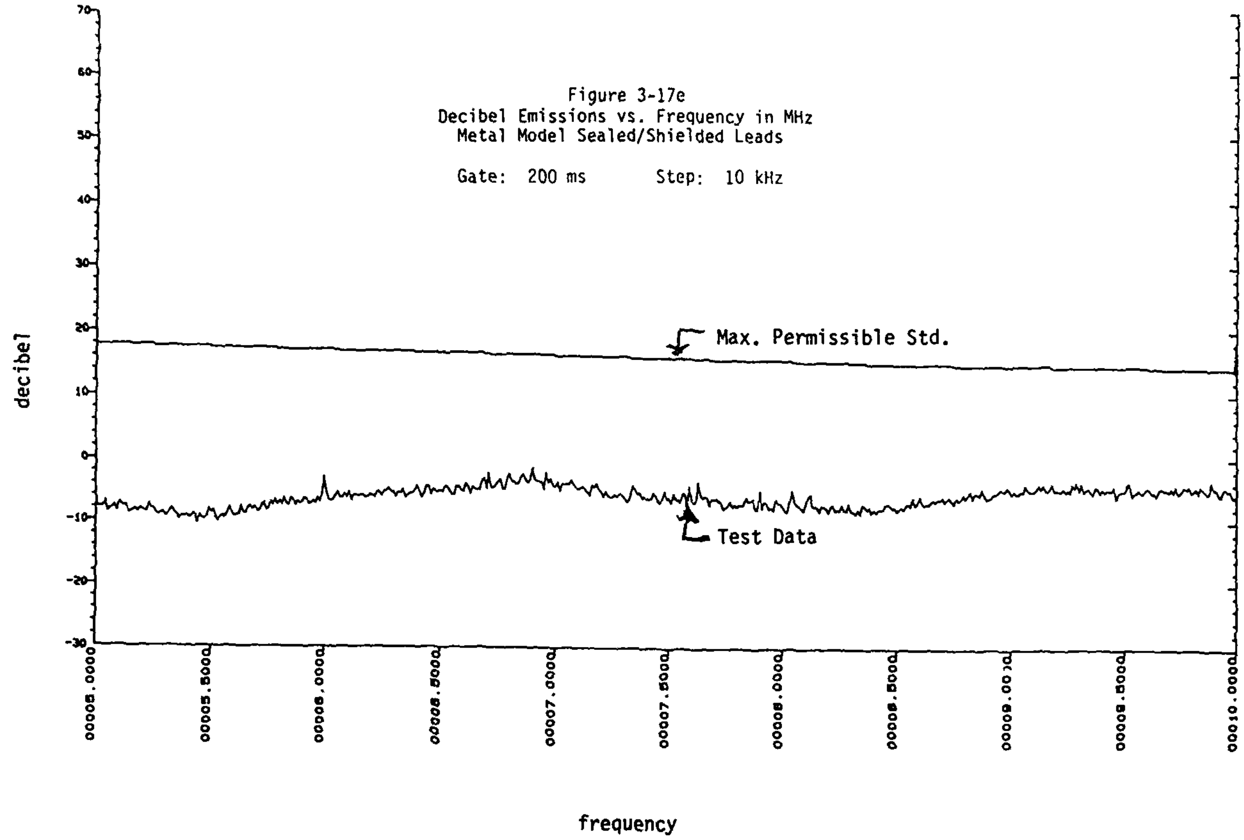
Figure 3-17e
Decibel Emissions vs. Frequency in MHz
Metal Model Sealed/Shielded Leads
Gate: 200 ms
Step: 10 kHz
Max. Permissible Std.
Test Data
decibel
70
60
50
40
30
20
10
0
-10
-20
-30
00005.0000
00005.5000
00006.0000
00006.5000
00007.0000
00007.5000
00008.0000
00008.5000
00009.0000
00009.5000
00010.0000
frequency

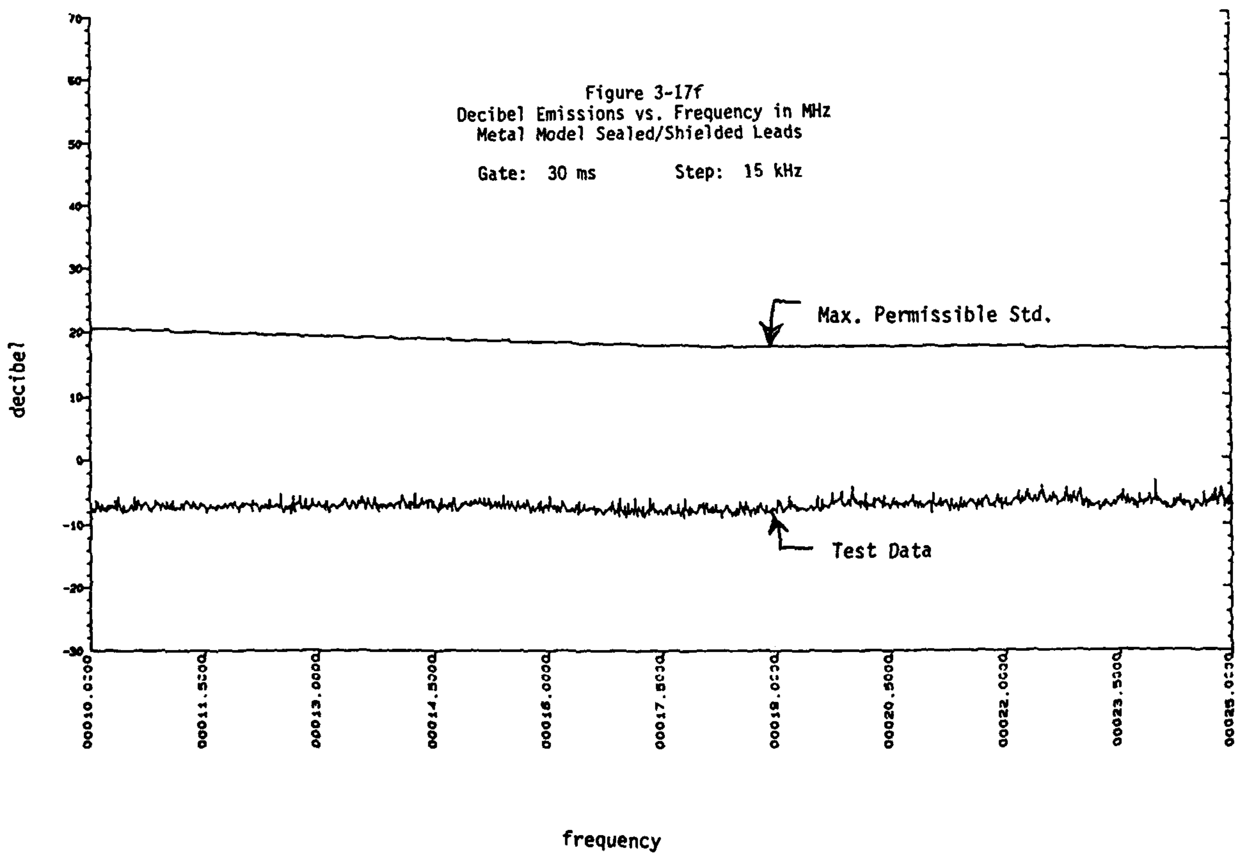
Figure 3-17f
Decibel Emissions vs. Frequency in MHz
Metal Model Sealed/Shielded Leads
Gate: 30 ms
Step: 15 kHz
Max. Permissible Std.
Test Data
decibel
70
60
50
40
30
20
10
0
-10
-20
-30
00010.0000
00011.5000
00013.0000
00014.5000
00016.0000
00017.5000
00019.0000
00020.5000
00022.0000
00023.5000
00025.0000
frequency

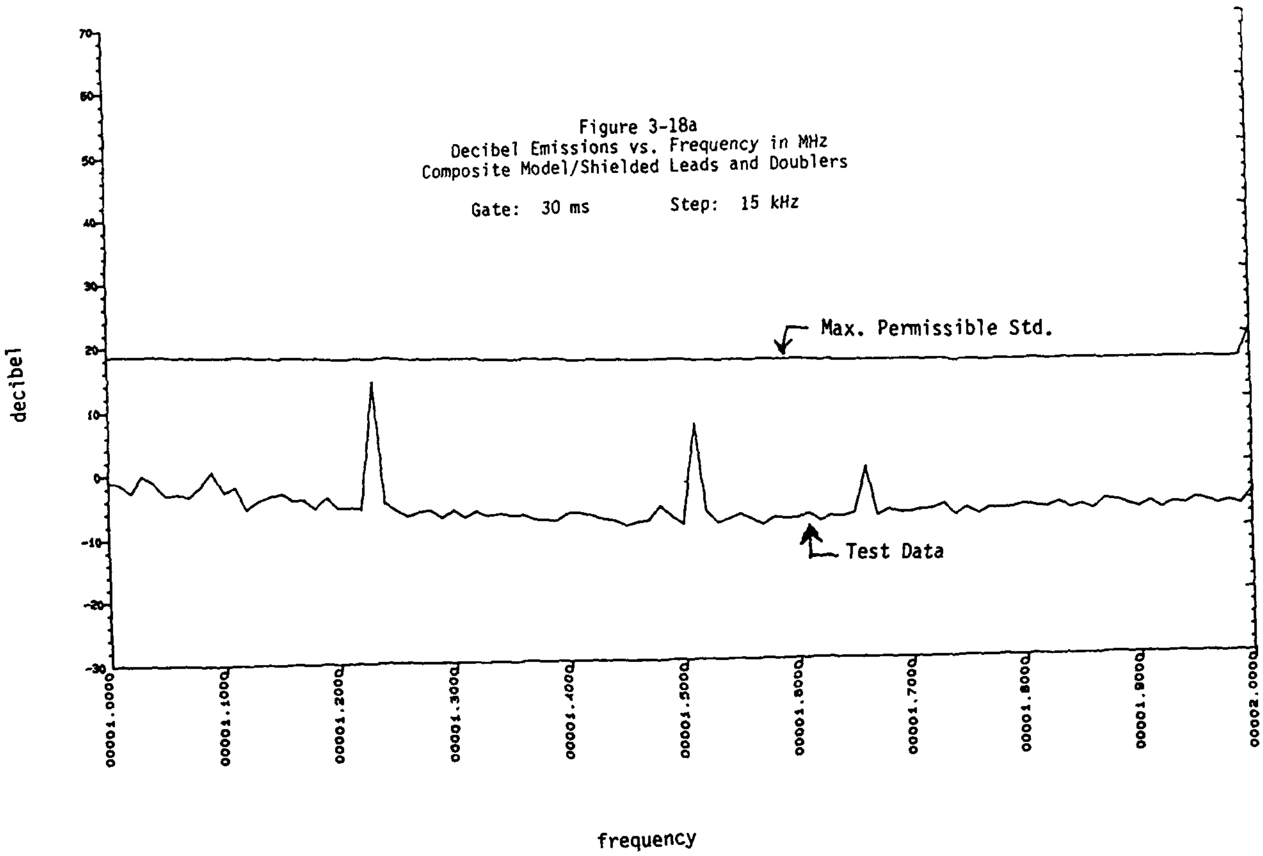
Figure 3-18a
Decibel Emissions vs. Frequency in MHz
Composite Model/Shielded Leads and Doublers
Gate: 30 ms Step: 15 kHz
Max. Permissible Std.
Test Data
decibel
frequency

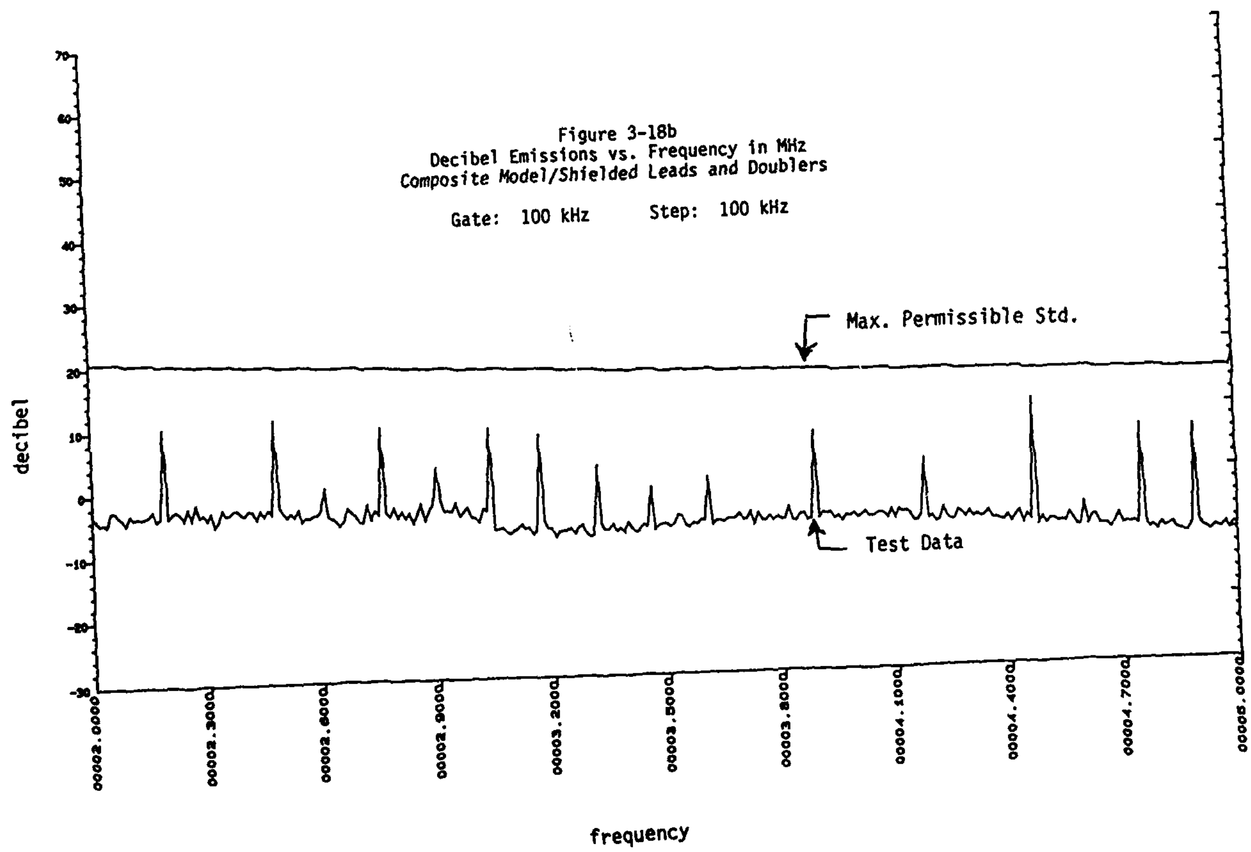
Figure 3-18b
Decibel Emissions vs. Frequency in MHz
Composite Model/Shielded Leads and Doublers
Gate: 100 kHz Step: 100 kHz
Max. Permissible Std.
Test Data
decibel
frequency

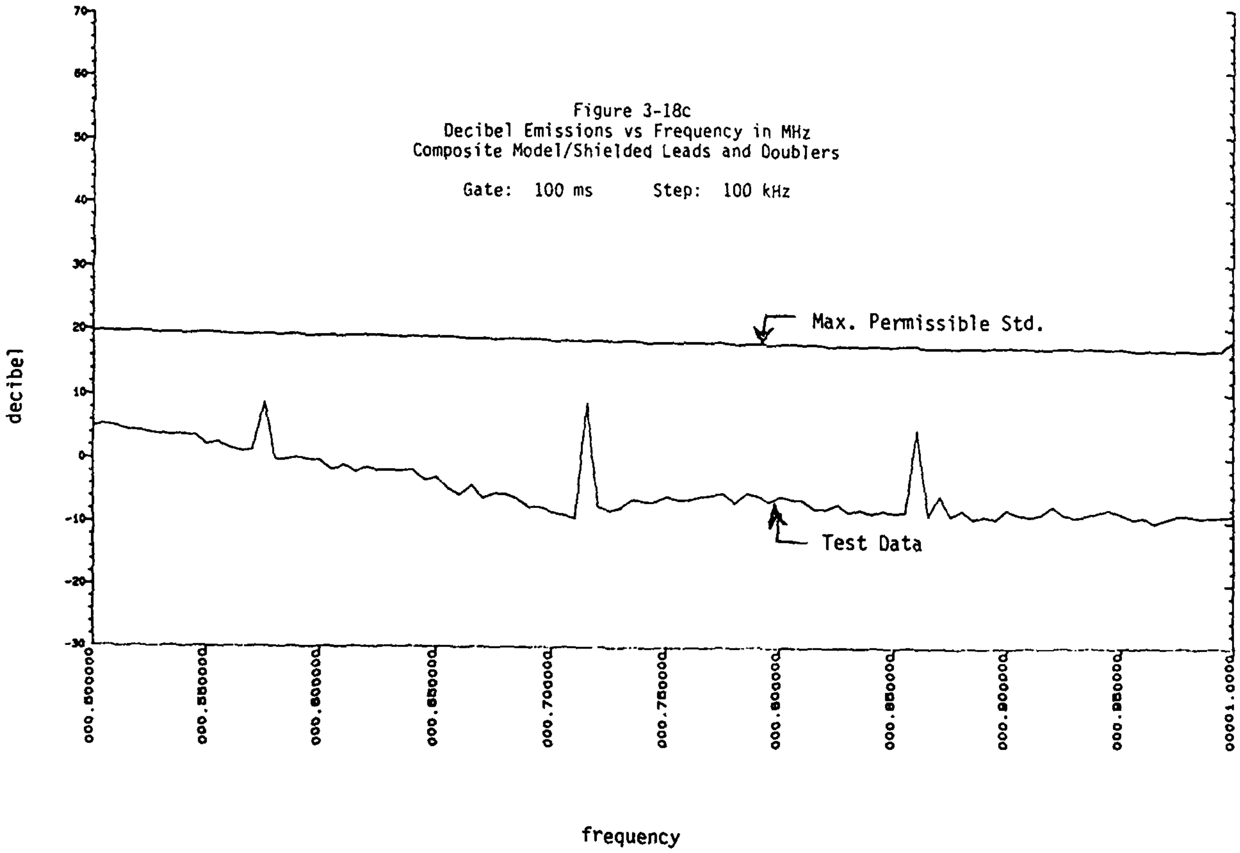

Figure 3-18c
Decibel Emissions vs Frequency in MHz
Composite Model/Shielded Leads and Doublers

Gate: 100 ms Step: 100 kHz

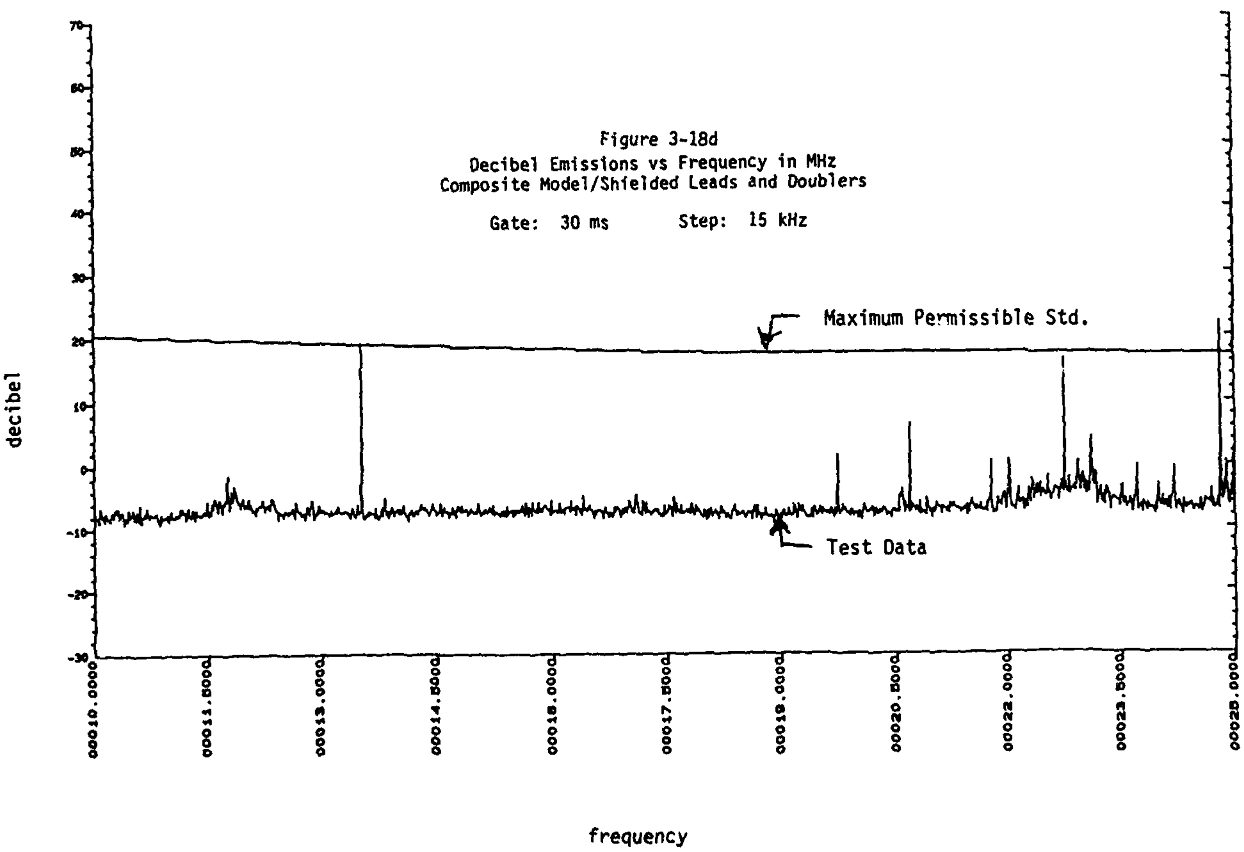

Figure 3-18d
Decibel Emissions vs Frequency in MHz
Composite Model/Shielded Leads and Doublers

Gate: 30 ms Step: 15 kHz

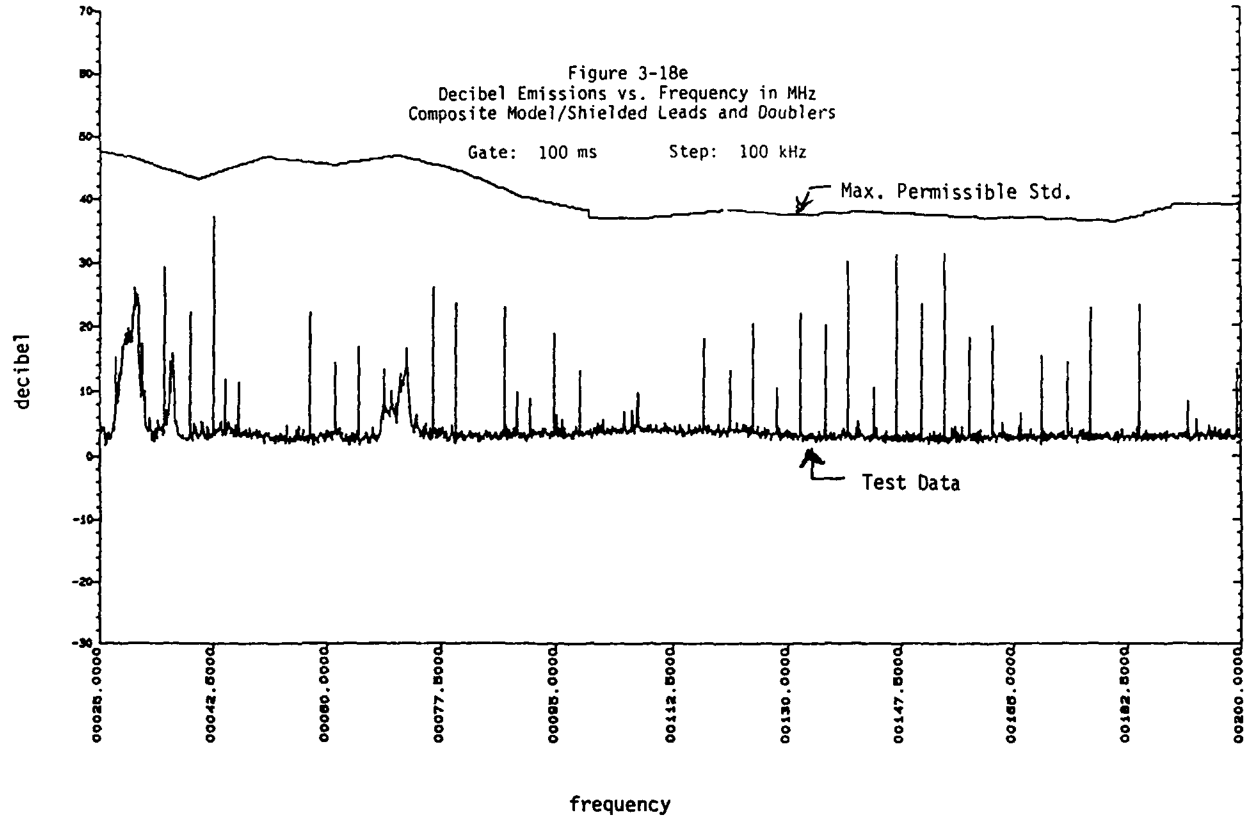
Figure 3-18e
Decibel Emissions vs. Frequency in MHz
Composite Model/Shielded Leads and Doublers
Gate: 100 ms
Step: 100 kHz
Max. Permissible Std.
Test Data
decibel
frequency

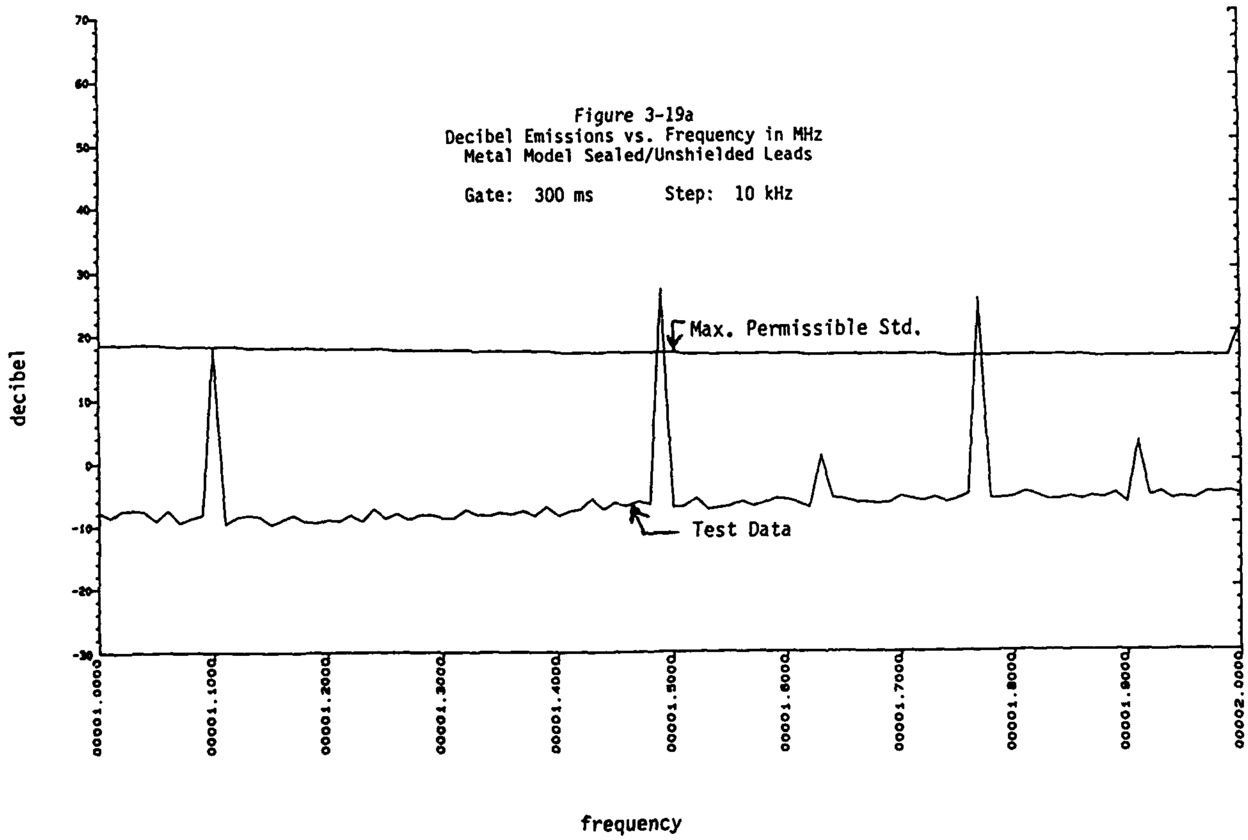
Figure 3-19a
Decibel Emissions vs. Frequency in MHz
Metal Model Sealed/Unshielded Leads
Gate: 300 ms
Step: 10 kHz
Max. Permissible Std.
Test Data
decibel
frequency

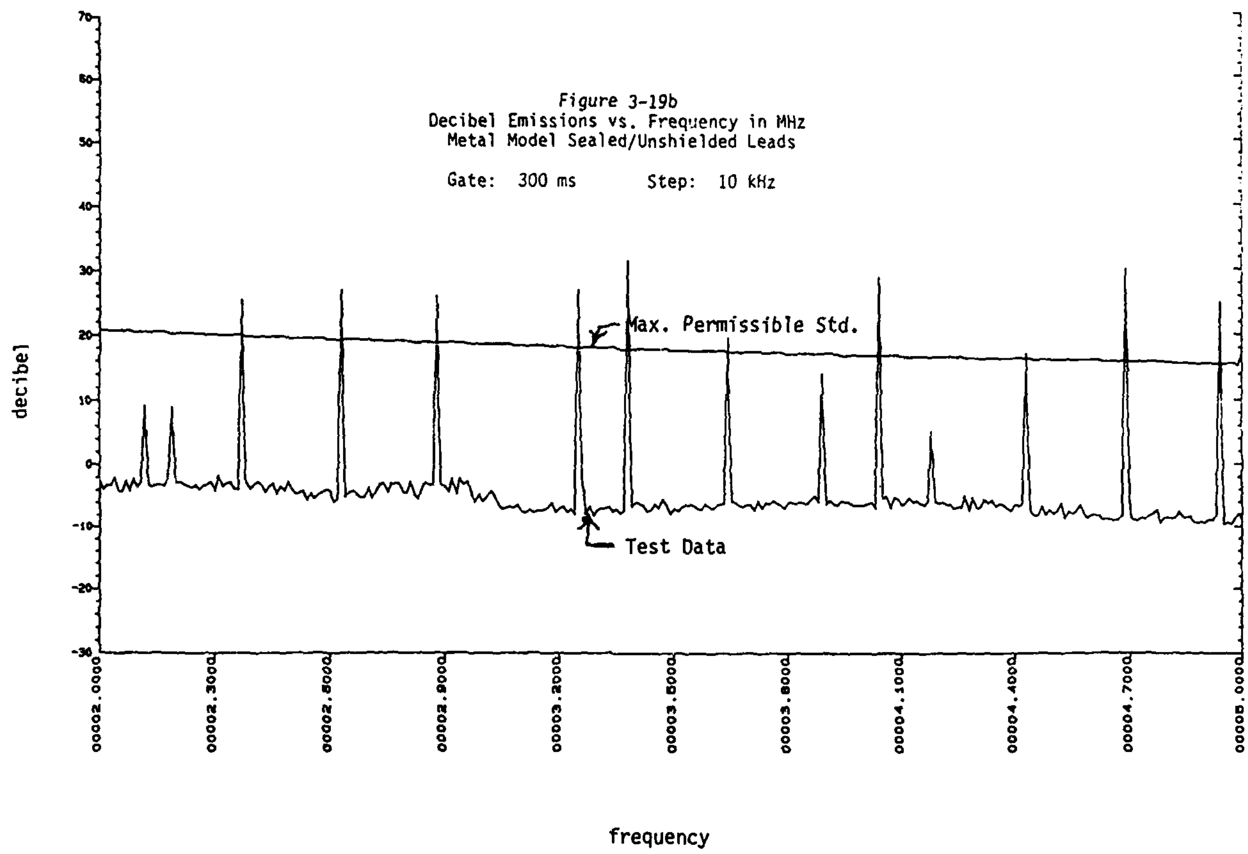

Figure 3-19b
Decibel Emissions vs. Frequency in MHz
Metal Model Sealed/Unshielded Leads
Gate: 300 ms Step: 10 kHz
Max. Permissible Std.
Test Data
decibel
70
60
50
40
30
20
10
0
-10
-20
-30
00002.0000
00002.3000
00002.6000
00002.9000
00003.2000
00003.5000
00003.8000
00004.1000
00004.4000
00004.7000
00005.0000
frequency

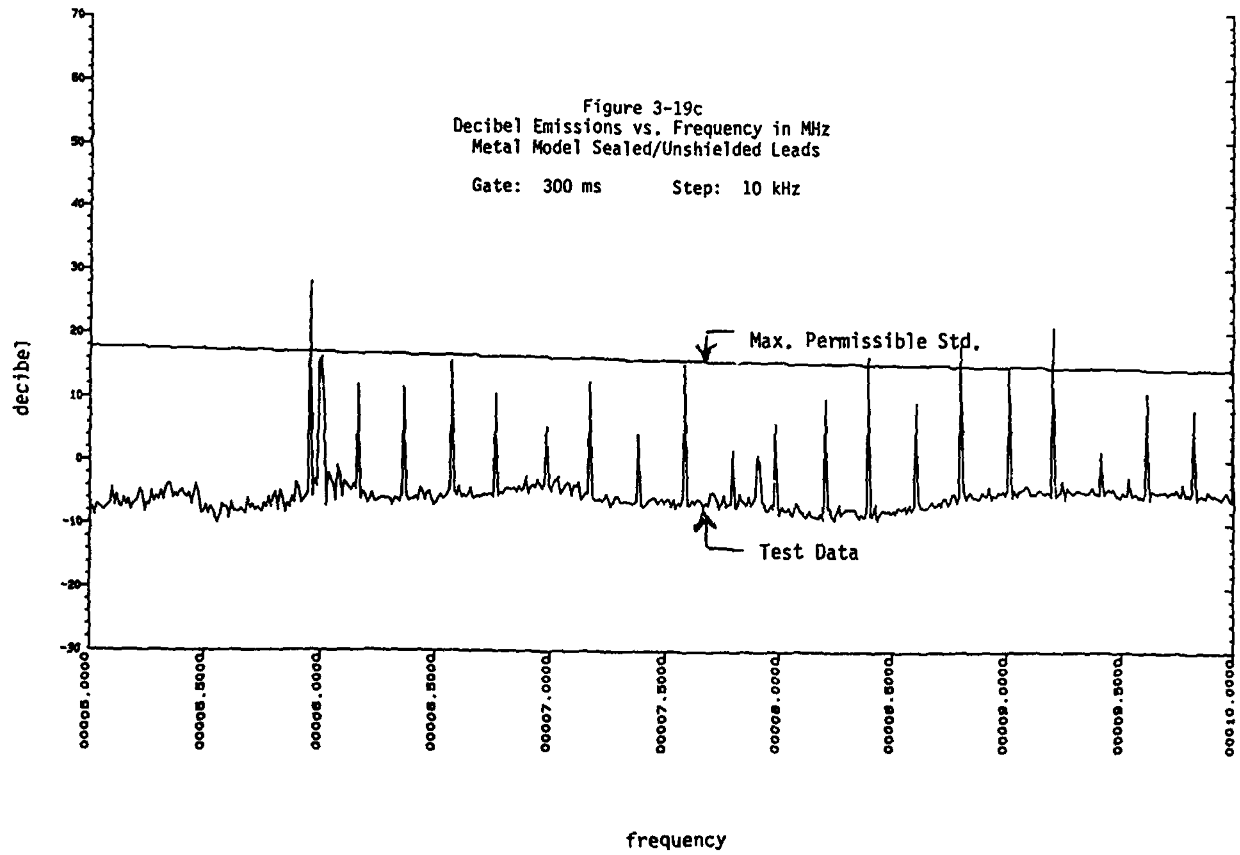

Figure 3-19c
Decibel Emissions vs. Frequency in MHz
Metal Model Sealed/Unshielded Leads
Gate: 300 ms Step: 10 kHz
Max. Permissible Std.
Test Data
decibel
70
60
50
40
30
20
10
0
-10
-20
-30
00005.0000
00005.5000
00006.0000
00006.5000
00007.0000
00007.5000
00008.0000
00008.5000
00009.0000
00009.5000
00010.0000
frequency

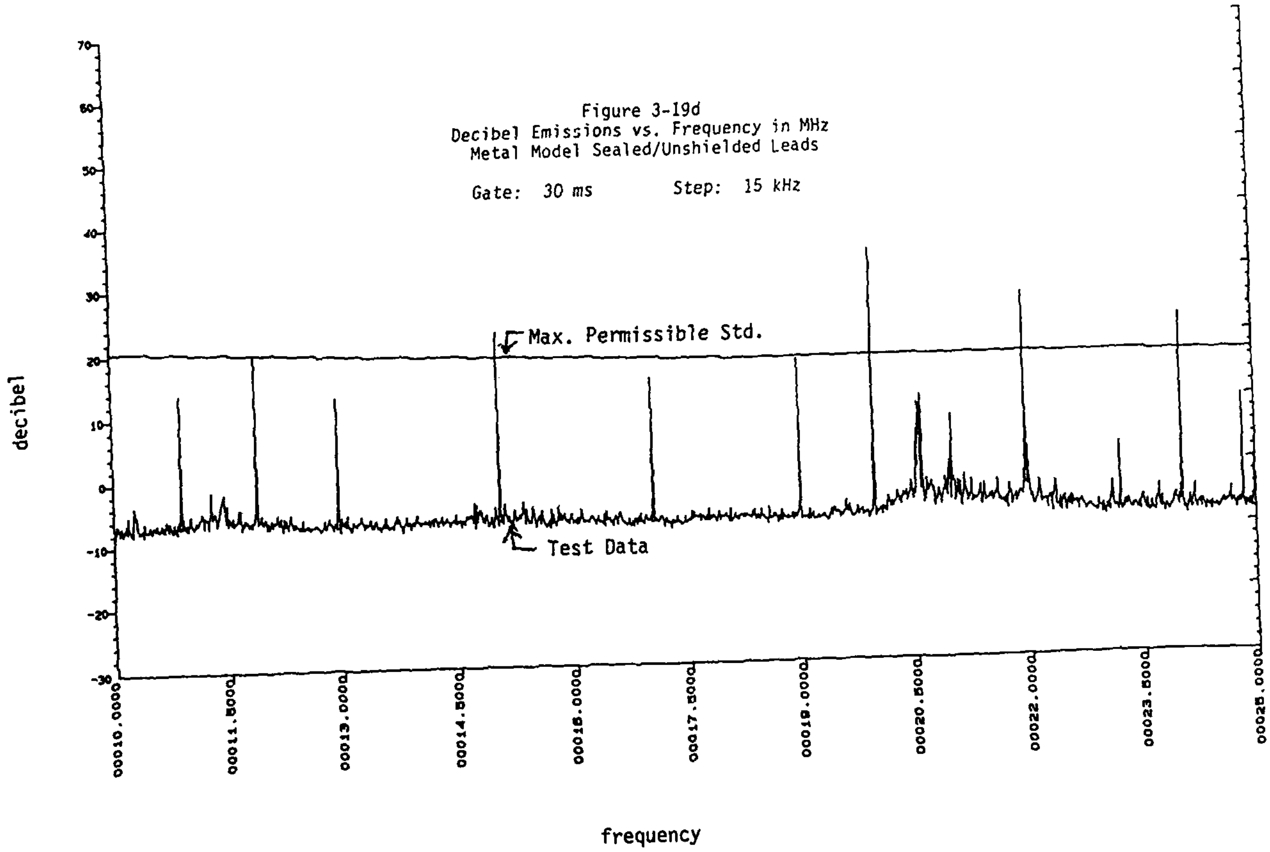

Figure 3-19d
Decibel Emissions vs. Frequency in MHz
Metal Model Sealed/Unshielded Leads

Gate: 30 ms Step: 15 kHz

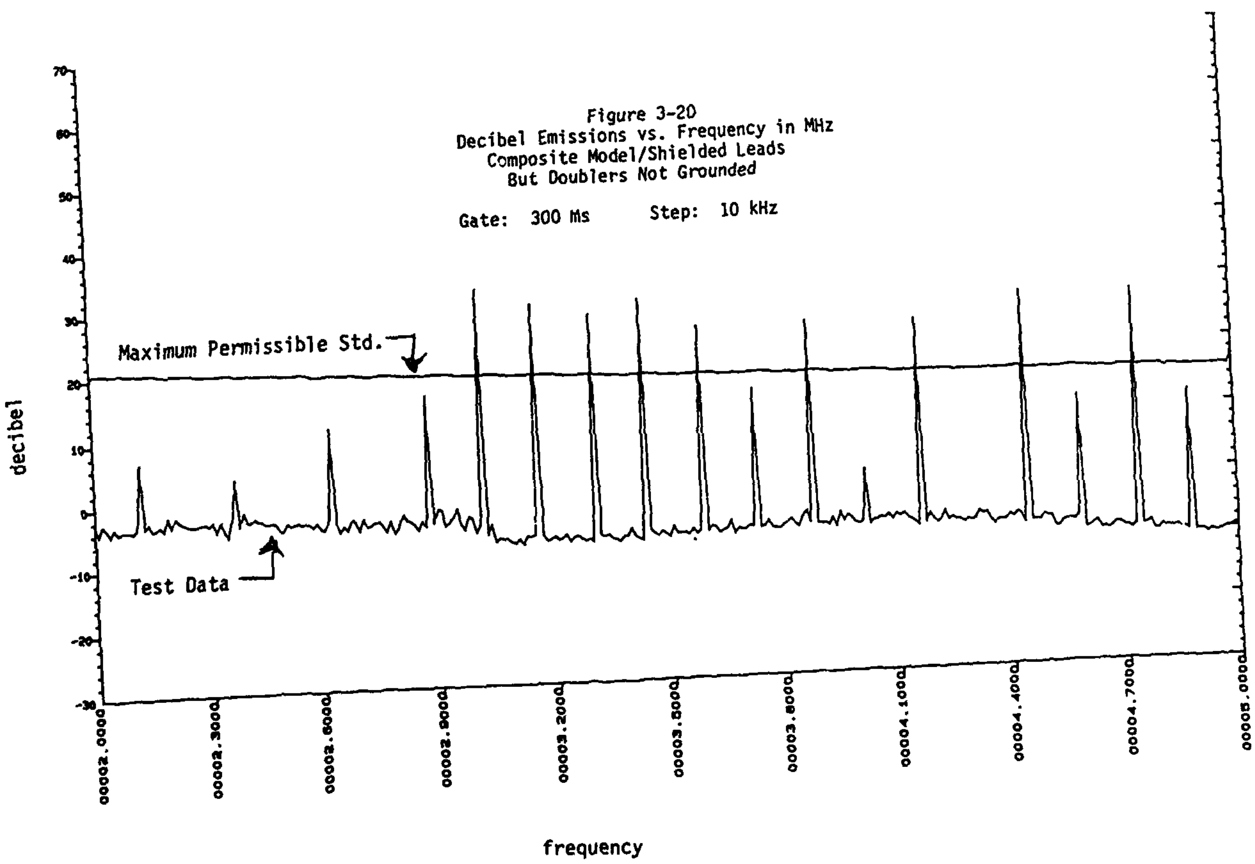

Figure 3-20
Decibel Emissions vs. Frequency in MHz
Composite Model/Shielded Leads
But Doublers Not Grounded

Gate: 300 Ms Step: 10 kHz